Determining the metabolic profiles in *Drosophila melanogaster*: Development and application of a novel ion-pairing liquid chromatography-mass spectrometry protocol

by

Jose Knee

A thesis submitted in partial fulfillment
of the requirements for the degree of
Master of Science (MSc) in Chemical Sciences

The School of Graduate Studies
Laurentian University
Sudbury, Ontario, Canada

THESIS DEFENCE COMMITTEE/COMITÉ DE SOUTENANCE DE THÈSE
Laurentian Université/Université Laurentienne
School of Graduate Studies/École des études supérieures

Title of Thesis Titre de la thèse	DETERMINING THE METABOLIC PROFILES IN *DROSOPHILA MELANOGASTER*: DEVELOPMENT AND APPLICATION OF A NOVEL ION-PAIRING LIQUID CHROMATOGRAPHY-MASS SPECTROMETRY PROTOCOL
Name of Candidate Nom du candidat	Knee, Jose
Degree Diplôme	Master of Science

Department/Program Département/Programme	Chemical Sciences	Date of Defence Date de la soutenance	January 20, 2014

APPROVED/APPROUVÉ

Thesis Examiners/Examinateurs de thèse:

Dr. Thomas Merritt
(Supervisor/Directeur de thèse)

Dr. James Watterson
(Committee member/Membre du comité)

Dr. Eric Gauthier
(Committee member/Membre du comité)

Dr. Tony Parkes
(Committee member/Membre du comité)

Dr. Laura K. Reed
(External Examiner/Examinatrice externe)

Approved for the School of Graduate Studies
Approuvé pour l'École des études supérieures
Dr. David Lesbarrères
M. David Lesbarrères
Director, School of Graduate Studies
Directeur, École des études supérieures

ACCESSIBILITY CLAUSE AND PERMISSION TO USE

Abstract

Genetic perturbations and foreign chemicals can result in a multitude of changes across a wide range of biochemical processes in a biological system. These perturbations may affect the metabolome, the small molecule metabolites in an organism. Recently, liquid-chromatography coupled to mass spectrometry (LC-MS) technology has been used to quantify large proportions of the metabolome, however standardized protocols are not yet available for use with *Drosophila melanogaster*. Here, I developed an ion-pairing LC-MS protocol for the metabolomic characterization of *D. melanogaster* and demonstrated its implementation in establishing the metabolomic profile of flies under oxidative stress and in the metabolic profiles of four different *Drosophila* species. I demonstrated that this new method allows for the detection of otherwise difficult metabolites and that it is repeatable and sensitive with acceptable levels of ion-suppression, matrix effects, limits of detection and quantification. I then used this method to determine and quantify the metabolomic fingerprints of loss of Superoxide dismutase activity and paraquat-induced stress. Comparing and contrasting the effects of these two sources of oxidative stress, I document both similarities and stressor-specific effects.

Keywords

LC-MS, Metabolomics, *Drosophila melanogaster*, oxidative stress

Co-Authorship Statement

Chapter 1 of this thesis concentrates on a review of many technological and biological concepts important to this project. I am the sole author of this chapter. Thomas Merritt contributed insight into experimental design and the conception of the projects, along with grammatical and structural guidance in all chapters of this thesis.

Chapter 2 is a restructured document of a published article in the *Journal of Chromatography B*. This article entitled, A novel ion-pairing chromatography LC-MS protocol for the study of biologically relevant polar metabolites, is authored by myself (first author), Teresa Z. Rzezniczak (TZR), Kevin K. Guo (KKG), Aiko Barsch (AB), and Thomas J. S. Merritt (TJSM). TZR contributed technical assistance during method development, validation, and various metabolomic analyses. KKG and AB contributed to the technological and conceptual design of the protocol developed in this thesis.

Chapter 3 is an early manuscript intended for submission into the journal, *Free Radical Biology and Medicine*. As in Chapter 2, I am the first author with TZR, Tony L. Parkes (TLP), and TJSM as authors on the manuscript. TZR contributed technical assistance for part of the metabolomic analysis in this manuscript. TLP has contributed the fly lines and his expertise with this particular biological system.

Chapter 4 is a discussion of aspects covered in this thesis including avenues for future research. I am the sole author to this chapter with conceptual, structural, and grammatical guidance from TJSM.

Acknowledgements

In the past two and a half years as an M.Sc. student at Laurentian University, I have had the pleasure of working with extraordinary people who have made my success possible. I would first like to thank my supervisor Dr. Thomas Merritt, for providing me with the wisdom, tools, and opportunities to become more of a well-rounded scientist. I would also like to thank Dr. Merritt for his unwavering support throughout all stages of my masters.

Secondly, I would like to thank my committee members Dr. Eric Gauthier, Dr. James Watterson, and Dr.Tony Parkes. My committee members have provided me with support and feedback that has positively affected my thesis and prepared me for the challenges I will face in the future.

Lastly, I would like to thank my family and friends who have supported me and made my experience throughout these years much more rewarding and enjoyable. I would like to thank my colleagues Teresa Rzezniczak, Ryan Auld and David Bing, without whom I would not have been able to complete my thesis, both in a technical sense and in comradery.

Table of Contents

List of Tables

List of Figures

List of Appendices

List of Abbreviations

Abbreviation	Definition
Å	Angstrom
ADP	Adenosine 5'-diphosphate
AMP	Adenosine 5'-monophosphate
ANOVA	Analysis of variance
APCI	Atmospheric pressure chemical ionization
ATP	Adenosine 5'-triphosphate
AUC	Area under the curve
^{o}C	Degree Celsius
C-18	Octadecyl silane
CDP	Cytodine diphosphate
CE	Capillary electrophoresis
CoA	Coenzyme A
CYA	Cornmeal-yeast-agar
D	Dimensional
Da	Dalton
DAA	Diamyl ammonium
DC	Direct current
DNA	Deoxyribonucleic acid
EC	Electrochemical
EI	Electron impact
ESI	Electrospray ionization
*e*V	Electron volt
FAD	Flavin adenine dinucleotide (oxidized)
FALS	Familial amyotrophic lateral sclerosis
FDR	False discovery rate
FMF	Find molecular features
g	Gravitational constant
G6PD	Glucose-6-phosphate dehydrogenase
GC	Gas chromatography
GLYP	Glycogen phosphorylase
GPDH	Glycerol 3-phosphate dehydrogenase
GSH	Glutathione (reduced)
GSSG	Glutathione (oxidized)
HEX	Hexokinase
HFBA	Heptafluorobutyric acid
HILIC	Hydrophilic interaction chromatography
I.D.	Internal diameter
i.e.	*id est*
IDH	Isocitrate dehydrogenase
IMP	Inosine monophosphate
IP	Ion-pairing
IPR	Ion-pairing reagent
KEGG	Kyoto Encyclopedia of Genes and Genomes

KO	Knock-out
kV	kilovolt
L	Liter
LC	Liquid chromatography
LOD	Limit of detection
LOQ	Limit of quantification
m/z	Mass-to-charge ratio
ME	Malic enzyme
mg	milligram
min	Minute
mL	milliliter
mM	millimolar
mRNA	messenger ribonucleic acid
MS	Mass spectrometery
NAA	n-Acetylaspartate
NAD	Nicotinamide adenine dinucleotide (oxidized)
NADH	Nicotinamide adenine dinucleotide (reduced)
NADP	Nicotinamide adenine dinucleotide phosphate (oxidized)
NADPH	Nicotinamide adenine dinucleotide phosphate (reduced)
NMR	Nuclear magnetic resonance
OS	Oxidative stress
oTOF	Orthogonal time of flight
PC	Principal component
PCA	Principal component analysis
PGI	Phosphoglucose isomerase
PGM	Phosphoglucomutase
pKa	Acid dissociation constant
ppb	Part per billion
ppm	Part per million
PQ	Paraquat
QC	Quality control
qTOF	Quadrupole time of flight
RF	Radio frequency
RNAi	Interfering ribonucleic acid
ROS	Reactive oxygen species
RP	Reversed phase
RSD	Relative standard deviation
SOD	Superoxide dismutase (protein)
Sod	Superoxide dismutase (mRNA)
SPE	Solid phase extraction
TBA	Tributylammonium
TCA	Tricarboxylic acid cycle
TFA	Triflouroacetic acid
TOF	Time of flight
UPD	Uridine 5’-diphosphate
(U)HPLC	(Ultra) high performance liquid chromatography

µL	microliter
µm	micrometer
UMP	Uridine monophosphate
UV	Ultra-violet
Vis	Visible
V	Volt
w/v	weight per volume
z	Charge (dimensionless)

Chapter 1

1 Introduction

1.1 Overview

Organisms rely on a multitude of biological processes that function not in isolation, but in an intricate ensemble of interactions. The study of these interactions has classically been limited to investigating isolated features, however advancements in network biology, and technological capabilities, have recently made insights into complex networks possible. In the network biology paradigm any phenotypic trait is the sum of all the interactions in a system (Barabási and Oltvai, 2004). Understanding the network biology of an organism requires the quantification of these interacting traits using large-scale data acquisition associated with functional genomics. Once quantified, these traits make up a profile that can be used to describe a complex phenotype, rather than a simple phenotype based on a limited amount of traits. With this large-scale paradigm in mind, the concentration and variation of metabolites in a system can be treated as a phenotypic trait that can be quantified and used to infer biological meaning (Kamleh et al., 2008; Want et al., 2013). Metabolites do not exist in isolation, but as components of biochemical networks that respond to genetic and environmental factors. Quantifying variation in metabolite levels can provide insights into underlying genomic functions and highlight networks of interests for future research.

1.1 Metabolomics

The complete set of small molecule metabolites in a system is known as the metabolome, and the aim of metabolomics is to detect and quantify as large a proportion of the metabolome as feasible, given technical and financial constraints (Dettmer et al., 2007). Recent advances in analytical technology allow us to analyze a substantial portion of the metabolome (Kamleh et al., 2008; t' Kindt et al., 2010). Wide-arrayed metabolomic methods offer the advantage of being able to discern concentration differences in a broad suite of metabolites in biological samples without previous genomic or biochemical information. These types of "untargeted" studies allow us to observe important differences in the metabolome, which may have otherwise been overlooked (Kamleh et al., 2008; t' Kindt et al., 2010).

From a genomics perspective metabolites are the products of upstream genomic processes: genes are transcribed into mRNA, mRNA is translated into protein, and proteins convert one metabolite to another. Metabolite levels then dictate various complex biological phenomena and can therefore be considered a link between genotype and phenotype. The *Isocitrate dehydrogenase* system in human oligodendroglioma cells is an example of such a connection. A mutation in the *Isocitrate dehydrogenase* (*Idh*) gene results in downstream alterations in metabolome (phenotype: Reitman et al., 2011). In this example, a genomic alteration resulted in an *Idh* knock-out (KO), manifesting in loss of transcribed *Idh* mRNA and functional IDH protein. IDH catalyzes the conversion of the metabolite isocitrate into 2-oxoglutarate. The author's metabolomic analysis revealed that 2-oxoglutarate was decreased in *Idh1* and *Idh2* mutants, as expected. The overall metabolite picture, however, was much more complicated as over 140 metabolites were significantly different in the *Idh* KO subjects than in control samples (Reitman et al., 2011). The breadth of this effect, 140 individual metabolites, highlights the usefulness of broad metabolomic analysis in revealing pleotropic effects of a gene alteration, by quantifying small molecule metabolites.

In contrast to transcriptomics, which involves the detection of polymers of four nucleotide bases, or proteomics, which involves the detection of polymers of 20 amino acids, metabolomics encompasses a much broader and diverse set of chemicals with a larger variety of physiochemical properties. The diverse set of compounds that make up the metabolome include amino acids, cofactors, vitamins, organic acids, sugars, drugs and other external chemicals, amongst others. Due to the wide diversity of compounds found in the metabolome, no single analytical platform can analyze it in, entirety, though some platforms can analyze a large suite of compounds.

1.2 Metabolite detection methods

The most common detection methods in metabolomic studies include ultraviolet-visible (UV-Vis) spectrophotometry, nuclear magnetic resonance (NMR) spectroscopy, mass spectrometry (MS), and electrochemical array (EC-array; Fiehn, 2002; Gamache et al., 2004). Each of these techniques has advantages and disadvantages for analysis of small molecule metabolites, and a suite of molecules for which they are best suited. NMR detection has the advantage of elucidating structural information that can be used for the identification of unknown compounds,

however it has the disadvantage of higher detection limits and it cannot easily differentiate between compounds being analyzed simultaneously as a part of a complex mixture (Wishart, 2008). UV-Vis detection shares disadvantages with NMR detection, however it offers simpler and more affordable systems, as well as established protocols. EC-array detection is capable of detection limits that are orders of magnitudes lower than any other detection method, however it is limited to compounds that are capable of oxidation or reduction (Gamache et al., 2004). Mass spectrometry (MS) displays the largest molecular versatility; it is compatible with a wide range of solvents and modifiers, it is able to detect a widest variety of chemicals, and it has exceptionally low detection limits that are being driven even lower as technology advances (Dettmer et al., 2007). In contrast to other techniques, accurate mass measurements from mass spectrometry can also differentiate between compounds introduced simultaneously, although with certain limitations that will be discussed in following sections. Further, many MS platforms are capable of tandem mass spectrometry, in which ions of a single mass are isolated and fragmented into reproducible patterns of daughter signals, which can aid in the elucidation of unknown compounds (Dettmer et al., 2007). MS platforms do, however, lack the ability to reveal the structural information that NMR analysis is capable of delivering. Alternatively, a combination of MS and NMR approaches can be employed to reveal the identification of a metabolite that neither approach can identify on their own (Eyres et al., 2008).

1.3 Mass spectrometry based metabolomics

Recent advancements in the technology of mass spectrometry based metabolomics, have made the technique more sensitive, versatile, and robust (Dettmer et al., 2007). Mass spectrometry is a powerful technique for determining the identity and concentrations of ions. Mass spectrometers determine the mass of an ion by manipulating it through its various components using electromagnetic fields. In order to be manipulated by electromagnetic fields, compounds need to be in a charged, gaseous state. Charge and mass are the largest factors affecting an ion's movement and the reported unit of measurement in MS is therefore, the mass-to-charge ratio (m/z). The components of a mass spectrometer that manipulate charged molecules are called ion guides, or mass analyzers, depending on their purpose.

Different mass spectrometers contain various forms of ion guides and mass analyzers, including various numbers of parallel rods (quadrupoles, hexapoles, *etc*.), stacked circular structures with

decreasingly small radii known as funnels, ion traps, and time of flight (TOF) chambers. All guides manipulate ions under high vacuum pressures to effectively guide ions to detectors while removing solvent and neutral gases. Movement is regulated axially, along the length of the instrument, and radially, perpendicular to axial movement. Ion guides confine ions within a narrow, radial, path, by interaction of the ion within an in-homogenous radio frequency (RF) field. The RF field will generate points of varying electrical potential energy, which act as potential barriers to ions moving within an instrument. Potential barriers reflect ions travelling down a path, and by oscillating the RF field and the location of potential barriers an instrument can guide ions within a predetermined path. Axial movement of ions is achieved with the use of a direct current (DC) gradient. For example, ion funnels have two DC voltage plates at each end of the funnel that guide ions through the funnel and the consecutively smaller rings have an applied RF frequency that concentrate the ions along a smaller path.

Multipole mass spectrometers are among the most common types of mass spectrometers used in metabolomic studies. Multipoles consist of a number of metal bars arranged circularly and in parallel, creating a path for ions to be manipulated within the bars. Multipoles and ion-traps, variations of the multipole, rely on the stability of an ion trajectory directed through the instrument with RF and DC voltages (De Hoffmann, 2005). If RF voltages alone are used across the bars, then ions of various masses can travel through the multipole and it acts as a guide. If both RF and DC voltages are applied to the poles then ions of a certain mass will be stable through a trajectory, while unstable masses will exit, or discharge on the poles. Ion traps are based on the same type of stable trajectory principle and the poles can be arranged linearly or non-linearly. The linear ion-trap variation is essentially a quadrupole with two reflecting potentials at each end of the quadrupole that trap an ion, while the non-linear variation is essentially a quadrupole bent into a ring structure (De Hoffmann, 2005).

Time-of flight (TOF) mass spectrometers have been used extensively for broad based metabolomic studies and rely on the separation of ions down a flight tube (De Hoffmann, 2005; Verhoeven et al., 2006). The time-of-flight (TOF) mass analyzer requires a voltage to accelerate ions into a field free drift stage before the ion reaches a detector (De Hoffmann, 2005). In TOF mass spectrometry the time it takes the ion to travel from the accelerated region to the detector is inversely proportional to the mass to charge ratio (m/z). Depending on the ionization source, or

components preceding a TOF chamber, ions entering the TOF component are often travelling perpendicularly to the path of flight, necessitating an orthogonal acceleration region. This type of MS is known as orthogonal time-of-flight (oTOF). In ion guiding steps preceding an oTOF component, ions travel in an axial direction towards the oTOF chamber, however they have a radial dimension, meaning at the moment of acceleration there is a distribution of kinetic energies causing some dispersion of the masses. A reflectron can be used to account for the distribution of kinetic energy during orthogonal acceleration and achieve a higher resolution. A reflectron is a region of steady electric field in which ions of different energies will be reflected to the detector. Ions with higher kinetic energies will travel further through the repulsive field correcting for the distribution of kinetic energy at the acceleration region, which standardizes the time-of-flight for molecules of the same mass.

Many modern mass spectrometry systems are essentially hybrid systems consisting of multiple ion guides and mass filters. The MS system in the Merritt laboratory in the Laurentian University Department of Chemistry & Biochemistry, for example, is a double-quadrupole time-of-flight (qTOF) mass spectrometer. The qTOF includes ion capillaries, gates, double funnels, a hexapole, double quadrupoles, and finally an oTOF chamber. Combining different MS systems provides better efficiencies and higher versatility. For example, a qTOF MS is capable of tandem MS, in which parent ions can be fragmented into daughter ions to allow better identification of unknown molecules. In tandem MS, ions enter the first quadrupole, which acts as either an ion guide in standard MS mode, or as a mass filter in tandem MS. Ions that leave the first quadrupole then reach the second quadrupole, which also acts as an ion guide in standard MS mode, however can act as a collision cell in tandem MS (Verhoeven et al., 2006). Following the quadrupole region of the MS, ions reach the TOF component, which is the main mass analyzer of the qTOF system.

1.3.1 Electrospray ionization source

There are several ionization sources available to introduce ions into the mass spectrometer depending on the preceding instrumentation; the most commonly used for broad scope metabolomic analysis include electron impact (EI), atmospheric pressure chemical ionization (APCI), and electrospray ionization (ESI) (Dettmer et al., 2007; Lee et al., 2010). ESI is a “soft

ionization" technique that does not require the fragmentation of compounds before introduction into a mass spectrometer simplifying analysis. Amongst all other ionization techniques ESI is capable of ionizing the broadest coverage of molecules for analysis (Wilm, 2011). These characteristics make ESI ideal for metabolomic studies and are why ESI is used for this work.

The exact ionization mechanism of ESI is currently unknown, however two of the most accepted models are the ion evaporation model (Iribarne and Thomson, 1976; Thomson and Iribarne, 1979) and the charge residue model (Dole et al., 1968; Wilm and Mann, 1994). In the ESI process a solution is sprayed from a capillary tube with an applied voltage and evaporated until the Raleigh limit is reached. The Raleigh limit is a situation in which an excess of ions lines the outer edge of a droplet and the surface charge density generates a surface tension equal to the coulombic repulsion of the ions (Wilm, 2011). The two proposed mechanism of ESI differ after the Raleigh limit. The ion evaporation model postulates that the molecular ion is expelled after the Raleigh limit is reached (Iribarne and Thomson, 1976; Thomson and Iribarne, 1979). In contrast, the charge residue model postulates that the droplets continue to evaporate until a single ion is contained in a charged droplet and is finally expelled by evaporation and declustering (Dole et al., 1968; Wilm and Mann, 1994). Regardless of the exact mechanism of ion formation, ESI is a highly versatile ionization source that is especially useful for metabolomic studies.

ESI is a powerful tool in bioanalytical investigations, however the ionization efficiency of ESI can be drastically affected by complex sample matrices resulting in ion suppression (Müller et al., 2002). Ion suppression occurs when multiple compounds exit an ESI source simultaneously affecting the ability of one, or more, of these molecules to ionize. Ion suppression results in lower amounts of analytes entering a mass spectrometer and by association reduced signals. The many compounds within complex matrices, such as biological metabolite extracts, are likely candidates for ion suppression and signals from such samples would likely be reduced if the complex matrices of compounds were not first separated before introduction into an ESI source. Several chromatographic separation techniques have been utilized in MS based metabolomics, however the three most common include gas chromatography (GC), capillary electrophoresis (CE), and high performance liquid chromatography (HPLC). Each technique has its own strengths and weaknesses. GC-MS and liquid chromatography (LC)-MS are often complementary techniques that can each resolve many compounds that cannot be resolved by the

other. The limitations of GC-MS include a fewer number of compatible mobile phases, it is limited to volatile compounds unless complex derivatization steps are used, and it has limitations on the size and polarity of the molecules it can detect (Koek et al., 2011; Schauer et al., 2005). CE-MS protocols are robust, reproducible, and sensitive, however the method's major limitation is a loading capacity of miniscule volume, a maximum of approximately 1µL. This weakness, however, can be a strength when only small sample volumes are possible, including proteomic applications (Mischak et al., 2009). Stringent sample preparation is necessary to accommodate the small loading capacity of CE, while LC based applications can be more forgiving. The relative versatility of LC-MS based metabolomics makes it a good general choice and is why this technology was used for my thesis research.

1.3.2 Column chemistry and ion pairing chromatography

In general, HPLC works by separating compounds based on their ability to pass through, be retained, or slowed, by an adsorbent material. Retaining compounds in LC is achieved by running a liquid sample over an adsorbent material (stationary phase) that is packed in a column, using a flow of solvent. The compounds in the sample interact with the adsorbent material to different extents and escape the column (elute) at different times, depending on the strength of interactions. The running solvent used for HPLC influences the retention of compounds. Parameters such as hydrophobicity, pH, ionic strength, and the temperature of the solvent all change the interactions of compounds with the adsorbent material. The adsorbent material can be a polymeric, or granular, solid containing different chemical moieties, which will change the strength and types of interactions between the analytes, solvent, and adsorbent.

The most widely used HPLC method is reversed phase (RP) C-18 chromatography, which uses a matrix of octadecyl silane (C-18) groups attached to free silanols as an adsorbent. RP chromatography utilizes polar solvents to carry samples over the stationary phase, enabling molecules in the samples to interact with C-18 groups on the stationary phase. Samples containing hydrophobic compounds will then adsorb to the hydrophobic alkyl chains of the column while polar compounds remain in the polar solvent. Increasing the ratio of organic solutions (non-polar) to polar solutions in the running solvent will displace the adsorbed compounds from the column and the compounds will elute from the column.

C18 chromatography has many applications, but the technique was developed in an effort to analyze compounds of higher hydrophobicity (Vo Duy et al., 2012). This makes the technique less than ideal for many biological applications in which analysis of small, polar, compounds is the goal. An earlier form of LC columns used free silica particles in columns using a normal phase solvent condition. Normal phase solvent conditions require a solvent with higher hydrophobic properties (Hydrophobicity: methanol < isopropanol < acetonitrile < heptane) to be used initially, in order to promote interaction of polar compounds with the stationary phase. The hydrophobic solvent is then replaced by an aqueous solvent, which will displace polar compounds interacting with silanols. The interaction of polar molecules with free silanols is a multi-modal combination of hydrogen bonding, liquid-liquid partitioning, adsorption, and dipole interactions. This type of chromatography was revisited in the 1990's and renamed hydrophilic interaction chromatography (HILIC) (Alpert, 1990). Since 1990, HILIC has been used extensively for analysis of small molecules with polar properties in a wide variety of applications (reviewed in: Buszewski and Noga, 2012).

HILIC is a highly sensitive and versatile method of separation, but does have many shortcomings of its own. Since HILIC is run in normal phase conditions, the initial solvent contains high proportions of acetonitrile, an aprotic (incapable of being a proton donor) solvent that limits the solubility of polar compounds. Dissolving in higher proportions of aqueous solvent is detrimental to the efficiency of the chromatography because water acts as the strong solvent in HILIC, and sample composition should be similar to initial running solvent composition for all types of liquid chromatography (Layne et al., 2001). HILIC is unable to resolve structural isomers such as glucose 6-phosphate and mannose 6-phosphate, although this is a failing common to most forms of chromatography (Bajad et al., 2006; Coulier et al., 2006; Luo et al., 2007). In order to re-equilibrate the silanol groups in HILIC columns with water, or "wet the column", long equilibration times with a high proportion of acetonitrile are required (Buszewski and Noga, 2012). In some cases long equilibration times can be an issue because of the high price of acetonitrile.

Ion-pairing liquid chromatography (IP-LC) is an alternative separation technique for the analysis of polar molecules that avoids some of the limitations of HILIC. This type of chromatography uses a hydrophobic stationary phase, such as a C18 column, in conjunction with an amphiphilic

ion. Much like the mechanism of ESI, the exact mechanism of IPC is still a matter of debate, however proposed mechanisms include a combination of adsorption, ion-exchange, and electrostatic forces that exist between the amphiphilic ions, the column, and counter ions (Ståhlberg, 1999). IP-LC is run under RP conditions, meaning solubility issues for polar molecules are avoided as they are dissolved in aqueous solvent (*i.e.* weaker mobile phase in RP). In several cases structural isomers, which cannot be separated by HILIC can be resolved using IP-LC (Coulier et al., 2006; Luo et al., 2007). Like HILIC, IPC requires long equilibration times, although equilibrating in aqueous solvent rather than more expensive organic solvents alleviates some financial burden.

1.4 *Drosophila melanogaster*: Model for LC-MS analysis

Drosophila melanogaster has served as a model species for studies in a wide variety of fields. *Drosophila* research has been taking place for over a century and through the organism's use as a model species, many fundamental principles of genetics have been elucidated (Rubin and Lewis, 2000). The usefulness of *D. melanogaster* stems from many aspects of the species including the short-lifespan, manageable genome size, cheap and easy laboratory rearing requirements, and a plethora of genetic information and tools accumulated from over a century of research. The near complete *D. melanogaster* genome was sequenced and annotated in 2000, setting the foundation for further functional genetic studies (Adams et al., 2000).

To date, *Drosophila* genetics remains at the forefront of functional genomic studies and new molecular insights (Czech et al., 2013; Mackay et al., 2012). Several levels of functional genomics have been extensively studied in *Drosophila*, including the transcriptome (Czech et al., 2013; Graveley et al., 2011), and the proteome (Brunner et al., 2007; Chang et al., 2013). Metabolomics studies, however, have not seen wide-spread attention as in other systems, though new studies are beginning to emerge (Bratty et al., 2011; Kamleh et al., 2008; Passador-Gurgel et al., 2007; Sarup et al., 2012). The relative scarcity of metabolomic *Drosophila* research leaves room for improved and standardized protocols, which have yet to be established. Standardized protocols would facilitate the transition into metabolomics for new researchers, and promote the development of support systems for researchers interested in determining the identity of unknown compounds, and accessing protocols and results from other groups, much like support systems for other organisms (Bais et al., 2010; Cui et al., 2008; Wishart et al., 2013).

1.5 Reactive oxygen species and oxidative stress

There are several intracellular molecules that are susceptible to oxidative damage by highly reactive chemical species, including reactive oxygen species (ROS) (Buonocore et al., 2010). ROS are generated as a result of aerobic metabolism and have vital roles in cell signaling, homeostasis, and microbial response (Buonocore et al., 2010). ROS can also be generated from environmental factors such as exposure to radiation or foreign chemicals (Hosamani and Muralidhara, 2013; Riley, 1994). While ROS are natural features in all biological systems, an excess of ROS concentrations can lead to rates of damage to lipids, DNA, proteins, and metabolites which cellular repair/turnover systems are inadequate to cope with. Molecular damage thus accumulates, with deleterious effects on several biological processes and normal physiology. The altered state resulting from over exposure of oxidative damage from ROS is known as oxidative stress (OS). An overabundance of ROS and conditions of OS are implicated in several degenerative diseases and disease states (Barber and Shaw, 2010; Dhalla et al., 2000). Though OS has been a major research interest for several decades, many processes are still not well understood and many avenues for research remain, LC-MS based metabolomics included. Organisms have multi-faceted antioxidant systems that neutralize the effects of ROS, however in conditions of overproduction or overexposure to ROS, the levels of ROS overwhelm an organism's ability to counteract these cytotoxic molecules (Hosamani and Muralidhara, 2013; Riley, 1994).

1.6 Superoxide dismutase

Organisms have extensive antioxidant defense systems that limit the deleterious effects of ROS, including enzymatic and small molecule antioxidants. In *D. melanogaster*, the cytosolic Superoxide dismutase 1 protein (SOD) is a major enzymatic antioxidant responsible for catalyzing the dismutation of superoxide into hydrogen peroxide. Other antioxidant enzymes such as catalase or glutathione peroxidases then break down the hydrogen peroxide produced by SOD. When SOD activity is lost in *D. melanogaster*, the ability of flies to remove free superoxide is reduced, and has been inferred to result in an accumulation of superoxide (Bernard et al., 2011; Phillips et al., 1989). Higher concentrations of superoxide result in more oxidative damage to intracellular molecules, which leads to the condition of oxidative stress (Bernard et al., 2011; Phillips et al., 1989). Physiological changes include reduced viability, drastically

reduced lifespan, sensitivity to ionizing radiation, sensitivity to superoxide generating chemical paraquat, and an overall enfeebled phenotype (Phillips et al., 1989). In addition to loss of SOD activity being deleterious, under certain conditions over expression of the SOD enzyme can result in an increase in lifespan (Parkes et al., 1998a).

The fly *cytosolic Sod-null* genotype, $cSod^{n108}$, has been extensively characterized both genetically and physiologically (Bernard et al., 2011; Campbell et al., 1986; Parkes et al., 1998b). The genomic location of the *Sod* gene and its molecular details of the mutant allele are known. One indication of the pleiotropic nature of SOD deficiency is that at a proteomic level, loss of SOD activity through the $cSOD^{n108}$ allele results in a general lowering of the activities of several enzymes involved in central carbon metabolism (Bernard et al., 2011). The enzymes and metabolites assayed by Bernard *et. al* (2011) were chosen based on evidence from other studies that the processes these enzymes are involved in are affected by OS (Parkes et al., 1993; Ying, 2008). Despite choosing to assay down-stream phenotypes which were suggested to be altered by loss of SOD function some were not significant, or significant but subtle in magnitude, highlighting the unpredictability of pleiotropic genetic lesions (Bernard et al., 2011). The unpredictability of downstream processes affected by pleiotropic genetic lesions makes these systems good candidates for untargeted, high throughput analysis, such as LC-MS based metabolomics.

Chapter 2

2 A novel ion-pairing chromatography LC-MS metabolomics protocol for the study of biologically relevant polar metabolites

We report a method of ion-pairing liquid chromatography coupled to mass spectrometry (IP-LC-MS) that we have developed for the sensitive detection and quantification of a variety of biologically relevant polar molecules. We use the ion-pairing agent diamyl ammonium (DAA) to improve chromatographic resolution of polar compounds, such as nucleotide cofactors, sugar phosphates, and organic acids, that are generally poorly retained by conventional reverse phase chromatographic methods. This method showed good linearity (Average *R* value of 0.996) and reproducibility (generally RSD values <10%) with a set of prepared standards. We demonstrate the utility of this method by investigating the metabolomic signature of three distinct biological systems: the metabolic response to lack of Superoxide dismutase activity and to paraquat induced oxidative stress, and the metabolic profiles of four different *Drosophila* species.

2.1 Introduction

Analysis of a broad suite of biologically relevant molecules, *e.g.* RNAs, proteins, or metabolites, is a central goal of many post-genomic era biological studies. For example, the qualitative and quantitative study of all transcripts and protein in a biological system is the goal of transcriptomics and proteomics, respectively. Similarly, metabolomic studies describe a comprehensive set of small molecule metabolites (Trethewey et al., 1999). Comprehensive screening of transcripts and proteins is crucial in understanding complex biological processes, but stops short of describing the actual biology of the system. In many cases, metabolites are the end products of these processes and understanding the metabolomic signature of a system can provide a more complete understanding of biological and biochemical processes (Fiehn, 2002). The metabolome is a highly complex and dynamic suite of molecules that can change in response to such factors as differences in gene activity (Reitman et al., 2011), various stresses (Smith et al., 2012; Wu et al., 2012), or xenobiotics (Giri et al., 2006). Metabolomic profiling studies specifically characterize the changes or differences in the metabolome between conditions or genotypes. This characterization is made challenging by the wide chemical diversity of metabolites. This diversity is in contrast to that in genomics or transcriptomics in

which the nucleotide subunits share a similar biochemistry of interaction (*i.e.*, Watson and Crick base pairing) and can all be identified and quantified with simple biochemical assays (nucleotide binding or synthesis). Even the field of proteomics, in which the 20 amino acids are more complicated to assay than the four nucleotide bases, does not face the same chemical complexity of hundreds or even thousands of chemically distinct metabolites. To analyze the entirety of the metabolome, multiple analytical platforms such as liquid chromatography-mass spectrometry (LC-MS), gas chromatography-mass spectrometry (GC-MS), or nuclear magnetic resonance spectrometry (NMR) are required, however an exhaustive survey is often technically or financially unfeasible. A compromise is to use an individual platform with a broad coverage of metabolites that can present researchers with a reasonable understanding of biological processes in a reasonable time frame and at manageable cost.

Mass spectrometry, combined with ultra-high performance liquid chromatography for sample separation, has been utilized in metabolomic studies for several years and can analyze a large set of polar to semi-nonpolar metabolites (Giri et al., 2006; Kristensen et al., 2012; Reitman et al., 2011). With effective sample preparation and chromatography, LC-MS strategies provide high sensitivity and specificity and a large dynamic range, advantages over some other metabolomic platforms. In addition, LC-MS techniques are compatible with most standard solvents, avoid complicated derivatization steps, and can analyze larger polar molecules such as NADH, advantages over GC-MS based studies (Koek et al., 2011; Schauer et al., 2005).

Broad metabolomic profiling is a developing field, and tested, widely applicable, protocols are still being developed. Metabolomic profiling of *Drosophila melanogaster* by LC-MS is particularly rare, surprising given the central role of this species as a model system, although a few laboratories (Bratty et al., 2011; Chambers et al., 2012; Passador-Gurgel et al., 2007) have demonstrated the power of these studies in this system and more articles are beginning to be published (Cheng et al., 2013). Reversed phase C18 chromatography (Chambers et al., 2012; Passador-Gurgel et al., 2007) and HILIC (Kamleh et al., 2008) have been utilized for profiling purposes however, the use of ion-pairing chromatography has yet to be explored.

Effective chromatographic separation facilitates the generation of high quality LC-MS data. The most common separation techniques for analysis of highly polar metabolites include Hydrophilic

Interaction Chromatography (HILIC) and Ion-pairing chromatography (IP-LC)(Cubbon et al., 2010; Tolstikov and Fiehn, 2002). Both techniques have advantages and disadvantages, which have been described in previous studies (Bajad et al., 2006). In the last decade, the use of HILIC as a polar compound separation technique has increased drastically. Unfortunately, HILIC can produce less than optimal peak shapes for many compounds including NADPH, NADH, and reduced thiols, and is generally unable to distinguish between structural isomers (Bajad et al., 2006). These compounds are central players in many biological systems including oxidative damage and stress and are of particular interest in our, and other, research group's work (Bernard et al., 2011). In addition, the reproducibility of HILIC can also be less than optimal: peak shape and retention time can be altered by subtle differences in temperature, pH, or solvent additive concentrations. Ion-pairing chromatography, however, has been successfully employed to analyze many of the metabolites that we are interested in and avoids some of the limitations of HILIC, e.g. it often demonstrates greater reproducibility and better peak shapes (Luo et al., 2007). IPC has its own disadvantages, however, most notably ion-suppression, reduced sensitivity, and system contamination (Mallet et al., 2004). In this paper we report a simple protocol for metabolomic analysis of polar metabolites using ion-pairing chromatography coupled to a qTOF mass spectrometer fitted with an Electrospray Ionization (ESI) source.

To demonstrate the broad applicability of our protocol, we have used it to describe the metabolomic profile of three different biological systems: loss of cytosolic superoxide dismutase (cSOD) function, paraquat-induced oxidative stress, and the metabolomic profile of four different fly species (Diptera: *Drosophila*). The superoxide dismutase protein (SOD) is a scavenger of reactive oxygen species (ROS) and loss of SOD function results in an accumulation of ROS, a state of chronic oxidative stress (Bernard et al., 2011; Campbell et al., 1986; Parkes et al., 1998b), and subsequent damage to the cell. Paraquat is a powerful chemical oxidant once widely used as an herbicide, now commonly used to generate oxidative stress in experimental biological systems. We use our protocol to determine the metabolomic profile of a *Sod null* mutant and chronic paraquat exposure induced oxidative stress in the model species *Drosophila melanogaster*. Oxidative stress has broad and pronounced pathophysiological effects (James et al., 2004) and recent work, focused on specific metabolites, has shown significant changes in metabolite presence/absence and concentrations (James et al., 2004; Liu et al., 2011; Singh et al., 2008). Here we show that these metabolic effects are far-reaching. We include our third

example, comparison of the metabolic profiles of *D. melanogaster* and three other cosmopolitan *Drosophila* species, to demonstrate the broad utility of our method across species boundaries. Different species, even four cosmopolitan species such as we have investigated, will have unique metabolic or physiological adaptations to their environments (Clark and Wang, 1994; Montooth et al., 2003). Here we show distinct differences in the metabolic profile of these four *Drosophila* species, all collected from a single environment and maintained under identical laboratory conditions.

We report here a versatile IP-LC-MS method for the simultaneous detection and quantification of hundreds of polar metabolites present in biological samples. We use the volatile ion-pairing reagent (IPR), diamyl ammonium (DAA), to resolve the polar molecules on a classical reverse phase column. Further, we demonstrate the utility of this method with examples from three distinct systems: a genetic knockout system, chemically induced oxidative stress and the metabolic characterization of four species on a common food. This untargeted approach balances good analytical performance with a simple protocol and opens the door to metabolic characterization of other genetic systems and organisms.

2.2 Materials and methods

2.2.1 Chemicals and reagents

All metabolite standards were obtained in high purity from Sigma Aldrich (St. Louis, MO) or Bioshop (Burlington, ON). The ion-pairing reagent, diamyl ammonium (DAA) acetate, was purchased from TCI America (Product Number A5704, Portland, OR). All solvents were high-purity LC-MS grade and were obtained from Fisher Scientific (Sunnyvale, CA).

2.2.2 Fly stocks

Superoxide dismutase mutant: Details of the *D. melanogaster Sod1*$^{-}$ null and *Sod*$^{+}$ control alleles have been described in earlier studies (Bernard et al., 2011; Campbell et al., 1986). Briefly, the *D. melanogaster Sod1*$^{-}$ null allele, *cSOD*^{n108}, has essentially no SOD activity (Campbell et al., 1986). The *Sod*$^{+}$ control genotype is a whole organism transgenic rescue line (w^{+}; T5/T5; *cSOD*^{n108}*red/TM3*) that was constructed in the same genetic background as the null, but has a

second chromosome SOD transgene under the control of the native *Sod1* promoter resulting in flies with approximately 50-60% of wildtype SOD1 activity (Parkes et al., 1998b). Despite the lower than wildtype activity, the T5 line is generally phenotypically indistinguishable from wild-type (Parkes et al., 1998b), and, as such, is used as a control.

Multiple *Drosophila* species: All fly lines were isofemale lines, lab cultures established from single wild-caught females, and were established from a compost heap in Sudbury, Ontario, Canada, in late July 2013. Three isofemale lines of *D. melanogaster* were identified morphologically. Three isofemale lines of *D. immigrans*, and *D. busckii,* and one isofemale line of *D. hydei* were identified morphologically and species identification confirmed by comparison of the "barcode" fragment of the COI gene (Goto and Kimura, 2001) with reference sequences in Genbank.

In all application examples, multiple samples of multiple flies were collected to account for fly-to-fly, and vial-to-vial, variation. Multiple vials were used to collect up to 15 flies. If 15 flies could not be collected, then the homogenization buffer was reduced accordingly. In the *Sod* experiment, we assayed 56 Sod^{+} and 56 $Sod1^{-}$ samples and 31 quality control (QC) injections, which consisted of a pooled mixture from extracts of both sample types. In the paraquat experiment, we assayed 20 paraquat treated T5 control samples and 20 T5 control samples (no paraquat), and 30 QC samples. In the metabolomic comparison across species, we assayed four samples from three isofemale lines of *D. melanogaster*, *D. busckii*, and *D. immigrans*, and four samples of one isofemale *D. hydei* line and 15 QC samples.

2.2.3 Culture conditions

Flies were maintained on a standard cornmeal-yeast-agar media (*Sod* and paraquat experiment) or Carolina Biological (Burlington, North Carolina) Formula 4-24 instant *Drosophila* medium (cross-species comparison) at 25 ^{o}C with a 12-hr/12-hr photocycle. For metabolomic profiling, groups of ten male, and ten female, *Drosophila* were placed in vials containing the appropriate medium and allowed to lay eggs for 5 days. Non-virgin adult male progeny of the desired genotype were collected and aged 3-4 days post-eclosure. After aging, flies were anesthetised and collected in groups of 15 flies, flash frozen in liquid nitrogen, and stored at -80 ^{o}C until further processing. Liquid nitrogen was used to quench metabolism and storage in -80 ^{o}C was

used to prevent degradation before analysis; techniques used with biological samples (Lu et al., 2008; Want et al., 2013).

2.2.4 Chemically induced oxidative stress

The *Sod*$^{+}$ T5 control line was utilized to metabolically assess the effect of paraquat induced stress by LC-MS analysis to allow more direct comparison of the results of this experiment to those of the *Sod-null* experiment. T5 flies were raised (as described above) in either standard cornmeal-yeast-agar media (control) or on the same medium treated to a final concentration of 0.5 mM paraquat (Rzezniczak et al., 2011). Non-virgin males that developed in paraquat treated medium were transferred to fresh paraquat treated medium on the day of eclosion and allowed to age for two more days before being flash frozen in liquid nitrogen and stored at -80^{O}C until further processing.

2.2.5 Sample preparation

The weight of individual flies often varies within, or between cultures, and can vary drastically across species. To account for differences in the amount of tissue between fly collections, we standardized the volume of extraction solvent to wet mass of the flies in each sample. All fly samples were weighed to the nearest 0.01mg with a microbalance (MX5 Balance, Mettler Toledo AG, Greifensee Switzerland). A volume of 6.35 µL/mg was used for *Sod-null* and paraquat stress experiments. Due to the relative difficulty in maintaining some *Drosophila* species under laboratory conditions, smaller sample sizes (fewer flies) were used for the multi-species comparison. Fewer flies per sample necessitated a larger extraction volume, 10 µL/mg, to achieve the minimum volume required for the assays. Metabolites were extracted from fly samples as follows. Samples were homogenized in extraction solvent (3:1:1 methanol:water:chloroform) in a mixer mill (TissueLyser, Qiagen) using 3.5mm stainless steel beads in 1.5 mL microcentrifuge tubes with screw caps at 30 Hz for one minute. Sample tubes were centrifuged at 13000 x g for 10 minutes at 4°C to pellet solids and 20 µL of homogenate was diluted in 60 µL of 10 mM DAA at pH 4.95 (Solvent A, see below). For quality control, homogenate from control and experimental, or from all four *Drosophila* species, were pooled and assayed at various points during analysis.

2.2.6 Instrumentation

All experiments were carried out on a Dionex UltiMate 3000 Rapid Separation LC system (Thermo Scientific, Sunnyvale CA) coupled to a Bruker micrOTOF-Q II™ electospray ionization-quadrupole-time of flight mass spectrometer (Bruker Daltonics, Billerica MA). The MS was operated in negative mode and was calibrated using sodium formate dissolved in water/isopropyl alcohol, infused at a flow rate of 0.18mL/hour using a KD Scientific 100L infusion pump. The ionization source working parameters were as follows: capillary voltage 4kV, ion energy of quadrupole 4eV/z, dry temperature 200°C, nebulizer 4.0 bar, and dry gas 9.0 L/min. Chromatographic separation was achieved at 0.400 mL/min using a Kinetex C18 RP 100 mm x 2.1mm I.D., 1.7 µm particle size, 100 Å pore size, column (Phenomenex, Torrance CA) at 50°C with eluent A (10mM diamylammonium acetate aqueous solution adjusted to pH 4.95 with acetic acid) and eluent B (methanol) following the gradient described in Table 1.

2.2.7 Data analysis

Data was acquired using the Hystar 3.2 software package and evaluated using Compass DataAnalysis 4.0 software package (Bruker Daltonics, Billerica MA). Principal component analysis (PCA) and t-tests were performed using ProfileAnalysis 2.0 software (Bruker Daltonics, Billerica MA), and standard curves were generated using QuantAnalysis software (Bruker Daltonics, Billerica MA). Metabolite peaks were detected and time aligned using the Find molecular features function (FMF) in DataAnalysis software works in conjunction with the ProfileAnalysis software. The analysis window used in these analyses commenced after the void and calibration segment (0.4 minutes), and stopped before the high organic washing step that reached the mass spectrometer at 24 minutes. Features were represented as buckets, consisting of a mass to charge ratio (m/z) and a retention time. Each bucket was normalized by the sum of all buckets in the analysis and Pareto scaling was used. Bucket intensity values of the top 30 features, ranked by T-test/ANOVA, were exported into MetaboAnalyst software (http://www.metaboanalyst.ca/MetaboAnalyst/faces/Home.jsp)(Xia et al., 2009, 2012), which was used for hierarchical clustering using a Spearman rank correlation and an average clustering algorithm.

2.2.8 Quantification and Validation procedure

2.2.8.1. Ion suppression

Ion suppression was quantified by comparing metabolite signal intensities between clean solvent conditions and pH adjusted solvent with DAA. Briefly, six candidate metabolites were chosen from each LC gradient (ATP – eluting at 40% Solvent A, ADP – eluting at 65% Solvent A, Arginine – eluting at 95% Solvent A, GSH – eluting at 90% Solvent A, Succinate – eluting at 80% Solvent A, NAD – eluting at 85% Solvent A). Standard solutions at 5ppm were made and these metabolites were individually directly injected into the ionization source using the LC injector, *i.e*. no LC column was used. The mobile phase was isocratic, with the percentage of Solvent B adjusted to reflect the gradient at which the metabolites elute when a column is used.

2.2.8.2. Matrix effects

We quantified potential matrix effects of fly homogenate using the post-extraction spike method (Matuszewski et al., 1998). Flies were collected and homogenized and the homogenate was divided into subsets: one subset (homogenate only) was used to determine the MS response from the metabolites in fly homogenate and the other subset was spiked with 5 ppm of standard. Both subsets were analyzed by LC‑MS as described above and the peak area of metabolite in the fly was subtracted from the peak area found in the spiked sample to correct for naturally-occurring concentrations of the metabolite in the fly. Candidate metabolites were selected as described for our testing of ion suppression (above). Corrected peak areas from spiked homogenate were then compared with peak areas from metabolite run in clean solvent (i.e., LC‑MS grade water) to determine the matrix effects of the fly homogenate.

2.2.8.3. Limits of detection/linearity

The calibration curve for 41 metabolites was obtained by analyzing standard solutions at ten concentrations: 50, 65, 85, 100, 500, 1000, 5000, 10000, 50000, and 100000 ppb. Calibration curves were generated using QuantAnalysis software (Bruker Daltonics, Billerica MA), which plots the area under the curve (AUC) against the concentration of the compound. Linear regressions were used and linearity was calculated from these curves. Limits of quantification (LOQ) and the limits of detection (LOD) were calculated for each metabolite.

2.3 Results and discussion

2.3.1 Method development

We have developed an ion-pairing chromatography method that resolves many polar compounds not well retained by typical chromatographic methods for use as part of a liquid chromatography – mass spectrometry protocol. Method development was performed by injecting prepared standard solutions of commercially available chemicals. Metabolite identification in flies was performed by comparing mass to charge ratios and retention times with prepared standards, and confirmed by injection of spiked homogenate solutions. We initially tested the resolving capabilities of reversed phase (RP) C-18 and similar column chemistries for a set of target polar compounds, but found that the polar compounds all eluted at, or near, the void volume (data not shown). While ion-pairing reagents (IPRs) are expected to improve retention of polar compounds, they may cause ion suppression, adduct formation, and MS source contamination (Hsieh et al., 2001; Luo et al., 2007). In an effort to avoid these issues, while gaining the longer retention times, characteristic of IPRs, we examined the utility of the volatile IPR diamyl ammonium. To our knowledge, the use of this agent in an LC/MS protocol has not previously been investigated, in particular for metabolic profiling workflows.

DAA acetate is a secondary ammonium salt with two amyl side chains that allow for interactions with C-18 carbons. DAA is less hydrophobic than quaternary and tertiary alkyl ammonium salts, traditional IPRs, yet yields acceptable retention of acidic-polar compounds (Fig. 1). In particular, phosphorylated nucleotide cofactors which are difficult to analyze using RP and HILIC (Bajad et al., 2006), had excellent retention with our protocol (Metabolites 27, 39-40 Fig. 1). Under acidic conditions reduced forms of nucleotide cofactors are unstable, however the moderate pH used in this protocol does not result in observable degradation of these compounds (Luo et al., 2007). With regular care and attention, DAA can be relatively easily cleaned from the LC/MS system. DAA is virtually undetectable following four hours of direct injection of clean solvent and an acid wash of the LC unit using a water/organic solution of 100mM sodium perchlorate and 0.1% (w/v) phosphoric acid (results not shown). It is worth stressing, however, that this cleaning should be regular. We have found that even this ion-pairing agent can become harder to remove if the system is run too long (weeks) without a regular cleaning.

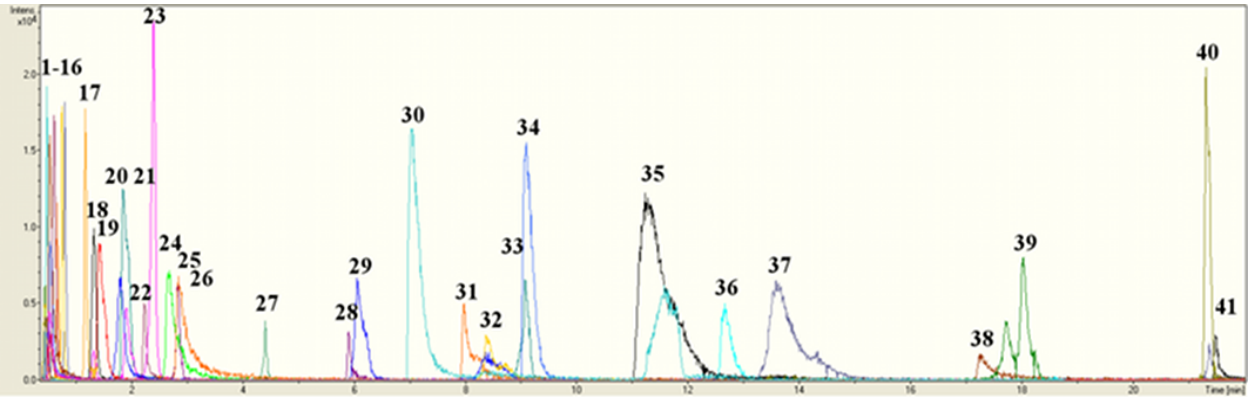

Figure 1: Combined extracted peak chromatograms of prepared standards in solution using solvent A. Peaks represent specific metabolites and numbers over peaks correspond to metabolites in Table 2.

The optimum pH for separation of a wide range of metabolites using the IPR tributylamine (TBA) has previously been determined to be 4.95 by Luo *et al.* (Luo et al., 2007). Considering the similar pKa values of TBA and DAA and the use of the same acetic acid buffer, we adjusted our DAA solution to a pH of 4.95. Similarly, the LC gradient utilized was adapted from Luo *et al.* (Luo et al., 2007) with the time adjusted to account for differences in column dimensions.

Table 1: Liquid chromatography gradient

Step	Total Time (min)	Eluent A (%)	Eluent B (%)
1	1.25	95	5
2	5.25	80	20
3	15.25	80	20
4	17.50	65	35
5	19.25	65	35
6	21.00	40	60
7	22.75	40	60
8	22.85	10	90
9	24.50	10	90

10	24.60	95	5
11	31.50	95	5

2.3.2 Ion suppression/enhancement

We observed both ion enhancement and suppression by DAA (Fig. 2). The level of ion suppression or enhancement across the LC gradient was estimated by comparing the signal strength of six different metabolites injected with clean solvent to that strength when injected with solvent containing DAA. At high DAA content (*i.e.*, when the LC gradient contained greater than 95% solvent A), we observed a 49.5% signal decrease for arginine (Fig. 2B, $F_{1,5}$=23.53, $P < 0.0167$) and a decrease of 25% for succinate (Fig. 2B, $F_{1,5}$=419.73, $P < 0.0003$) . This suppression is substantially lower than that with traditionally used ion-pairing reagents. Ion suppression with trifluoroacetic acid (TFA), for example, averaged 87% under similar conditions (Mallet et al., 2004b). We observed ion enhancement for the remaining tested metabolites (GSH, NAD, ADP & ATP; see Fig. 2A and 2B). The ion enhancement caused by DAA for GSH and NAD was relatively small with signal increases of 3.9% ($F_{1,5}$ = 10.30, $P < 0.0490$) and 34.8% ($F_{1,5}$ = 153.39, $P < 0.0011$) respectively. On the other hand, when the LC gradient contained less DAA (*i.e.,* 40 – 65% DAA Solvent) the ion enhancement observed was much greater: a 94.4% increase in the signal of ADP ($F_{1,5}$ = 619.5, $P < 0.0001$) and a 2328.0% increase in ATP signal ($F_{1,5}$ = 4137, $P < 0.0001$). Nucleotide cofactors were used to estimate ion suppression/enhancement at lower levels of DAA, because these were the only compounds in the standards that we assayed that elute at higher organic solvent concentrations. Ion suppression or enhancement from solvent conditions is compound specific and the values obtained in this study are used for a rough estimate of overall values. The high level of ion enhancement for ATP and ADP could be a result of the chemical properties of the compounds, and other compounds that elute at, or near, the same time may be affected differently by DAA in the solvent.

2.3.3 Matrix effects

Our protocol is intended for fast and simple analysis of a wide variety of compounds. To minimize time, cost, and the potential loss of some metabolites (e.g. through retention on Solid Phase Extraction columns), we included a minimum of sample preparation and clean up. The quick protocol allows for the processing of many samples in a short period of time, but the relatively "dirty" sample homogenate may impact resolution of some metabolites. The simplicity of our sample preparation protocol leaves analyses susceptible to ion suppression from phospholipids and/or co-eluting compounds, *i.e.* matrix effects (Müller et al., 2002). To address the extent of this potential problem, we quantified matrix effects by comparing the signal intensities of candidate metabolites in "clean" solution to the standards in complex fly homogenate (Fig. 3). Of the five tested candidate metabolites, two metabolites (glycerol-1-phosphate and tryptophan) did not have any significant matrix effects, while three metabolites (arginine, succinate, and aspartate) had significant positive or negative effects. Signal intensity was suppressed in fly matrix by 59.6% for arginine and by 50% for succinate and enhanced by 31% for aspartate (Fig. 3; $F_{1,5} = 26.104$, $P > 0.0069$; $F_{1,5} = 85.710$, $P > 0.0008$; $F_{1,5} = 227.522$, $P > 0.0001$, respectively). Although matrix effects were relatively high for some compounds (arginine and succinate), they were within acceptable range based on current opinion for a untargeted, whole-metabolome approach (Böttcher et al., 2007). More thorough sample clean up may reduce such matrix effects, but runs the risk of also removing metabolites. We suggest that researchers should weigh these pros and cons on a case-by-case basis.

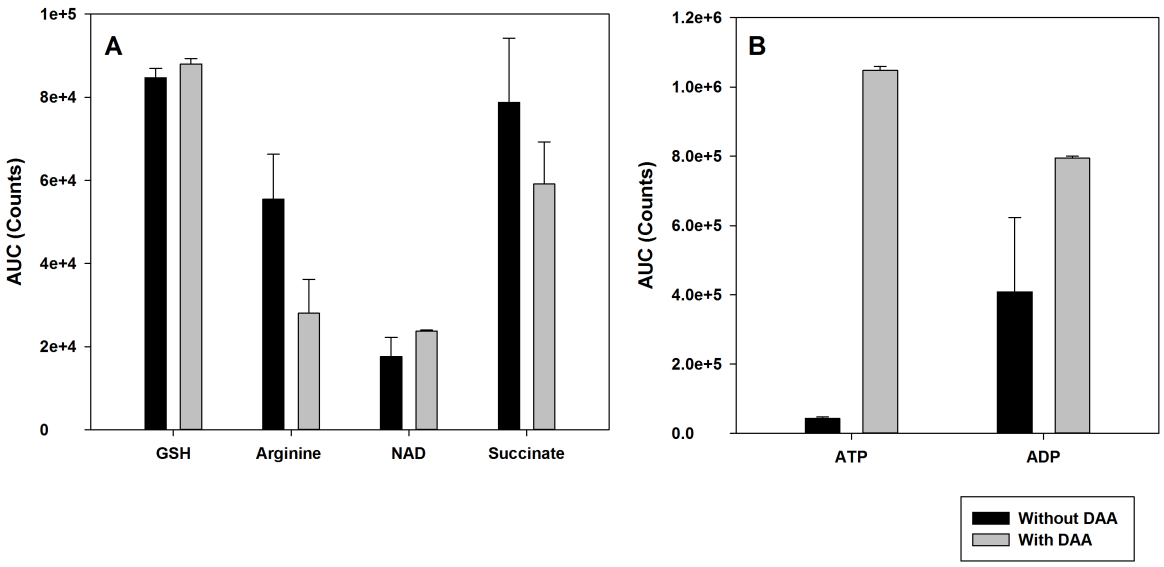

Figure 2: Ion suppression/enhancement caused by the ion-pairing reagent, DAA. Signal intensities, measured through area under the curve (AUC), for candidate metabolites, were quantified in the absence of DAA (black bars), and in the presence of DAA (grey bars). Changes in the signal intensities are shown for (A) the nucleoside phosphates: adenine 5'-triphosphate (ATP) and adenosine 5'-diphosphate (ADP), and for (B) reduced glutathione (GSH), arginine, nicotinamide adenine dinucleotide (NAD), and succinate. Overall, the compounds show lower ion suppression than traditional ion-pairing reagents (data not shown).

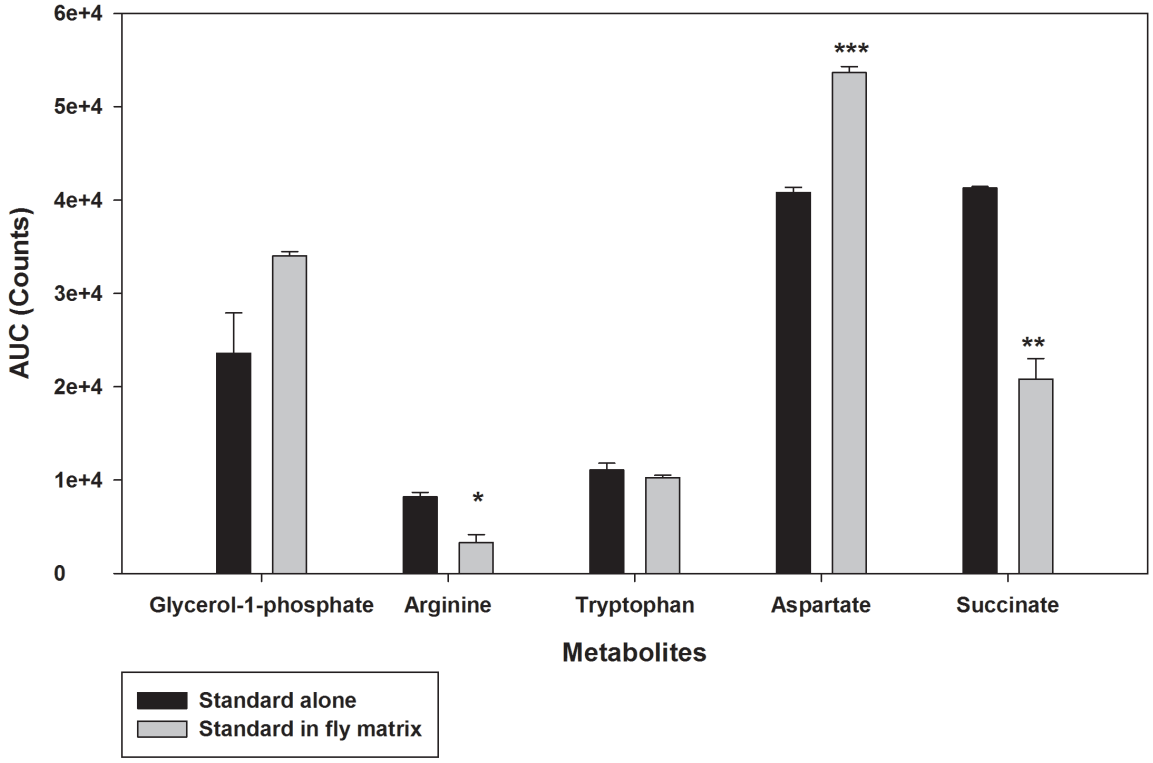

Figure 3: Matrix effects in *Drosophila* homogenate. The amount of ion suppression or enhancement caused by fruit fly homogenate was quantified using the post-extraction addition method. Matrix effects were quantified for candidate metabolites by the area under the curve (AUC) for each metabolite, at a concentrations of 5 ppm, in clean solution, which consisted of mobile phase (black bar) and 5 ppm of metabolite spiked into fly homogenate (grey bar) after correcting for the amount of metabolite in the homogenate alone.

2.3.4 Linearity and quantification

Calibration curves were determined for 41 metabolites using 10 µL injections of concentrations ranging from 0.050 ppm to 100 ppm. In general, the metabolites showed excellent linearity over three or greater orders of magnitude, with correlations coefficients (R^2) of ≥ 0.95. On average, the LOD and LOQ were comparable to those found in previous studies (van Dam et al., 2002; Huck et al., 2003; Soga et al., 2009), but were approximately an order of magnitude greater than those found by Luo et al. (2007). The difference in these values may be due to the nature of the different IPR in either study. The LOD and LOQ were higher for certain metabolites including ADP, AMP, ATP, malate, NADH, NADP and NADPH.

Table 2: Retention times, linearity of calibration, limits of detection and limits of quantification

	Compound	Retention time (min)	Linearity		LOD (ppm)	LOQ (ppm)
			Range (ppm)	R^2		
1	Ornithine	0.46	0.5 - 100	0.996		
2	Lysine	0.46	0.5 - 50	0.998	0.298	0.996
3	Arginine	0.47	0.5-10	0.999	0.288	0.960
4	Dopamine	0.50	5-100	0.997	0.184	0.613
5	Histidine	0.51	0.085 - 5	0.998	0.025	0.082
6	Asparagine	0.55	0.1 – 10	0.978	0.100	0.653
7	Glutamine	0.55	0.1 - 100	0.995	0.100	0.423
8	Threonine	0.55	0.85-10	0.999	0.396	1.319
9	Serine	0.56	0.5 -10	0.996	0.153	0.508
10	Trehalose	0.56	0.5 -100	0.999	0.383	1.277
11	Proline	0.58	0.5 - 100	0.999	0.486	1.620
12	Cysteine	0.59	5-50	1.000		
13	Valine	0.62	0.5-100	0.993	0.476	1.587
14	Methionine	0.68	0.05 - 100	0.989	0.050	0.445
15	Tyrosine	0.76	0.05 - 100	0.998	0.050	1.015
16	Leucine	0.82	0.085 - 50	0.997	0.085	0.660
17	Phenylalanine	1.20	0.085 - 10	0.995	0.085	0.504
18	Glutamate	1.33	0.05 - 10	0.984	0.050	0.312
19	Aspartate	1.41	0.05-10	0.992	0.050	0.356
20	CDP-Choline	1.81	0.5 - 100	0.998	0.359	1.196
21	Tryptophan	1.89	0.5 - 100	0.999	0.210	0.700
22	Glucose-6-Phosphate	2.33	10 - 100	0.999	1.772	5.908
23	Pyroglutamate	2.42	0.05-10	0.999	0.022	0.072

	Compound	Retention time (min)	Linearity		LOD (ppm)	LOQ (ppm)
			Range (ppm)	R^2		
24	Glycerol-1-Phosphate	2.48	0.5 - 50	0.999	0.500	1.867
25	Glutathione (reduced)	2.85	0.1 – 100	0.999	0.100	1.400
26	β-glycerophosphate	2.87	0.5 - 100	0.995	0.281	0.935
27	NAD+	4.47	0.5 - 100	0.999	0.500	2.834
28	AMP	6.01	5 - 100	0.997	5	25.107
29	Succinate	6.07	0.05 -100	0.993	0.050	2.948
30	Malate	7.04	5 - 100	0.993	3.054	10.182
31	Glutathione (oxidized)	7.87	0.5-50	0.998	0.500	1.690
32	α-Ketoglutarate	8.35	1 - 100	0.999	0.231	0.771
33	6-phosphoglucanate	9.04	5-100	0.999	0.620	2.066
34	Fumarate	9.18	0.5 - 50	0.996	0.500	6.531
35	Fructose-1,6-Bisphosphate	11.15	10 – 100	0.999	0.859	2.862
36	Phosphoenol pyruvate	12.67	1-50	0.996	0.509	1.700
37	NADP+	13.60	10 - 100	0.999	6.706	22.353
38	ADP	17.53	10 - 100	0.982	10	43.648
39	NADH	18.02	5 –50	0.999	5	20.663
40	NADPH	21.31	10 – 100	1.00	2.948	9.829
41	ATP	21.53	10 - 100	0.998	10	65.153

2.3.5 Reproducibility

Across the triplicate injections, the relative standard deviations (RSD) of the peak area for 5 ppm and 50 ppm injections were used to assay intra-day variation for all metabolites listed in table 2. Inter-day variation was assessed using 5ppm and 50 ppm injections in triplicate over three days for a subset of 10 metabolites. In general, the RSD of metabolites are below 15 %, which are comparable to similar IPR and HILIC methods (Bajad et al., 2006; Coulier et al., 2006; Luo et

al., 2007). The first 16 metabolites elute quickly, at or near the void volume, potentially leading to poor reproducibility of their identification and quantification. To address the issue of reproducibility, we performed a spike-in experiment with these 16 metabolites at 3 different concentrations. For each of the three concentrations, all 16 standards were spiked into fly homogenate (to account for possible matrix effects) and 5 replicates run through our LC/MS protocol. The standards injected in combination showed good reproducibility across all three concentrations, although methionine, valine, and dopamine demonstrate reduced stability in signal at lower concentrations (Appendix D). The intra-day reproducibility for the majority of compounds fall below 15%, a criterion previously applied by the Food and Drug Administration (FDA) which is followed by other bioanalytical studies, although an RSD of up to 20% is acceptable for low intensity signals (Center for Drug Evaluation and Research (CDER) and Food and Drug Adminstration (FDA), 2001; Dunn et al., 2008; Gika et al., 2007). The low RSD values indicate that our method is reproducible even in this short retention time region.

Table 3: Reproducibility of LC-MS signals

	Compound	Retention time (min)	Intra-Day Reproducibility		Inter-Day Reproducibility	
			50ppm	5ppm	50ppm	5ppm
1	Ornithine	0.46	1.78	4.26		
2	Lysine	0.46	2.61	2.93	9.18	11.36
3	Arginine	0.47	0.568	2.19		
4	Dopamine	0.50	1.43	3.54		
5	Histidine	0.51	1.20	1.58		
6	Asparagine	0.55	1.77	1.41		
7	Glutamine	0.55	0.42	8.43		
8	Threonine	0.55	2.36	4.91		
9	Serine	0.56	NA	4.52		
10	Trehalose	0.56	2.08	11.51		
11	Proline	0.58	0.84	5.76		
12	Cysteine	0.59	2.77	8.25		

	Compound	Retention time (min)	Intra-Day Reproducibility		Inter-Day Reproducibility	
			50ppm	5ppm	50ppm	5ppm
13	Valine	0.62	0.381	1.46		
14	Methionine	0.68	1.51	4.45		
15	Tyrosine	0.76	2.02	3.85		
16	Leucine	0.82	1.89	5.47	0.03	
17	Phenylalanine	1.20	5.53	1.66	0.47	
18	Glutamate	1.33	NA	2.02		
19	Aspartate	1.41	1.43	2.21		
20	CDP-Choline	1.81	1.65	0.995		
21	Tryptophan	1.89	0.58	4.30	8.15	13.70
22	Glucose-6-Phosphate	2.33	17.68	7.97	16.43	2.99
23	Pyroglutamate	2.42	2.59	3.18		
24	Glycerol-1-Phosphate	2.48	0.619	9.97		
25	Glutathione (reduced)	2.85	2.05	3.94		
26	β-glycerophosphate	2.87	1.52	2.11		
27	NAD+	4.47	1.95	3.86	12.48	16.72
28	AMP	6.01	5.16	48.28	8.53	
29	Succinate	6.07	1.42	0.288		
30	Malate	7.04	3.60	12.06		
31	Glutathione (oxidized)	7.87				
32	α-Ketoglutarate	8.35	2.80	35.98		
33	6-phosphoglucanate	9.04	0.757	0.411		
34	Fumarate	9.18	0.918	1.32		
35	Fructose-1,6-Bisphosphate	11.15	4.03	NA		
36	Phosphoenol pyruvate	12.67	2.91	5.56		
37	NADP+	13.60	2.38	NA		

	Compound	Retention time (min)	Intra-Day Reproducibility		Inter-Day Reproducibility	
			50ppm	5ppm	50ppm	5ppm
38	ADP	17.53	16.8	7.33	6.88	18.92
39	NADH	18.02	26.03	25.08		
40	NADPH	21.31	4.03	NA		
41	ATP	21.53	12.49	NA	13.77	

2.3.6 Application

We assessed the general applicability of our LC-MS protocol to variety biological questions by using it to determine the general metabolic profile of three diverse systems: loss of cytosolic SOD function, the effect of chemical-induced oxidative stress, and the metabolite profiles of four different fly species.

2.3.7 The effect of loss of cytosolic Superoxide dismutase function

Loss of SOD function results in a pronounced and widespread effect on the metabolome: almost one third of the features differ in concentration between *Sod-null* and control flies. We detected 594 putative metabolites (automatically extracted features) within our analysis window and of these, 168 (28%) features had significantly different concentrations between *Sod-nulls* and controls using an uncorrected *P*-value cut-off of 0.05, 138 using a value of $P \leq 0.01$. Clustering of the top 30 significantly regulated features clearly resolves the Sod^- and Sod^+ flies (Fig. 4). In Fig. 4 it is apparent that there is variation in biological response between samples, which is expected in biological systems (Bernard et al., 2011; Merritt et al., 2005; Rzezniczak and Merritt, 2012), and highlights the need for replication in the experimental design. Principal Component Analysis (PCA) also captures the impact of loss of SOD function on the metabolome (Fig. 5). $Sod1^-$ lines differed from controls along principal component 1 (PC_1), which captured 15.8% of variation. Several features, including glutamine and $C_{15}H_{20}O_{11}$, that drive variation along PC_1 in Fig. 5 also contribute to the separate clustering of $Sod1^-$ and Sod^+ genotypes in Fig. 4. The fact that many of the metabolite differences are statistically robust, but of relatively small absolute

magnitude, strongly suggests that biological replication is absolutely crucial in capturing trends that are variable yet biologically interesting. In addition to subtle differences, there are also many features with distinct and pronounced differences between null and control that show limited variability between samples. Given the central role of the SOD protein in the fly (Campbell et al., 1986), the distinct metabolic signature between null and control was expected, but the scope of the difference, almost one third of features differing, is striking. The relatively small differences in fold change are a function of the biology of this system – many biologically interesting differences are of small absolute magnitude – not the protocol we have developed. The ability of our protocol to resolve these small differences in biological responses is an advantage of untargeted mass spectrometry based metabolomic techniques (Weckwerth et al., 2004).

The group of metabolites that significantly differed between the Sod^- and Sod^+ flies included both identified and unidentified metabolites. Eighteen of the 45 metabolites we used in optimizing the protocol differed significantly in concentration between the null and control flies; the remaining metabolites have not yet been identified. Fig. 8A shows the difference in concentration of three representative metabolites: glutamine, oxidized glutathione, and the unknown metabolite with a predicted molecular formula ($C_{15}H_{20}O_{11}$).

2.3.8 The effect of paraquat induced stress

PQ-induced oxidative stress also had a pronounced effect across the metabolome, although not as widespread as that of loss of SOD activity. We identified 459 common features, 59 of which had significantly different concentrations between experimental and control samples using a $P < 0.05$, 40 features differ using $P < 0.01$. The metabolite profiles of the top 30 features, ranked by t-test, cluster the treated and control samples separately, as depicted in the heat map (Fig. 6). uaThe differences in the metabolic profiles of treated and control flies are also reflected in PCA (Appendix A). The stressed samples could be distinguished on PC_2, which together with PC_1 captures 28.2% of the variation. Fig. 8B shows three representative metabolites that differ between treated flies and controls: glutamine and two unidentified compounds with predicted molecular formulas of ($C_9H_{16}NO_5$) and ($C_6H_{12}O_7$).

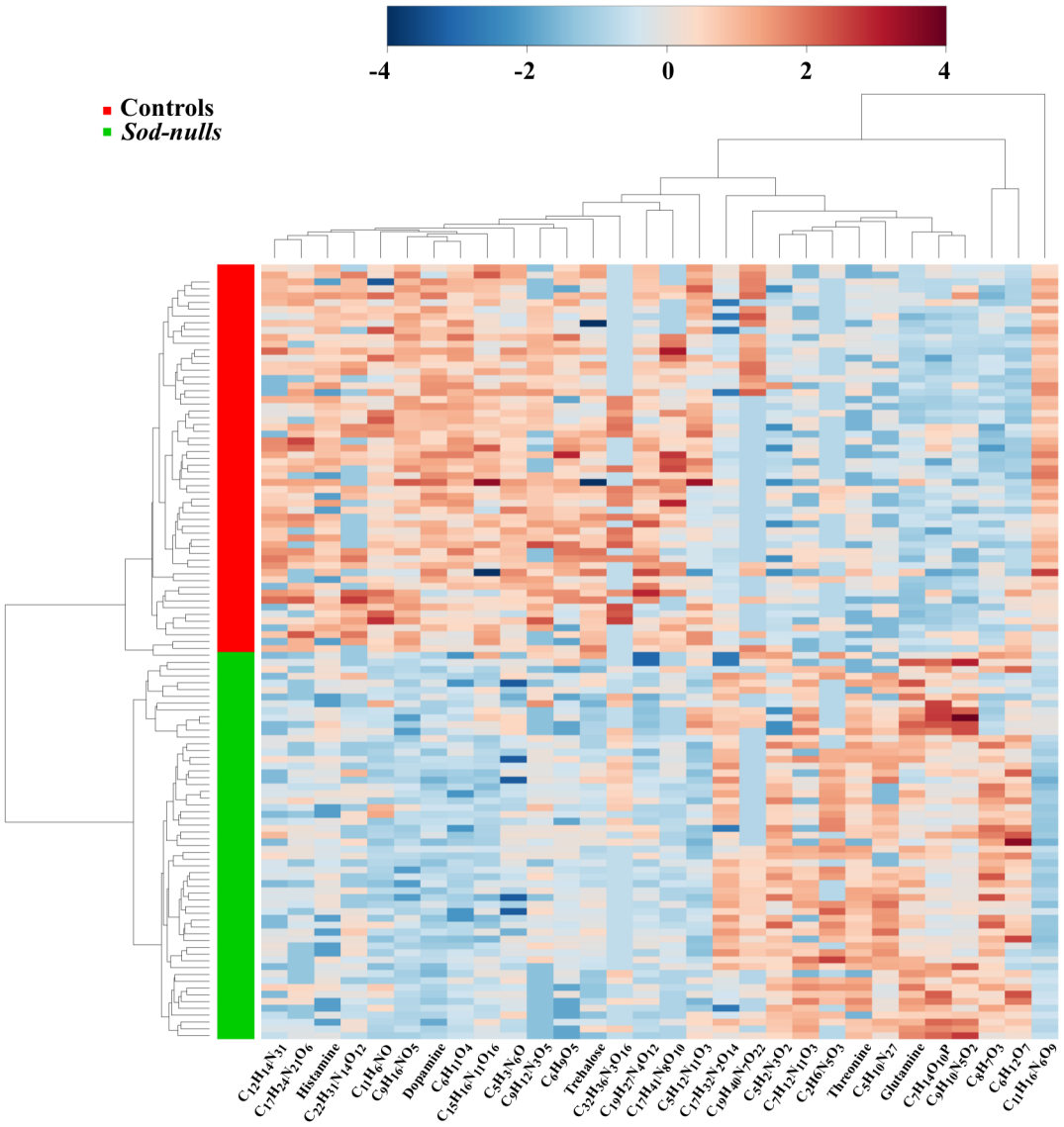

Figure 4: Heat map of metabolite profiles for the top 30 significantly different metabolites for *Sod-nulls* vs. T5 control lines. The level of each compound (*x*-axis) in each sample (*y*-axis) is represented as the fold change above the mean level of that compound. Along either axis, the compounds and samples are arranged by unsupervised hierarchical clustering.

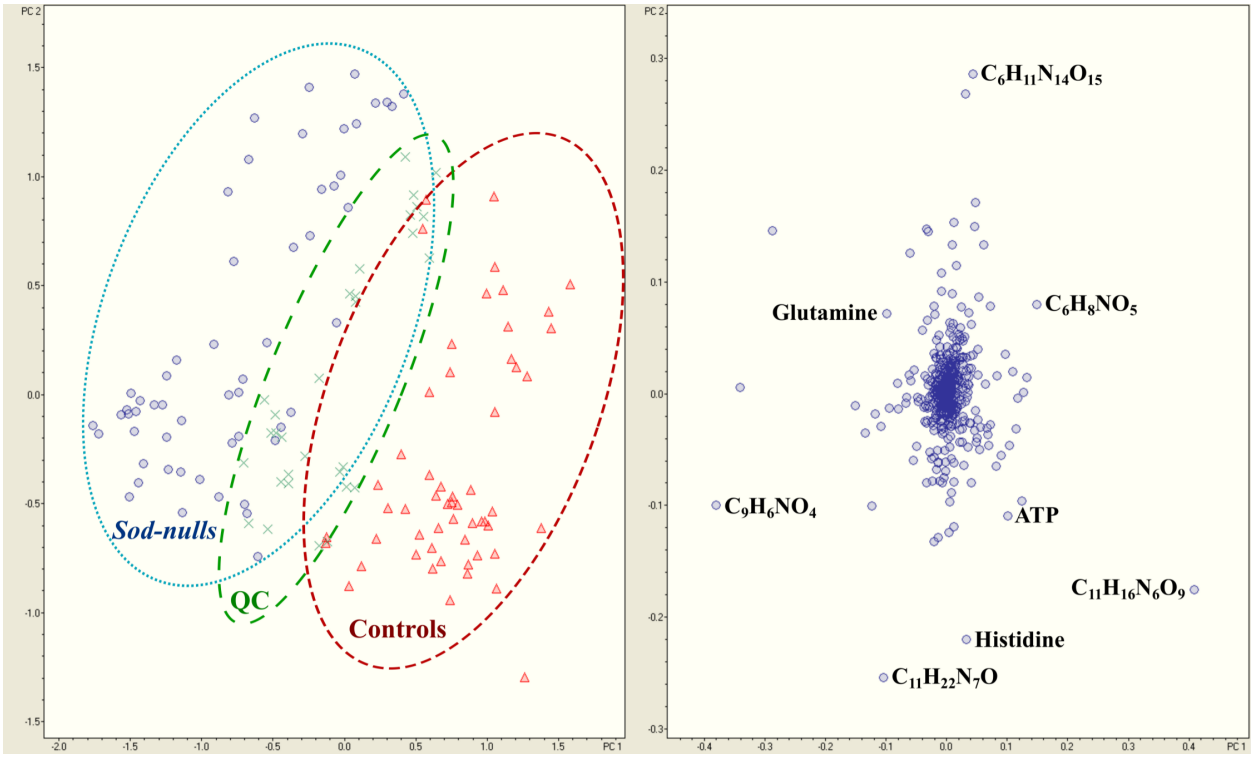

Figure 5: Principal component analysis (PCA) loadings and score plots representing the metabolic profiles of the *Sod-nulls* vs. T5 control lines. Quality control (QC) injections are included in the plot. Axes represent principal component one (PC_1) and principal component two (PC_2) for both loadings and score plots.

Loss of SOD activity and paraquat treatment have been proposed to both create a condition of chronic oxidative stress (Bernard et al., 2011; Rzezniczak et al., 2011). Given this prediction, it is interesting to compare our metabolomic signature of loss of SOD activity with that of PQ-induced oxidative stress. Both sources of oxidative stress resulted in broad metabolic changes (Fig. 4 and 5). While the majority of metabolite differences in response to loss of SOD activity or paraquat stress were specific to either system, 18 putative metabolites did show similar responses to either stressor. Presumably, the shared responses reflect the general condition of oxidative stress while the differences reflect the different mechanism of stress (genetic versus chemical) and other unique features of each treatment. For example, glutamine concentration was higher in both genetically and chemically stressed flies (*Sod-nulls* 1.42 fold, $P = 2.54e\text{-}22$; Paraquat treatment 1.90fold, $P = 6.56e\text{-}10$; fig. 8A and B). Glutamine is an important intermediate in nucleotide synthesis (Neu et al., 1996), provides a source of energy when

glycolysis is shunted for other purposes or the electron transport chain is disrupted (Piva and Mcevoy-Bowe, 1998), and is involved in anti-apoptotic (Matés et al., 2002) and autophagic (Jardon et al., 2012) signaling. All of these functions can be responses to oxidative stress. Glutamine is also a precursor to the tri-peptide anti-oxidant, glutathione (GSH), which reduces ROS and becomes an oxidized dimer (GSSG) (Matés et al., 2002). GSH is a major antioxidant component of biological systems and is elevated in paraquat treated flies (1.31 fold, P = 8.87e-8). In contrast, GSSG was detected at higher levels in the *Sod-null* genotype compared to controls (1.48 fold, P = 3.02e-6) while GSH levels remained the same. These commonalities and differences in metabolome response are the focus of an ongoing investigation of oxidative stress in *D. melanogaster* in the Merritt Laboratory.

2.3.9 Species specific metabolic signature

As a test of the broad applicability of our protocol to general systems beyond oxidative stress and *D. melanogaster*, we compared the metabolite profiles of four *Drosophila* species collected from the wild and reared on a common diet: *D. melanogaster*, *D. hydei*, *D. immigrans*, and *D. busckii*. Diet can have a pronounced impact on an organism's metabolome (e.g. Matzkin et al., 2011, 2013). Given that different species can have different metabolic requirements or optima (e.g. (Matzkin et al., 2011) we tested to see if we could resolve the different metabolic signatures from species raised on a common laboratory food. Species were chosen that occupy a similar "wild" environment (a local compost heap) and lines were chosen that had similar, short, laboratory histories to avoid potential differences in adaptation to the laboratory and media (e.g. Orozco-terWengel et al., 2012). In this experiment, we detected 650 putative metabolites within our analysis window. All four species are clearly resolved by clustering of the top 30 metabolites determined by ANOVA (Fig. 7). *D. melanogaster* and *D. busckii* are resolved, between themselves, and between *D. hydei* and *D. immigrans*, which share similar global metabolic profiles, determined by PCA (Appendix B). Many features were detected at different levels between species. Thirty of these are represented in Fig. 7 and three that differentiate between species are represented in Fig 8c. Pyroglutamate was detected at higher levels in *Drosophila busckii* than in all other *Drosophila* species. The unknown feature at ($C_{16}H_{24}N_5O_{10}$) was higher in *D. immigrans* compared to *D. melanogaster* and *D. busckii*, however was not statistically different from *D. hydei*. Interestingly, the unknown feature $C_{15}H_{20}O_{11}$ was not only higher in *D.*

melanogaster than all other species but was also a distinguishing feature of the *Sod-null* genotype. *D. hydei* did not have any one particular metabolite that was statistically higher or lower than in all other species, however the metabolic profile was able to isolate the species on a separate cluster (fig. 7). Overall, these applications demonstrate that we have successfully developed an LC-MS protocol that can screen for hundreds of polar molecules in biological samples.

2.3.10 Conclusion

We have developed a robust and versatile IP-LC-MS method for the simultaneous detection of hundreds of small polar molecules that are virtually impossible to analyze with classical reversed phase chromatography. With regular cleaning this method avoids the contamination usually associated with typical IPRs while benefiting from the chromatographic resolution that that these compounds allow. We have successfully applied the protocol to quantify the metabolic effect of a *Sod-null* genotype in *D. melanogaster*, chemically induced oxidative stress in *D. melanogaster*, and determine the metabolic profiles of four different *Drosophila* species. By applying this protocol to three distinct biological questions, we demonstrate that this LC-MS method can be used to detect and quantify a diverse suite of molecules that are likely to be biologically relevant in a variety of systems. Identification of currently unknown features using tandem mass spectrometry and applying this protocol to different systems, species, and even organisms is currently in progress. Positive mode analysis with alkyl ammonium salts results in a constant background signal of the IPR, which can contribute to higher levels of ion suppression and system contamination. Complementary protocols for positive mode analysis are currently being developed.

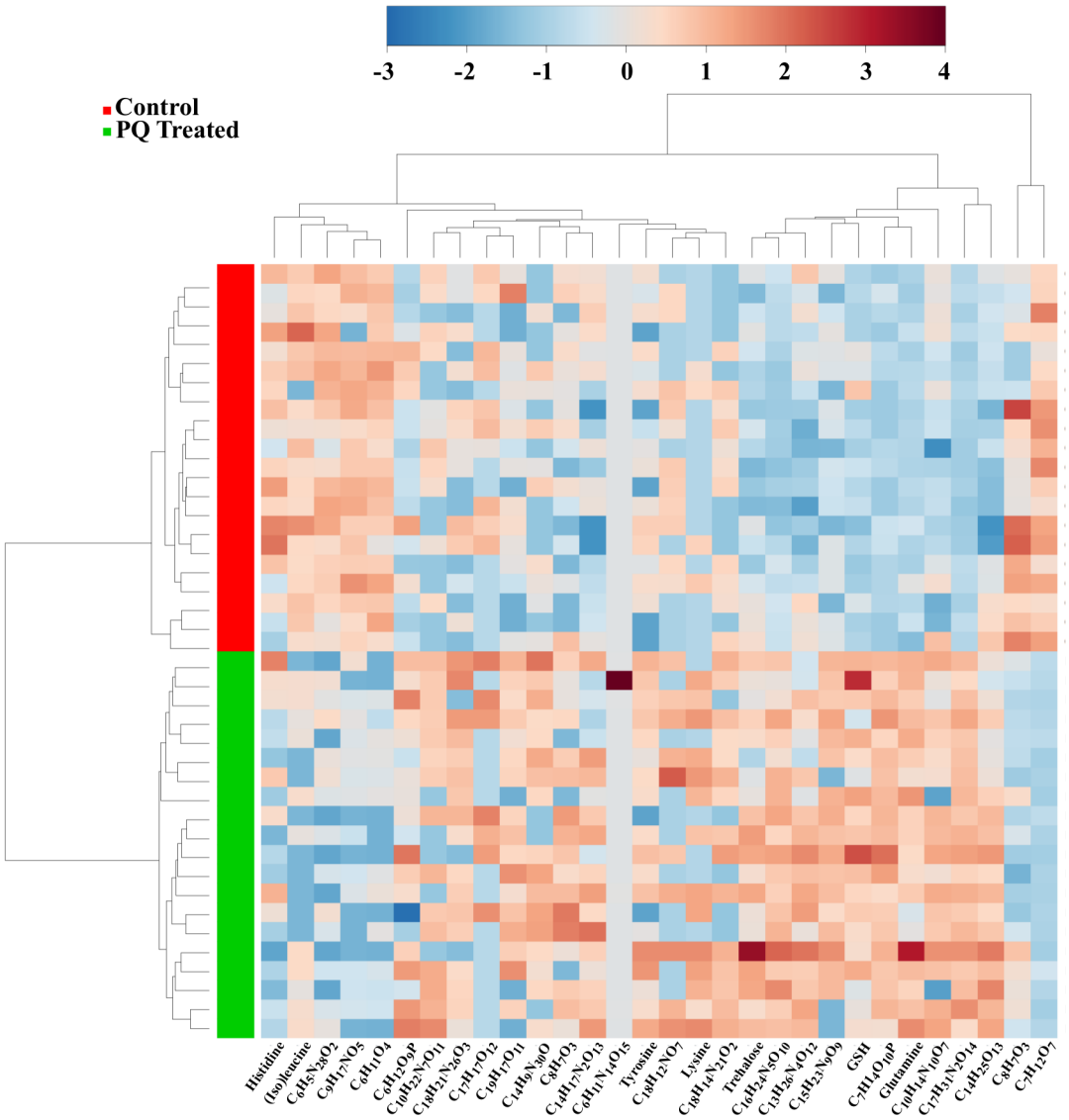

Figure 6: Heat map of metabolite profiles for the top 30 significantly different metabolites for Paraquat treated T5 lines vs. T5 control lines. The level of each compound (*x*-axis) in each sample (*y*-axis) is represented as the fold change above the mean level of that compound. Along either axis, the compounds and samples are arranged by unsupervised hierarchical clustering.

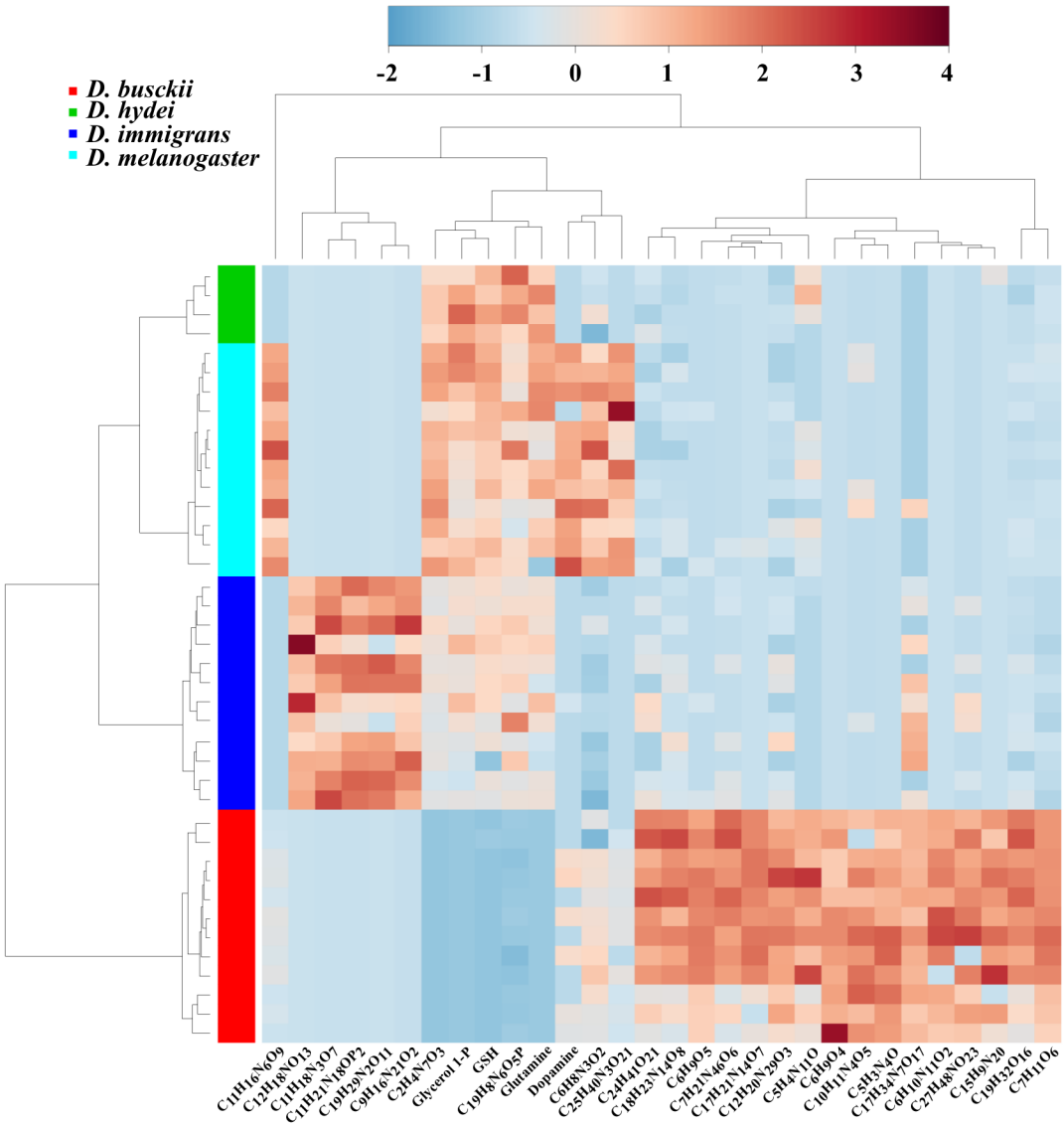

Figure 7: Heat map of metabolite profiles for the top 30 significantly different metabolites for four *Drosophila* species. The level of each compound (*x*-axis) in each sample (*y*-axis) si represented as the fold change above the mean level of that compound. Along either axis, the compounds and samples are arranged by unsupervised hierarchical clustering.

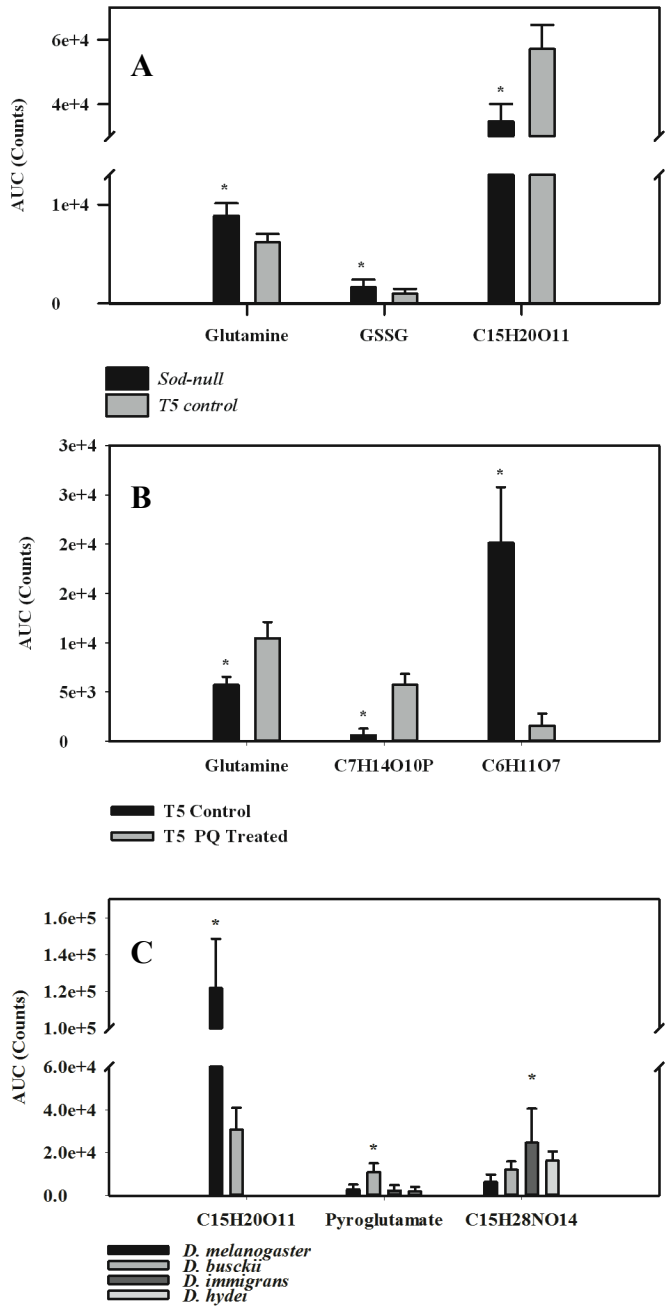

Figure 8: A comparison of metabolite levels between (A) *Sod-nulls* vs. T5 controls, (B) Paraquat treated T5s vs. control T5s, (C) Four *Drosophila* species. "*" denotes significant difference of a sample (P<0.001) compared to all other samples unless otherwise clarified with lines. Error bars represent standard deviation.

Chapter 3

3 LC-MS metabolomic analysis of a *Sod-null* mutant and paraquat induced stress in *Drosophila melanogaster*

Oxidative stress results in substantial biochemical and physiological perturbations in *Drosophila melanogaster*. To generate oxidative stress, we have used both a *Superoxide dismutase* null-allele and exposure to the chemical paraquat. In this study we used liquid chromatography - mass spectrometry to quantify a large suite of metabolites and discovered wide spread changes to the metabolome in response to both stresses compared to control flies. Glucose metabolism, pantothenate and coenzyme A biosynthesis, purine metabolism, and glutathione levels were all altered as a result of both experimental conditions. We also discovered that, although either source results in oxidative stress, many metabolite levels differ between the two sources. In fact, many features are significantly different between stress and control, but in opposite directions in the two different stressors. The results from this study present a more complete survey of the metabolomic effects of oxidative stress in *D. melanogaster* than previous research and a more complete understanding of the metabolic consequences of this stress in general.

3.1 Introduction

In all organisms, oxidative stress (OS) results in a suite of detrimental physiological effects, many of which have been explored through the use of the *Drosophila* model system. *D. melanogaster* have been used in studies of OS because of their ease of culturing and plethora of available genetic tools. Surprisingly, even with extensive study, there is still little known about the effects of OS on global metabolite levels in this organism. Description of a global response will allow us to better understand the metabolic processes affected by oxidative stress and possibly find novel biomarkers for OS. To address this void in our knowledge, we set out to describe the global metabolic profiles of OS in *D. melanogaster* using liquid chromatography coupled to mass spectrometry (LC-MS) using two known sources of oxidative stress, one genetic, a *Superoxide dismutase* null allele, and one chemical, paraquat induced stress.

The enzyme Superoxide dismutase (SOD) is part of the biological anti-oxidant defense mechanism, responsible for the dismutation of superoxide to hydrogen peroxide (Riley, 1994). Impairments in SOD function have been implicated in several diseases including Familial

amyotrophic lateral sclerosis (FALS), Parkinson's disease, Alzheimer's disease, dengue fever, cancer, Down's syndrome, and cataracts (Noor et al., 2002). The SOD family of enzymes is evolutionarily ancient, likely evolving soon after organisms developed the ability to survive in oxygen, and SOD homologs are found in essentially all groups of organisms from microbes to humans (Zelko et al., 2002). In *D. melanogaster*, three isoforms of SOD are currently annotated: cytosolic SOD (SOD1), mitochondrial SOD (SOD2), and an extracellular SOD (SOD3). This investigation focuses the effects of knocking out the *Sod1* gene. In *D. melanogaster*, the loss of SOD1 function results in drastic physiological changes with wide ranging effects, including a reduced lifespan, infertility, neurodegeneration, sensitivity to other oxidative sources, and an increase in spontaneous DNA damage (Bernard et al., 2011; Parkes et al., 1998b; Woodruff et al., 2004). The adverse effects of the *Sod-null* mutation are believed to stem from oxidative damage associated with an accumulation of free radicals, generated via the Fenton reaction and the Haber-Weiss reaction. This process begins with the reduction of iron by superoxide in the Haber-Weiss reaction. Following the reduction of iron, the Fenton reaction can take place, in which iron reacts with hydrogen peroxide to generate hydroxyl radical, which is likely the cause of most oxidative damage (Buonocore, et al., 2010).

Paraquat (PQ), a superoxide generating chemical that has historically been used as a herbicide, is commonly used in *D. melanogaster* as an experimental source of OS (Hosamani and Muralidhara, 2013; Phillips et al., 1989; Rzezniczak et al., 2011). *In vivo*, PQ is reduced to a radical species in an NADPH-dependent matter. The PQ radical spontaneously reacts with molecular oxygen to generate the superoxide radical and regenerate the non-radical form of PQ. Like a *Sod-null* mutation, paraquat treatment confers widespread, detrimental, physiological changes to *D. melanogaster* (Phillips et al., 1989; Rzezniczak and Merritt, 2012). Though both a *Sod-null* mutation and paraquat treatment result in elevated levels of OS, little is known about specific similarities or differences between the stresses. Assessing the particular changes to metabolite levels in each case may thus shed light on the mechanisms by which these stressors induce OS, as well as how OS is manifested within the larger metabolomic network.

Physiological changes resulting from oxidative stress are a function of the accumulation of oxidative damage, driven by reactive oxygen species (ROS). ROS can oxidize almost every type of cellular component including fatty acids, proteins, small molecule metabolites, and DNA.

Oxidative damage can lead to changes in gene expression, cell signaling and many other cellular processes (Girardot et al., 2004; Zou et al., 2000). Gene expression and enzymatic activities are upstream processes that lead to changes in levels of metabolites. The study of the entire set of metabolites and their levels in a system is known as metabolomics (Trethewey et al., 1999). Much like other wide-ranging biological analyses, e.g. genomics or transcriptomics, broad scoped, or untargeted, metabolomics offers insights into many biological processes and physiological states simultaneously. Untargeted metabolomic approaches can also reveal unexpected changes to metabolic networks that were not, or could not be, predicted and would otherwise have been missed by smaller-scale, targeted, assays. Liquid chromatography coupled to mass spectrometry (LC-MS) based metabolomic analyses are growing in popularity for broad-based studies (Bogdanov et al., 2008; Kamleh et al., 2008; Sreekumar et al., 2009; Want et al., 2013). Since oxidative stress results in wide-scale changes in several biological processes, we suspect that alterations to metabolite levels will be present in flies under OS. In fact, a broad array of changes to metabolite levels are observed under conditions associated with OS in different species (Bogdanov et al., 2008; Ho et al., 2013; Serkova et al., 2006; Sreekumar et al., 2009).

In this study, we use LC-MS based metabolomics to quantify the consequence of OS in *D. melanogaster* driven by two distinct sources of OS, a *Sod-null* mutation and PQ. We determine the unique metabolic profiles of both forms of oxidative stress to assess the similarities and differences between them with an ultimate goal of identifying common markers of OS. In both cases, we found large-scale metabolic differences between OS conditions and control lines. Overall, we find that OS leads to broad changes in the metabolome: 28% of metabolites are affected in *Sod-null* flies, 13% in paraquat treated flies. We find both similarities in the stress response (23 known metabolites altered in the same direction under both stressors), and striking differences (17 features of known structure that were significant in opposite directions).

3.2 Materials and methods

3.2.1 Fly stocks and treatment

The c*Sod1-null* genotype and the transgenic *Sod* rescue control have been described previously (Campbell et al., 1986; Parkes et al., 1998b; Phillips et al., 1989), but will be briefly described

here. The *Sod1-null* allele, *cSod^{n108}*, hereafter simply the *Sod-null*, was generated via ethylmethylsulfonate mutagenesis (Campbell et al., 1986), and introduced into Oregon R recipient strain to generate *w^{+}; T0/T0; cSOD^{n108}red/TM3* (Parkes et al., 1998). The *Sod* transgenic rescue control line w^{+}; T5/T5; cSOD^{n108}red/TM3, here referred to as T5 controls, was generated by introducing a *Sod* transgene under control of the native *Sod1* promoter into the same background.

The data used in this analysis is the same raw data used by Knee et al. (2013) (Chapter 2), which focused on method development. This study expands on the scope of previous results by inclusion of metabolite identities revealed by tandem mass spectrometry and subsequent confirmation by purchased standards. The current study also uses all the currently identified metabolites and their concentrations to identify biochemical pathways affected by the two sources of OS. Both the previous study (Knee et al., 2013; Chapter 2) and the current use a very lenient missing value cut-off. For further publication purposes, we are investigating more conservative analysis schemes, i.e. including only features that are present in at least some minimum percentage (e.g. 50 or 80%) of a sample type. Such cut-off values have been demonstrated more consistently result in biologically meaningful results (Hrydziuszko and Viant, 2012; Smith et al., 2006).

For the *Sod-null* vs. control experiment, groups of five males and five females were placed in over 20 vials containing standard cornmeal-yeast-agar-corn syrup medium and allowed to lay eggs for four days. All flies, in this and all other experiments and treatments were maintained at 25^0 C with a 12 hour light:dark cycle. Adult male progeny from several vials, aged 2-4 days, were anesthetized by CO_2, pooled, and collected into vials with 15 individuals before being flash frozen with liquid nitrogen and kept at -80 ^{o}C until the day of extraction. This analysis used 56 biological replicates for each sample type.

In the PQ induced stress experiment three SOD+ lines, the T5 'rescue' control line, *w*;6326;6326, a sub-line of the isogenic 6326 (Hoskins et al., 2001), and *w*;VT83;VT83 inbred lines isolated in Vermont, USA, were either exposed to paraquat or kept under benign conditions. Three lines were chosen to assess natural variability in response to PQ treatment. For each line, over 20 vials were set-up to contain five males and five females which were

allowed to lay eggs in either standard medium or medium treated with a final concentration of 0.5 mM paraquat. Newly emerging flies were transferred to fresh vials of paraquat treated, or standard, CYA medium and aged for two more days before being flash frozen and stored. To develop this protocol for inducing chronic OS across multiple life stages, we screened nutrient medium supplemented with a series of paraquat concentrations. At concentrations of 1mM or higher, the T5 control lines did not produce viable flies (data not shown). This analysis used 20 biological replicates of each sample type.

Our metabolite extraction protocol has been described previously (Knee et al., 2013). Briefly, groups of 15 adult male flies were weighed to the nearest 0.01mg with a microbalance (MX5 Balance, Mettler Toledo AG, Greifensee Switzerland) and extraction buffer was added in a concentration of 6.35 µL/mg. The extraction solvent used in this study was 3:1:1 mixture of ice-cold methanol:chloroform:water (adapted from Kamleh et al., 2008). The flies were homogenized with a bead beater (TissueLyser, Qiagen) and centrifuged, at 4^0C and 13000 x g, and the supernatant recovered to remove protein and debris. Extracts were kept at -80^0C until LC-MS analysis was run. Before injection into the LC-MS, fly extracts were thawed and diluted with solvent A (below) to reduce the combined methanol:chloroform content to approximately 20%.

3.2.2 LC-MS parameters

LC-MS analysis was performed on an Ultimate3000RS (Dionex, ThermoScientific) (U)HPLC system coupled to a MicroTOF QII (Bruker Daltonic, Billerica, MA) mass spectrometer with an electrospray ionization (ESI) source as previously described (Knee et al., 2013; Chapter 2). Separation was achieved at 0.4 ml/min on a 1.7 µm, 2.1x100 mm Kinetex C18 column (Phenomenex, Torrance, CA) maintained at 50^0 C. Solvent A consisted of 10 mM diamyl ammonium acetate (DAA) at pH 4.95. Solvent B was 100% methanol. The gradient used for these analyses is represented on Table 1.

The mass spectrometer was run with the following ESI parameters: capillary: 4 kV; nebulizer pressure: 4 bar; dry gas flow: 9Lmin−1; dry gas temperature: 200^0 C. At the beginning of each chromatographic run, sodium formate (0.5 mg/mL in an equivalent mixture of water and isopropanol) was injected into the mass spectrometer, in a separate segment for automatic

calibration. Quality control (QC) and blank injections were used periodically (approximately every 10 samples) throughout each analysis.

3.2.3 Data handling and statistical tests

Raw MS data was acquired using Hystar 3.2 software and evaluated using DataAnalysis 4.0 (Bruker Daltonics, Billerica MA). FindMolecularFeatures (FMF; Bruker Daltonics, Billerica MA) automatic peak finding software was used in conjunction with DataAnalysis 4.0 to generate a retention time: mass to charge ratio (m/z) pair termed a bucket. FMF compounds in the analysis window were imported into ProfileAnalysis 2.0 software (Bruker Daltonics, Billerica MA). The analysis window included the area after the calibration segment starting at 0.4 minutes and ending before the high organic wash stage at 24 minutes. ProfileAnalysis 2.0 was used for principle component analysis (PCA) and t-test analysis. Bucket features were normalized by the sum of all buckets in the analysis for t-test, and further Pareto scaling was used for PCA.

Features of known structure were validated using commercial standards and buckets generated from PCA were exported into comma separated value format and uploaded to MetaboAnalyst software (http://www.metaboanalyst.ca/; Xia et al., 2009, 2012). Pathway analysis was run on the MetaboAnalyst server, which uses Goemanós Globaltest (Goeman and Bühlmann, 2007) for pathway enrichment analysis, and a relative-betweeness centrality measure for pathway topology analysis. Pathway enrichment is a type of quantitative enrichment analysis similar to analyses used for gene expression datasets. Pathway enrichment combines over-representation analysis, in which metabolite sets are given a significance based on their representation on (i.e. presence/absence in) a particular pathway, and concentrations of the metabolites within these pathways (Xia et al., 2009, 2012). The results of pathway enrichment analysis are represented on the *y*-axis of the metabolome view of a pathway analysis. Pathway topology analysis takes into account pathway structure to determine which pathways are most likely affected by conditions under study (Xia et al., 2009, 2012). The results of topology analysis are represented on the *x*-axis and expressed as an impact. The impact is based on connectivity of metabolites in a particular pathway and normalized by the impact of the individual metabolites in that pathway. MetaboAnalyst uses the Kyoto Encylopedia of Genes and Genomes (KEGG) database for its

back end knowledge and uses the *Drosophila melanogaster* reference genome for the analysis (Xia et al., 2009, 2012). The global metabolic profile was reconstructed in Fig. 11 also using the KEGG database.

3.3 Results

3.3.1 Metabolomic analysis of a *Sod-null* mutation

We used an LC-MS protocol for the comprehensive screening of small molecule metabolites in *D. melanogaster* to determine the effects of a *Sod-null* mutation. Chromatography was performed with an ion-pairing reagent and a C-18 column and MS analysis was performed in negative mode. Previous studies of a variety of complex phenotypes, have shown that *Sod-null* flies are under chronic OS, presumably caused by the inability to remove superoxide anion (Bernard et al., 2011; Campbell et al., 1986; Parkes et al., 1998b). Here, we quantify the effects of a *Sod-null* mutation on the metabolomic profile of *D. melanogaster*, effects that likely contribute to many, if not all, of the larger-scale phenotypes previously established for this genotype. We found that the loss of SOD activity leads to significant and substantial, broad reaching effects across the metabolome. A total of 168 out of 594 shared features (potential metabolites), 28 %, were detected at significantly different concentrations in the *Sod-null* and control flies (Table 4). Out of the 594 shared features, 53 were confirmed metabolites, and 38 of these known metabolites were significantly different between *Sod-nulls* and controls. The broad differences in metabolite levels between the sample types allowed for the clear separation of the *Sod-null* and control flies along Principal component 1 (PC1) in principal component analysis (PCA; Fig. 9a). *Sod-null* mutants were also distinguishable from control flies using hierarchical clustering in heat map analysis (Fig. 10a).

3.3.2 Metabolomic analysis of paraquat-induced stress

We used the same UHPLC-MS protocol for the comprehensive screening of small molecule metabolites in flies exposed to the superoxide generating chemical, PQ, as we did for the *Sod-null* flies. PQ is commonly used to experimentally generate OS and its exposure to *D. melanogaster* causes broad reaching physiological and biochemical changes (Hosamani and Muralidhara, 2013; Rzezniczak et al., 2011). Flies from the T5 *Sod* control line were reared

under constant exposure to low levels of paraquat and compared to T5 flies reared on standard lab media. Chronic PQ exposure across the life stages of *D. melanogaster* resulted in a large metabolic response. A total of 59 out of 459 shared features (potential metabolites), 13 %, were detected at significantly different concentrations between PQ treated and control flies (Table 4). Out of the 459 shared features, 41 were confirmed metabolites, and 17 of these known metabolites were significantly different in paraquat treated and control flies. The wide, metabolic differences detected in paraquat treated flies, is reflected in separation of the two sample types along PC1 in the PCA (Fig. 9B).

3.3.3 Metabolic comparison between stresses

Comparison of the similarities and differences between genetically and chemically driven OS allows us to draw conclusions about OS in general. Both sources of OS resulted in substantial changes to the *D. melanogaster* metabolome, however the *Sod-null* allele had a significantly wider effect (Table 4; Fisher Exact Test $P<0.0001$). The number of detected metabolites of known structure was higher in the *Sod-null* analysis compared to the paraquat analysis, 55 and 45, respectively. The difference in detected metabolites of known structure may be attributed to PQ stress drastically reducing the concentrations of these metabolites below our limits of detection. The *Sod-null* allele and paraquat treatment are both used for models of oxidative stress, however the significantly altered features in both stresses differed both qualitatively and quantitatively suggesting that these two stress conditions are actually significantly different at the metabolomic level. Only approximately half (23 out of 45) of significantly different features in paraquat-induced stress were significantly altered in the same direction as the *Sod-null* genotype.

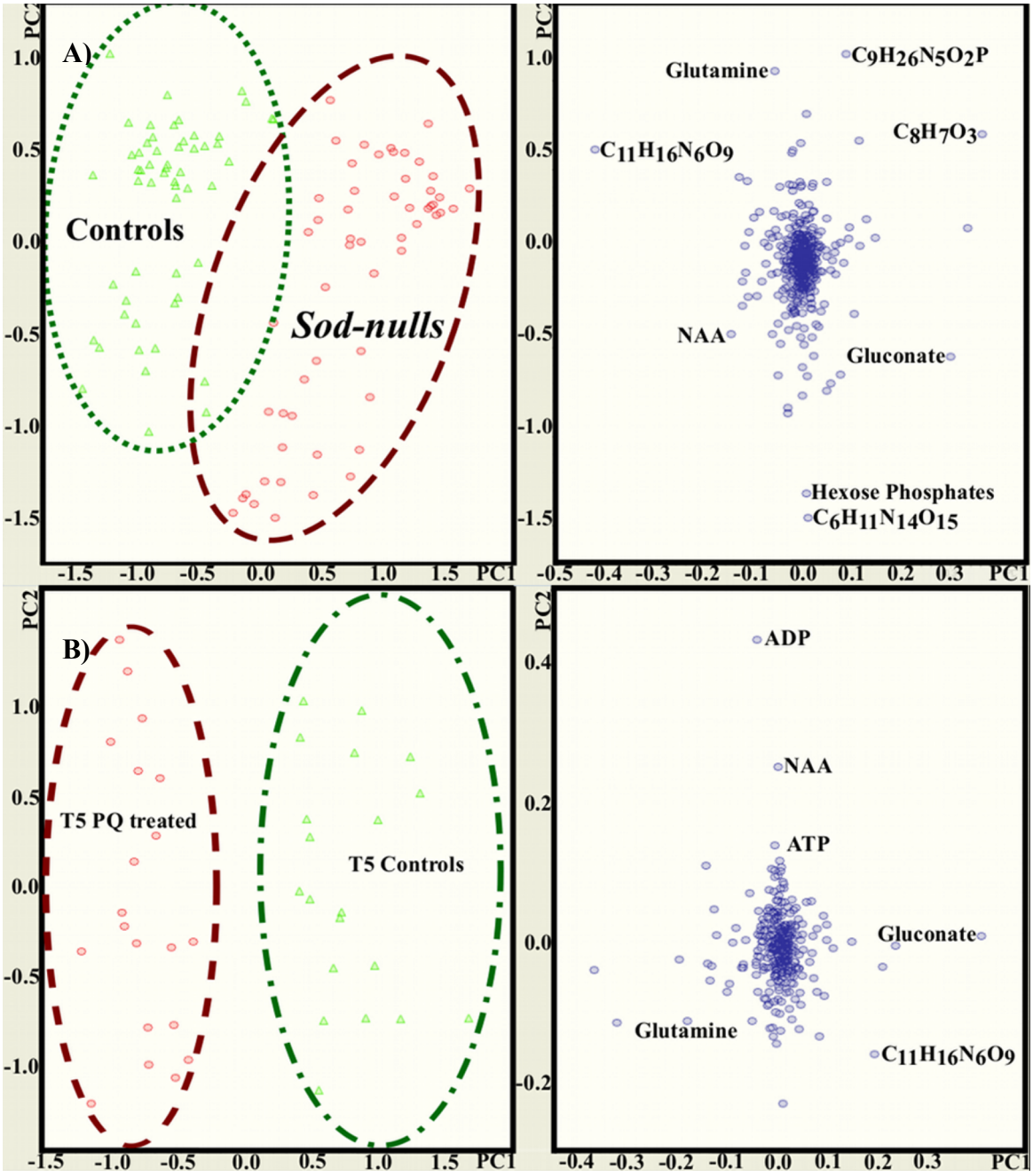

Figure 9: PCA scores and loading plots of the metabolic profiles representing A) the *Sod-null* vs. T5 control lines and B) T5 control lines under paraquat stress and control parameters.

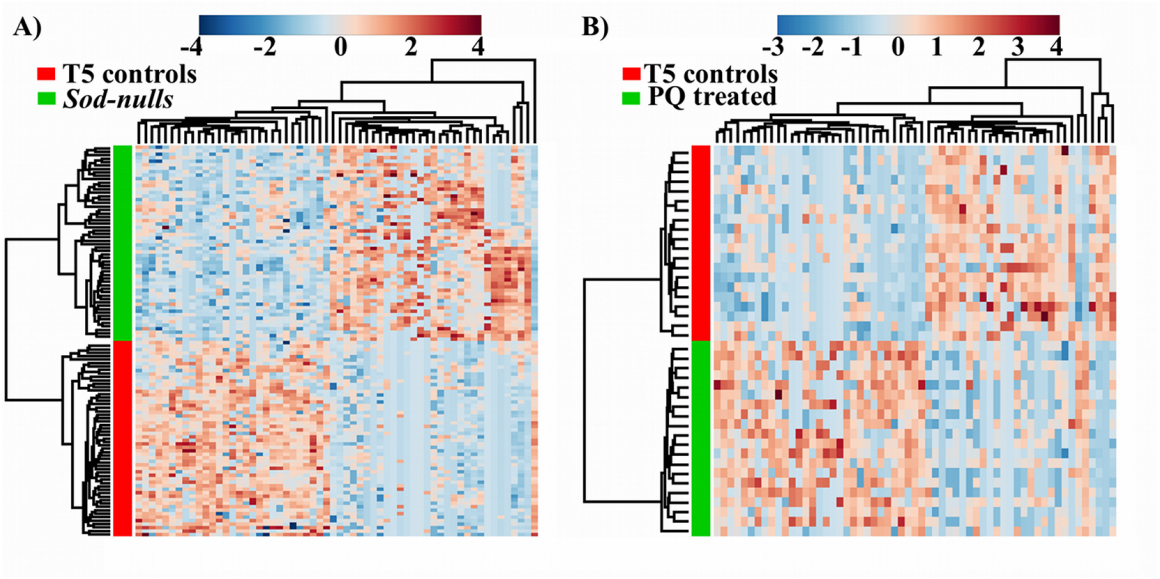

Figure 10: Heat maps of the metabolic profiles, consisting of the top 59 significantly different features, of A) *Sod-nulls* vs. T5 controls and B) PQ treated flies vs. controls. The level of each compound (*x*-axis) in each sample (*y*-axis) represented as the fold change above the mean level of that compound. Along either axis, the compounds and samples are arranged by unsupervised hierarchical clustering.

3.3.4 Metabolic pathways affected by a genetic and chemically induced oxidative stress

The *Sod-null* mutation and paraquat induced stress resulted in a suite of differences across the fly metabolome. Some individual metabolites may be interesting in themselves, but our larger interest is in the pathways and networks affected by these stresses. Pathway analysis, combining enrichment analysis and topology analysis, was used identify pathways affected by both stresses (Wu et al., 2012; Xia et al., 2009) and results are summarized in Fig. 11. Tables 5 and 6 list the metabolic pathways, extracted from the KEGG database, that affected by the *Sod-null* mutation and paraquat induced stress, respectively. An overall, simplified, metabolome view of metabolites detected and altered in levels is represented in Fig. 12. A colour gradient represents the metabolite levels in stressed samples compared to controls (Fig. 11). Figures 11 and 12 highlight the conclusions that both the *Sod-null* allele and paraquat treatment result in substantial changes to the metabolome, and that each source of oxidative stress results in distinct responses to metabolite and affected pathways.

Table 4: Summary of metabolomic comparisons

Stress	Total Features	Significantly different features	Features of known structure	Significantly different known compounds	Significant shared responses	Significant opposite responses
Sod-null	594	168 (28%)	55	36	23	17
Paraquat	459	59 (13%)	45	17		

3.3.5 Glutathione metabolism and related pathways

Glutathione metabolism was similarly affected by genetic and chemically induced stress (Fig. 12; pathway 19). The relative concentration of oxidized glutathione (GSSG) was higher in both sources of oxidative stress compared to controls (*Sod-nulls*: $P<1x10^5$; PQ: $P(0.02696)$). The reduced form of glutathione (GSH) was not affected by the *Sod-null* genotype ($P(0.95)$), however there was a significant 1.31 fold increase in PQ treated flies ($P<1x10^5$). Glutamate, a precursor to glutathione synthesis, was not altered in response to either stress. Cysteine, another precursor to glutathione, was not altered in response to the *Sod-null* stress, but was undetectable in PQ induced stress experiment. The mass of glycine, a precursor to glutathione, falls below the detectable scope of this study.

3.3.6 Glutamine and purine metabolism

The amino acid glutamate is involved in several pathways including conversion into glutamine (Fig. 12; pathway 5 & 23). The relative concentration of glutamine is increased in both genetically (1.42 fold: $P<1x10^5$) and chemically (1.90 fold: $P<1x10^5$) generated OS. Glutamine is also involved in purine metabolism (pathway 18), a pathway largely affected by the *Sod-null* mutation, but not paraquat treatment. Adenosine monophosphate (AMP) ($P<1x10^5$), adenosine triphosphate (ATP) ($P(0.01047)$), and urate ($P(0.00724)$), metabolites in the purine metabolism pathway, were reduced in *Sod-nulls* compared to controls.

3.3.7 Pantothenate and CoA biosynthesis

Pantothenate concentration was consistently lower in *Sod-nulls* (2.1 fold: $P<1x10^5$) and in PQ treated flies (1.83 fold: $P<1x10^5$), than in controls, suggesting this compound may be an appropriate general biomarker for oxidative stress in flies. Coenzyme A (CoA) was also reduced in *Sod-nulls* by a factor of 1.2 (*P*(0.00855)), while it remained undetected in paraquat treated flies. One downstream metabolite product of the pantothenate and CoA biosynthesis pathway with several functions is acetyl-CoA, which was reduced in *Sod-nulls* (1.37 fold: *P*(0.0136)), and undetected in the PQ comparison.

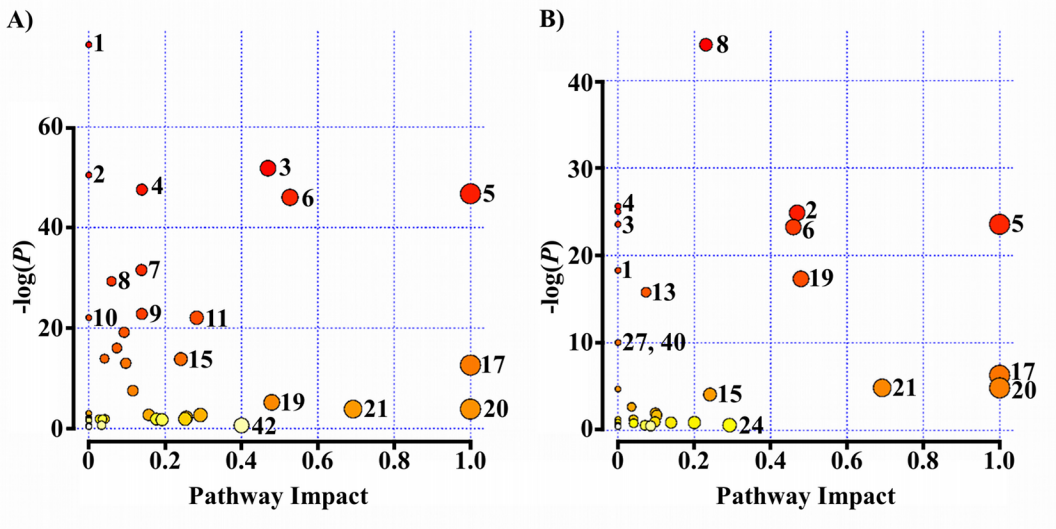

Figure 11: Predicted impact and significance of metabolic pathways in A) *Sod-null* and B) Paraquat treated flies

3.3.8 Changes to amino acid concentrations

The two sources of OS both affected the concentrations of amino acids in in *D. melanogaster* (Appendices E and F). Chemically and genetically driven OS impacted amino acid metabolism, however the effects that each stress had on amino acid metabolism were different (Tables 5 and 6). *Sod-null* flies had significantly higher concentrations of arginine (*P*(0.00001)), methionine ($P<1x10^5$), ornithine (0.00289), threonine ($P<1x10^5$) and valine (*P*(0.00074)), compared to control flies. PQ treated flies had higher concentrations of lysine (*P*(00063)) and tyrosine (*P*(0.00074)) compared to controls, while phenylalanine (*P*(0.01427)) was detected at lower concentrations. In both sources of OS, asparagine (*Sod-nulls*: *P*(0.00026; PQ: *P*(0.00483)) and

glutamine (*Sod-nulls*: $P<1x10^5$; PQ: $P<1x10^5$) concentrations were elevated, while histidine (*Sod-nulls*: *P*(0.00001); PQ: *P*(0.00179)) and proline (*Sod-nulls*: *P*(0.01899); PQ: *P*(0.00318)) concentrations were reduced. The concentration of (iso)leucine (*P*(0.0028)) was elevated in *Sod-nulls*, in contrast to PQ treated flies where (iso)leucine concentration was reduced (*P*(0.00048)).

Table 5: Pathway analysis of *Sod-null* genotype

	Pathway	Total Compounds	Hits	Raw p	-log(*P*)	Holm adjust	FDR	Impact
1	Pantothenate and CoA biosynthesis	12	1	6.78E-34	76.374	3.05E-32	3.05E-32	0
2	Arginine and proline metabolism	37	5	3.20E-23	51.796	1.41E-21	7.20E-22	0.46944
3	Nitrogen metabolism	7	2	1.24E-22	50.439	5.35E-21	1.87E-21	0
4	Pyrimidine metabolism	41	3	2.28E-21	47.53	9.58E-20	2.57E-20	0.13888
5	D-Glutamine and D-glutamate metabolism	5	3	5.17E-21	46.711	2.12E-19	4.65E-20	1
6	Alanine, aspartate and glutamate metabolism	23	6	1.05E-20	46	4.21E-19	7.90E-20	0.52703
7	Aminoacyl-tRNA biosynthesis	67	12	2.01E-14	31.538	7.84E-13	1.29E-13	0.13793
8	Pentose phosphate pathway	19	1	1.89E-13	29.297	7.18E-12	1.06E-12	0.05931
9	Amino sugar and nucleotide sugar metabolism	34	2	1.25E-10	22.802	4.63E-09	6.25E-10	0.13889
10	Valine, leucine and isoleucine biosynthesis	13	1	2.67E-10	22.045	9.60E-09	1.10E-09	0
11	Glycine, serine and threonine metabolism	25	2	2.69E-10	22.035	9.60E-09	1.10E-09	0.2825
12	Cysteine and methionine metabolism	25	2	4.82E-09	19.15	1.64E-07	1.81E-08	0.09236
13	Starch and sucrose metabolism	17	2	1.11E-07	16.009	3.68E-06	3.86E-07	0.07338
14	Glycerolipid metabolism	16	1	9.26E-07	13.893	2.96E-05	2.98E-06	0.04096
15	Tyrosine metabolism	30	2	1.01E-06	13.809	3.12E-05	3.02E-06	0.24096
16	Glycerophospholipid	27	2	2.28E-06	12.993	6.83E-05	6.40E-06	0.09682

	Pathway	Total Compounds	Hits	Raw p	-log(*P*)	Holm adjust	FDR	Impact
	metabolism							
17	Histidine metabolism	7	2	3.34E-06	12.61	9.68E-05	8.83E-06	1
18	Purine metabolism	64	6	0.0005358 7	7.5316	0.015004	0.001339 7	0.11528
19	Glutathione metabolism	26	6	0.0055828	5.1881	0.15074	0.013222	0.4794
20	Phenylalanine, tyrosine and tryptophan biosynthesis	4	2	0.021147	3.8562	0.54983	0.045316	1
21	Phenylalanine metabolism	10	2	0.021147	3.8562	0.54983	0.045316	0.69231
22	Riboflavin metabolism	7	1	0.050198	2.9918	1	0.10268	0
23	Citrate cycle (TCA cycle)	20	4	0.066843	2.7054	1	0.12927	0.15712
24	Nicotinate and nicotinamide metabolism	9	2	0.068946	2.6744	1	0.12927	0.29231
25	Fatty acid metabolism	38	2	0.11241	2.1856	1	0.19276	0.25512
26	Butanoate metabolism	21	4	0.1211	2.1111	1	0.19276	0
27	Lysine degradation	17	2	0.14734	1.915	1	0.19276	0
28	Fatty acid elongation in mitochondria	27	1	0.15161	1.8864	1	0.19276	0.2522
29	Glycolysis or Gluconeogenesis	25	1	0.15161	1.8864	1	0.19276	0.04208
30	Valine, leucine and isoleucine degradation	35	1	0.15161	1.8864	1	0.19276	0.0357
31	Fatty acid biosynthesis	38	1	0.15161	1.8864	1	0.19276	0.02717
32	Synthesis and degradation of ketone bodies	5	1	0.15161	1.8864	1	0.19276	0
33	Tryptophan metabolism	23	1	0.15161	1.8864	1	0.19276	0
34	Inositol phosphate metabolism	24	1	0.15161	1.8864	1	0.19276	0
35	Terpenoid backbone biosynthesis	13	1	0.15161	1.8864	1	0.19276	0
36	Fructose and mannose metabolism	18	1	0.15421	1.8695	1	0.19276	0.17705

	Pathway	Total Compounds	Hits	Raw p	-log(*P*)	Holm adjust	FDR	Impact
37	Sphingolipid metabolism	18	2	0.16179	1.8215	1	0.19677	0.03571
38	Pyruvate metabolism	24	2	0.17452	1.7457	1	0.20137	0.19182
39	Glyoxylate and dicarboxylate metabolism	16	2	0.17452	1.7457	1	0.20137	0
40	Biotin metabolism	5	1	0.20033	1.6078	1	0.22537	0
41	Propanoate metabolism	18	2	0.52684	0.64086	1	0.57247	0.03333
42	Methane metabolism	9	1	0.54702	0.60326	1	0.57247	0.4
43	Cyanoamino acid metabolism	6	1	0.54702	0.60326	1	0.57247	0
44	Porphyrin and chlorophyll metabolism	23	1	0.56942	0.56314	1	0.58236	0
45	Ubiquinone and other terpenoid-quinone biosynthesis	3	1	0.68549	0.37762	1	0.68549	0

Table 6: Pathway analysis of paraquat induced stress.

	Pathway	Total Compounds	Hits	Raw p	-log(*P*)	Holm adjust	FDR	Impact
8	Pentose phosphate pathway	19	2	7.05E-20	44.099	2.54E-18	2.54E-18	0.23048
4	Pyrimidine metabolism	41	1	7.31E-12	25.641	2.56E-10	1.32E-10	0
7	Aminoacyl-tRNA biosynthesis	67	10	1.38E-11	25.004	4.70E-10	1.42E-10	0
2	Arginine and proline metabolism	37	5	1.58E-11	24.872	5.21E-10	1.42E-10	0.46944
5	D-Glutamine and D-glutamate metabolism	5	2	5.86E-11	23.56	1.88E-09	3.52E-10	1
3	Nitrogen metabolism	7	2	5.86E-11	23.56	1.88E-09	3.52E-10	0
6	Alanine, aspartate and glutamate metabolism	23	5	8.04E-11	23.244	2.41E-09	4.14E-10	0.45946
1	Pantothenate and CoA biosynthesis	12	1	1.14E-08	18.287	3.31E-07	5.14E-08	0
19	Glutathione metabolism	26	5	3.01E-08	17.319	8.43E-07	1.20E-07	0.4794
13	Starch and sucrose metabolism	17	2	1.39E-07	15.791	3.74E-06	4.99E-07	0.07338
27	Lysine degradation	17	1	4.38E-05	10.035	0.0011392	0.00013145	0
40	Biotin metabolism	5	1	4.38E-05	10.035	0.0011392	0.00013145	0
17	Histidine metabolism	7	2	0.0018535	6.2907	0.044484	0.0051328	1
20	Phenylalanine, tyrosine and tryptophan biosynthesis	4	2	0.0078395	4.8486	0.18031	0.018815	1
21	Phenylalanine metabolism	10	2	0.0078395	4.8486	0.18031	0.018815	0.69231
45	Ubiquinone and other terpenoid-quinone biosynthesis	3	1	0.0089931	4.7113	0.18886	0.020235	0
15	Tyrosine metabolism	30	2	0.016711	4.0917	0.33422	0.035388	0.24096
37	Sphingolipid metabolism	18	1	0.068977	2.674	1	0.13795	0.03571
25	Fatty acid metabolism	38	1	0.14081	1.9603	1	0.2668	0.09789
18	Purine metabolism	64	5	0.1797	1.7165	1	0.32346	0.10119
11	Glycine, serine and threonine metabolism	25	1	0.28987	1.2383	1	0.47433	0.04054
10	Valine, leucine and isoleucine biosynthesis	13	1	0.28987	1.2383	1	0.47433	0
16	Glycerophospholipid metabolism	27	2	0.38268	0.96054	1	0.57515	0.09682
41	Propanoate metabolism	18	1	0.39389	0.93169	1	0.57515	0

	Pathway	Total Compounds	Hits	Raw p	-log(*P*)	Holm adjust	FDR	Impact
9	Amino sugar and nucleotide sugar metabolism	34	2	0.41309	0.88409	1	0.57515	0.13889
36	Fructose and mannose metabolism	18	2	0.41538	0.87855	1	0.57515	0.2
14	Glycerolipid metabolism	16	1	0.44915	0.8004	1	0.59886	0.04096
24	Nicotinate and nicotinamide metabolism	9	1	0.55702	0.58516	1	0.64815	0.29231
44	Porphyrin and chlorophyll metabolism	23	1	0.56131	0.57748	1	0.64815	0
23	Citrate cycle (TCA cycle)	20	2	0.56661	0.56809	1	0.64815	0.07086
26	Butanoate metabolism	21	2	0.60712	0.49903	1	0.64815	0
22	Riboflavin metabolism	7	1	0.60832	0.49706	1	0.64815	0
29	Glycolysis or Gluconeogenesis	25	1	0.61214	0.4908	1	0.64815	0.0855
34	Inositol phosphate metabolism	24	1	0.61214	0.4908	1	0.64815	0
38	Pyruvate metabolism	24	1	0.65503	0.42307	1	0.65503	0
39	Glyoxylate and dicarboxylate metabolism	16	1	0.65503	0.42307	1	0.65503	0

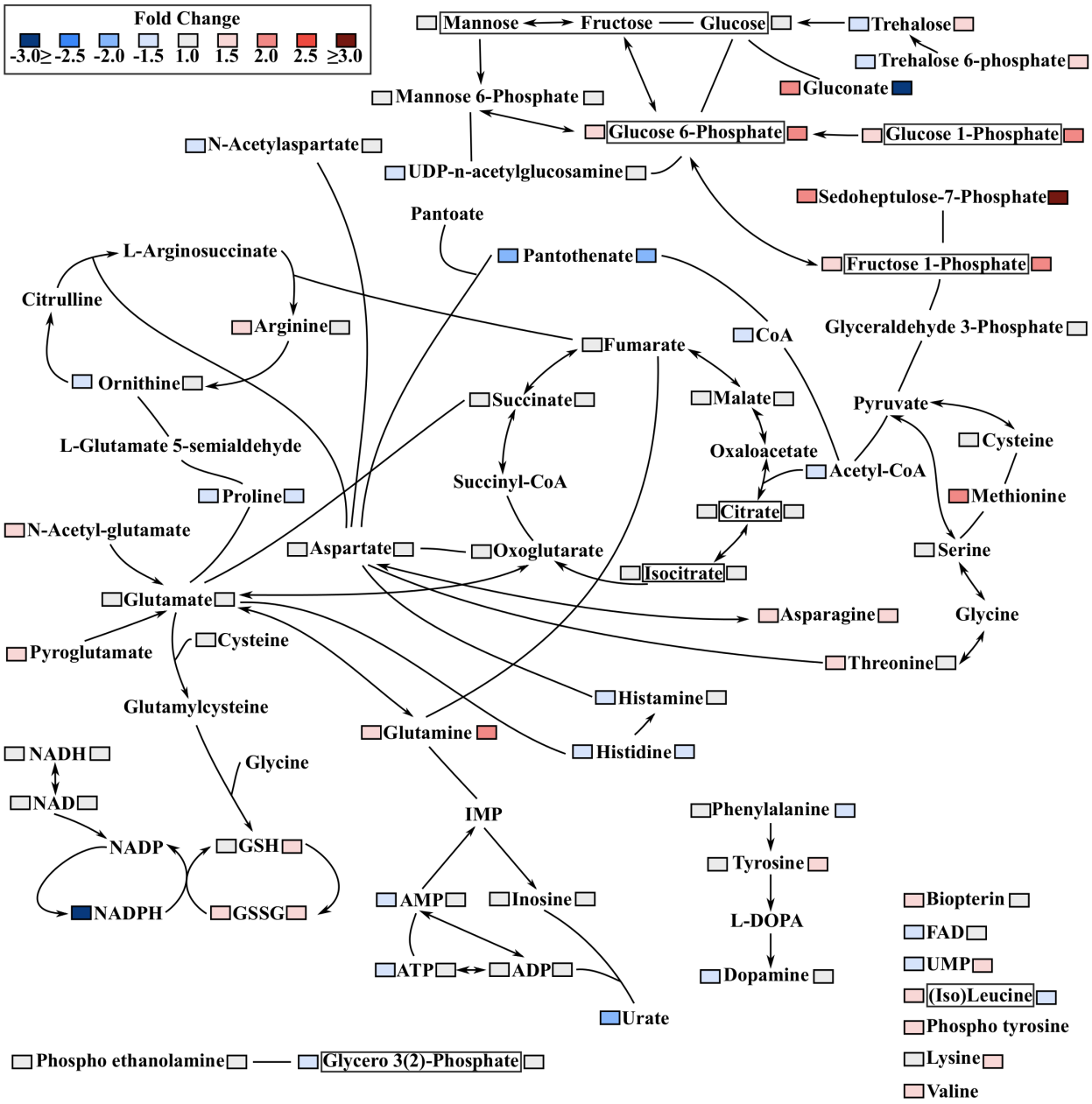

Figure 12: Simplified metabolic architecture of *Sod-null* and paraquat induced stress. Colour-coded box to the left of the metabolite corresponds to the *Sod-null* vs. control comparison and the box on the right corresponds to the paraquat treated vs. control comparison. Metabolites surrounded by a box indicate the metabolite is an isomeric compound that cannot be distinguished from other isomer forms. Metabolites without a colour-coded box on one side, or both, were not detected in the respective analyses. Lines with arrows indicate direction and

single enzyme conversion between two metabolites. Lines without arrows indicate multi-step conversion to connected metabolites.

3.4 Discussion

3.4.1 Oxidative stress leads to changes in the metabolic profile of *Drosophila melanogaster*

OS is a degenerative condition and in humans is associated with several diseases and pathologies including cardiovascular disease (Dhalla et al., 2000), Parkinson's disease (Jenner, 2003), and FALS (Barber and Shaw, 2010). Here, we use the *D. melanogaster* model system to demonstrate substantial changes in the metabolic profile in response to OS arising from two sources of OS: a *Sod-null* genotype and a chemical oxidant. Considering the breadth and magnitude of physiological and biochemical changes that both these stresses confer (Bernard et al., 2011; Hosamani and Muralidhara, 2013; Parkes et al., 1998b; Phillips et al., 1989), metabolic changes were expected, however, changes in the measured metabolome of up to 28% were surprising.

Sod knock-out/null alleles and paraquat have been used as models of oxidative stress and disease states in a variety of organisms (Van Raamsdonk and Hekimi, 2009; Sentman et al., 2006; Wei et al., 2001). Relatively little is known about global metabolomic response to OS in *D. melanogaster*, although we do have a better understanding of the metabolomic effects in other model species, including human cells and mice (Ho et al., 2013; Jozefczuk et al., 2010; Weeks et al., 2006). The suite of metabolites that are significantly altered by either source of OS in our models are interesting both in the unique features and in the features that are shared with other sources of oxidative stress.

3.4.2 Glutathione metabolism

The *Sod-null* mutation and PQ exposure lead to changes to glutathione metabolism (Fig. 11, pathway 19). Glutathione is a major anti-oxidant source in most cells; its reduced form (GSH) reacts with ROS, and substrates oxidized by ROS, to generate the oxidized form (GSSG) (Owen and Butterfield, 2010). The GSH/GSSG ratio is considered an indicator of cellular health and

decreases in the GSH/GSSG ratio have been observed in other studies of OS and OS related diseases (Bogdanov et al., 2008; Ho et al., 2013; Serkova et al., 2006; Tissot van Patot et al., 2009). Decreases in GSH levels as a result of OS, have been demonstrated to increase levels of pyroglutamate (Pederzolli et al., 2007a), a metabolite involved in glutathione metabolism. Although we do not detect decreases in GSH in *Sod-nulls*, we did observe increased levels of pyroglutamate, suggesting increased production of this compound, possibly to increase availability for protection from OS. The lack of change in GSH may reflect increased GSH synthesis, although two of the precursors, glutamate and cysteine, were not detected at different levels between conditions. To maintain the available GSH needed to reduce ROS, GSSG may be cycled back to GSH using the reducing power of NADPH, which may partly explain the observed large decrease in NADPH.

Glutathione metabolism was also affected by chronic PQ exposure, although to a different extent. GSSG levels were also elevated in PQ exposed flies, reflecting the *Sod-null* model and underscoring the importance of GSSG as a marker of oxidative stress. In PQ induced stress, glutamate, a precursor used in glutathione synthesis, was not different between samples. In contrast to the *Sod-null* analysis, GSH was detected at higher concentrations. The differences in the concentrations of GSH and GSSG between each stress may be attributed to the different standing concentrations of different ROS present in each stress.

3.4.3 NADPH, the pentose phosphate pathway, and glucose metabolism

NADPH, which functions in the reduction of GSSG back to GSH, is an important cofactor involved in many cellular processes and our observation of reduced concentrations in *Sod-nulls* is consistent with previous studies in the Merritt lab (Bernard et al., 2011). Glucose 6-phosphate dehydrogenase (G6PDH), 6-Phopshogluconate dehydrogenase (6PGDH), NADP-Isocitrated dehydrogenase (IDH), and malic enzyeme (ME) are involved in central metabolism and the pentose phosphate pathway, and are largely responsible for the reduction of NADP to NADPH. G6PDH, IDH, and ME have lower activities in *Sod-nulls* under benign conditions (Bernard et al., 2011). These lower activities likely contribute to the lower NADPH concentration we observe. In addition, NADPH is likely being consumed in recycling GSSG. Sedoheptulose 7-phosphate, an intermediate in the pentose phosphate pathway, was increased in both stresses. The increase

of sedoheptulose 7-phopshate in both stresses highlights this molecule as a possible marker of OS and reinforces the notion that OS affects the pentose phosphate pathway. Overall, the previous study of this *Sod-null* in the Merritt lab found a general reduction in many enzymes involved in central metabolism (Bernard et al., 2011). The current metabolomics study finds alterations to central metabolism and the pentose phosphate pathway, consistent with this pattern of reduced metabolic activity in the *Sod-null* flies (Table 5; Pathways 8, 23, & 29).

Sugar and sugar phosphates are important metabolites involved in central metabolism and the pentose phosphate pathway. Despite alterations to pathways 8, 9, 13 and 29 (Fig. 11), the combined sum of all hexoses was not significantly affected by either of the two sources of oxidative stress. A balance between synthesis and catabolism of gluconate and trehalose 6-phosphate might explain the consistent concentration of hexoses. Gluconate was elevated, and trehalose 6-phosphate was reduced in *Sod-nulls*, while the pattern was opposite in PQ treated flies. Gluconate and trehalose 6-phosphate represent alternative pathways for glucose metabolism and their substantial changes in concentrations, in opposite directions, may balance the synthesis and catabolism of glucose. Trehalose has been observed to have a functional role in protection against OS in *C. albicans* and the protection conferred was observed to be higher under direct OS from hydrogen peroxide as opposed to under oxidative tolerance (Alvarez-Peral et al., 2002). The distinction between tolerance and acute exposure, may underscore the difference seen between our models. While the *Sod-null* model has a reduced ability to remove endogenous superoxide and metabolize it to hydrogen peroxide, treatment with PQ generates exogenous superoxide, in the presence of normal levels of SOD enzyme. It might therefore be expected that the principal imbalance in ROS in the two OS models would be fundamentally different; in the *Sod-null* model superoxide should be elevated and hydrogen peroxide reduced, while in the PQ model the functional SOD should largely remove excess superoxide and generate more hydrogen peroxide.

Despite the well-known effects of oxidative stress on mitochondrial function and energy production (Cheng et al., 2013), we did not detect any variation in metabolite concentrations across the tricarboxylic acid (TCA) cycle in response to either stress. Interestingly, (iso)citrate and oxoglutarate concentrations were not influenced by the *Sod-null* genotype although *Isocitrate dehydrogenase,* responsible for the conversion of isocitrate to oxoglutarate, was

previously described to be reduced in *Sod-nulls* (Bernard et al., 2011). The lack of change in the concentrations of metabolites involved in the TCA cycle that we observe may result from metabolic rewiring geared towards the synthesis of other compounds. The lower FAD concentration that we observe in *Sod-nulls* may result from such a rewiring as succinate dehydrogenase converts succinate into fumarate using FAD as a cofactor. We did not, however, find a reduction in succinate or fumarate in *Sod-nulls*.

3.4.4 Oxidative phosphorylation and purine metabolism

Oxidative phosphorylation, which utilizes FAD(H_2), is responsible for generating adenosine triphosphate (ATP) from adenosine diphosphate (ADP), both high energy molecules with many functions. ATP, ADP, and adenosine monophosphate (AMP), are synthesized *de novo* in the purine metabolism pathway. This pathway can be fed by, or generate, glutamine, and glutamine concentrations were higher in both models of OS. Under various conditions, glutamine can act as a major energy source (Fox et al., 1996; Matés et al., 2002). The low ATP concentrations in the *Sod-null* flies suggest that energy reserves are low in these flies and the higher glutamine concentrations could reflect shunting of metabolic resources to this alternative energy source in the *Sod-nulls*. An alternate explanation for low ATP concentrations may be that under SOD-depleted conditions cellular metabolism is diverted away from energy production, so as to reduce flux through the electron transport chain from which superoxide is inevitably released. Whether glutamine is being funneled towards, or away from, purine metabolism is unclear, but glutamine may be being used to counteract reduced levels of metabolites in purine metabolism. Dysfunction in purine metabolism leads to activation of apoptotic pathways (Holland et al., 2011), and glutamine also plays important roles in the regulation of apoptosis (reviewed in: Matés et al., 2006). The interplay between purine metabolism and glutamine levels may be underlying the response of *D. melanogaster* to OS. Purine metabolism also generates urate, one of the most important anti-oxidants in humans (Liu et al., 2011). The decrease in urate in *Sod-nulls* is likely a result of increases in urate oxidation products, and has previously been described to be decreased under OS conditions in humans (Bogdanov et al., 2008).

3.4.5 Evidence of OS associated neurodegeneration

Both sources of OS resulted in changes in concentrations of metabolites in the pantothenate and coenzyme A (CoA) synthesis pathway (Fig. 11; pathway 1). Pantothenate concentrations were lower in both sources of OS, suggesting that this metabolite may be a general biomarker of OS in flies. The changes of metabolite concentrations in this pathway are consistent with previously reported changes in expression of genes involved in the pantothenate and CoA synthesis pathway (Zou et al., 2000). Zou *et al.* (2000) observed a decrease in acetyl-CoA synthase mRNA required for the synthesis of the enzyme responsible for the production of acetyl-CoA from CoA. Both of these metabolites are reduced in *Sod-nulls*. Acetyl-CoA synthase also produces AMP, a metabolite also decreased in *Sod-null* flies. Dysfunction in the pantothenate and CoA synthesis pathway is implicated in OS associated neurodegeneration (Brunetti et al., 2012). Our results indicating alterations in this pathway in the *Sod-nulls* are thus consistent with earlier work using *Sod-null* alleles as models of neurodegeneration (Elia et al., 1999; Mockett et al., 2003; Parkes et al., 1998b; Phillips et al., 1989; Watson et al., 2008). In addition, previous work has associated loss of SOD activity and OS with the loss of dopaminergic neurons in *D. melanogaster* models of Parkinson's disease (Botella et al., 2008; Neckameyer and Weinstein, 2005). Consistent with these studies, we find lower concentrations of dopamine in *Sod-null* flies, although two of the precursors to dopamine synthesis, phenylalanine and tyrosine, were not affected by the stress. In contrast, PQ treated flies show no reduction in dopamine concentration, but were found to have lower concentrations of phenylalanine, and higher concentrations of tyrosine. Our results across these two pathways reinforce the utility of the *Sod-null* genotype as a model of OS associated neurodegeneration in future studies.

3.4.6 Amino acid metabolism affected by OS

In addition to glutamine several other amino acids, and their associated metabolic pathways, were affected by the *Sod-null* mutation (Fig. 12). Amino acids are not only building blocks for proteins but also have many intracellular roles, particularly under OS. Proline, for example, has diverse anti-oxidant properties, modulates the redox environment, and contributes to the regulation of apoptosis in mammalian cells (Krishnan et al., 2008). Proline concentrations were lower in flies exposed to both sources of OS, possibly because it is being expended for protective

purposes, or being funneled into glutamate synthesis. In contrast to previous studies that document lower levels of arginine in disease related OS (Kochar and Umathe, 2009; Rodrigues Pereira et al., 2010), we find increased concentrations of arginine in *Sod-nulls* and unchanged levels in PQ treated flies. The amino acid histidine has been demonstrated to reduce OS and tumor necrosis factor alpha-induced interleukin-8 secretion, which itself is linked to the pro-oxidant inflammatory response, in intestinal cells (Son et al., 2005). Lower concentrations of histidine may reflect it being expended to reduce OS and inflammation in the *Sod-null* and PQ treated flies. Under OS, *Pseudomonas fluorescens* can repurpose histidine for the formation of the anti-oxidant, 2-oxoglutarate (Lemire et al., 2010), a response that flies under OS may share. Histidine concentrations are lower in *Sod*-nulls and PQ treated flies, possibly, because of demand for the metabolite in OS defense. Histidine can be converted into the neurotransmitter histamine, which was also in lower concentration in *Sod-nulls*. Histamine concentrations may be lower in *Sod-nulls* because of demand in OS defense, a role previously reported for the metabolite in cells supplemented with histamine (Hellstrand et al., 2000; Mahmood et al., 2012). Alternatively, this may be part of a biochemical adaptation promoting dampened neuronal function, reducing the energetic demand for ATP synthesis via the electron transport chain. Concordantly, the amino acid derivative N-acetylaspartate (NAA), which other studies have found to be located primarily in neural tissues (Clark, 1998), was in lower concentrations in *Sod-nulls*. Increased NAA concentrations in mammalian brains results in higher levels of OS (Francis et al., 2012; Pederzolli et al., 2007b). Decreased concentrations in *Sod-nulls* and unchanging concentrations in PQ treated flies may reflect a response to limit other sources of OS.

3.4.7 Conclusions and future directions

The *Sod-null* and PQ models of OS were used in this study as complementary systems to allow us to draw broader conclusions about the metabolomic response to OS. The systems are similar in that they both generate excess concentrations of intracellular superoxide. The systems are different in that in the PQ system the flies have functional SOD and can dismutate the radical to hydrogen peroxide. The concentrations of superoxide or hydrogen peroxide in both systems are not yet known, though the differences in their concentrations may drive the metabolic differences seen between each stress.

In the PQ investigation, we initially screened two other wild-type lines along with the T5 controls line from the *Sod* study. The two wild-type lines were viable in concentrations at least an order of magnitude higher than T5 flies (data not shown). To keep the concentrations consistent between T5 fly lines and wild-type lines, a 0.5 mM concentration was used. This concentration did not elicit broad metabolic differences in the wild-type flies: a PCA could not differentiate between PQ treated wild-types and wild-types under benign conditions (data not shown). Future studies will involve metabolomic analysis of more wild-type lines (genetic backgrounds) under further PQ induced stress. Although T5 control lines were more sensitive to PQ exposure than wild-type lines, the metabolic profiles of T5 flies were similar to wild-type lines under benign conditions (Appendix C). This similarity in metabolic profiles suggests that T5 control flies are good controls for metabolic analysis against the *Sod-null* model.

Future investigations would benefit from an assessment of the contribution of genetic background to the metabolomic response of OS in *D. melanogaster*. Genetic background effects can have substantial impact on the manifestation of genetic lesions or stress responses (reviewed in: Chandler et al., 2012; Gibson and Reed, 2008). The results from this study provide insights into the metabolic response of *D. melanogaster*, however broad based conclusions could only be made once testing across multiple backgrounds can be completed.

In this investigation we describe substantial changes to the metabolic profiles of *D. melanogaster* under genetic and chemical induced OS. Almost a third of the measured metabolome of the *Sod-null* model was altered in response to OS, and 13% of the measured metabolome was altered in flies chronically exposed to PQ. The two sources of oxidative stress resulted in changes to glutamine metabolism, pantothenate and CoA synthesis, and central metabolism, highlighting the role these pathways have in OS. The sources of OS were complementary to each other, however large differences in the metabolic profiles of flies under each stress highlight the general differences in the mechanisms of each stress. Future studies will involve assessments of the role of genetic background on the metabolic profiles of flies under each stress.

Chapter 4

4 General conclusions and future work

We have developed a novel ion-pairing chromatography - mass spectrometry protocol for the resolution, detection, and quantification of biologically relevant, polar, molecules. The newly developed protocol was validated through a reasonably extensive set of assessments including, ion-suppression, matrix effects, linearity, and limits of detection and quantification. Using this protocol the metabolic profiles of a *Sod-null* genotype, paraquat induced stress, and four *Drosophila* species were determined. We found that all components of all three biological systems could be differentiated base on metabolic profiles. Future work will cover two large aspects of this research: the technological and the biological. Currently, our metabolite coverage identifies pieces of networks and processes that are affected by certain conditions. Future technological endeavors will aim to increase the comprehensiveness of our detected metabolites, which will fill in dimensions of networks that are currently incomplete, and provide us with a better understanding of biological implications. The *Sod-null* experiments were performed on one genetic background, and the paraquat experiments on one genotype of the species. Consequently, the metabolic responses observed in Chapters 2 and 3 may not reflect the entire suite of possible OS-induced changes across the species, or may only reflect line specific alterations. Future work will investigate the effect of genetic background on metabolic profiles of *Sod-null* or paraquat induced stress. This chapter will focus on avenues for future work that the current project could not focus on.

4.1 Expanding metabolite coverage

4.1.1 Chromatography: Implications for increased metabolite detection

Mass spectrometry using an ESI source is susceptible to ion suppression by compounds in the solvent and in complex biological matrices (Müller et al., 2002), an issue reviewed in section 1.3. In sections 2.3.2 and 2.3.3 both ion-suppression and matrix effects were determined to influence the signal of molecules in our samples using our protocol. Although these levels of ion-suppression are within acceptable limits (Böttcher et al., 2007; Knee et al., 2013), no amount of ion-suppression is ideal. In targeted analyses with extensive sample preparations, ion-

suppression can virtually be eliminated, however when the goal is comprehensive metabolite coverage, ion-suppression may be inevitable and can only be limited.

The amount of ion suppression may be reduced with an effective chromatographic separation step preceding the mass spectrometer, for example IP-LC. The IPR used in our protocol is effective at forming ion-pairs with negatively charged compounds, however compounds with more positive charges are not resolved. Further, a large proportion of detected compounds in my analyses are found within the first minute of analysis (Fig. 1; Chapter 2). These compounds containing more basic moieties are subject to the highest levels of ion-suppression (section 2.3.3), complicating quantification of molecules in two ways. Firstly, low abundance metabolites will not be detected in some, possibly any, analyses, because ion suppression will result in higher detection limits. Secondly, the amount of ion suppression on a particular metabolite can vary between samples resulting in irreproducible peak areas, and by association, artifacts in statistical tests (Mallet et al., 2004b).

Future endeavors in the Merritt lab will aim to resolve the molecules eluting early in the chromatographic run, effectively reducing, or eliminating, the effects of ion-suppression for these types of molecules. Complementing our positively charged ion-pairing reagent, a negatively charged ion-pairing reagent is a possible direction for future separations. For example, the negative charge from heptafluorobutyric acid (HFBA) has previously been used for analysis of positively charged ionic species, including many poorly retained in our protocol, in LC-MS based metabolomics (Vo Duy et al., 2012; Liu et al., 2013). Negative and positive ionization modes correspond to analytical modes in which different charged species are drawn into a mass spectrometer. During the ESI process, metabolites can be given a positive or negative charge. Each metabolite has different susceptibilities to become negatively, or positively, charged depending on their chemical moieties, solvent pH and ionic strength, and co-eluting molecules. By switching the polarity of the mass spectrometers ion optics, either negative or positively charged species alone are introduced into the mass spectrometer and analyzed. Ion-pairing reagents are undetectable in their respective analysis mode, negative or positive, because of their inability to be ionized in that polarity, but can be detected in the other mode. For example, when a positively charged ion-pairing reagent is used in negative mode it is not detected, but when it is used in positive mode a signal will be seen and could contribute

greatly to ion-suppression and contamination within the mass spectrometer. A negatively charged ion-pairing reagent would complement our analysis, however it would lead to system contamination in both analytical modes, which would be detrimental to analysis in either mode.

A possible alternative to ion-pairing agents for the analysis of polar molecules is the use of HILIC as a separation technology. The multi-modal separation properties of the silanols that make up the stationary phase in HILIC provide a level of versatility that can be used to retain different compounds by using various solvent conditions. The acidity, composition, and presence of modifiers in the solvent can be altered to allow for different interactions amongst neutral, negatively, and positively charged compounds with the stationary phase. This versatility suggests that many of the compounds eluting near the void volume can be analyzed with HILIC either in a complementary protocol or simultaneously with compounds already resolved within our protocol.

The versatility of HILIC can be increased through the addition of various moieties to the stationary phase. For example, having an alkylamide or an sulfoalkylbetaine moiety can add to the different levels of interactions with solvent, additives, and compounds (Buszewski and Noga, 2012). These types of zwitterionic moieties may facilitate the analysis of a wide range of compounds ranging in polarity and pKa because of the interactions between the positive and negatively charged species of the column. In the Merritt lab, our goal is to perform comprehensive analysis, and these column types could provide the versatility we are trying to achieve (Bajad et al., 2006; Bratty et al., 2011; Kamleh et al., 2008).

Broad metabolite coverage could also be achieved using multi-dimensional chromatographic systems (Dixon et al., 2006). Multi-dimensional LC systems apply two or more, independent, orthogonal separations to a sample. The aim of multi-dimensional chromatography is to use one, or multiple, separation techniques orthogonally on a sample that will resolve compounds that could not be resolved by the first dimension of separation. This type of technique is particularly useful in separating complex matrices of compounds with varying chemical properties and has previously been demonstrated to be capable of resolving more features than 1D separation alone (Dixon et al., 2006; Li et al., 2013). Multi-dimensional LC systems require a quaternary pump, capable of pumping four solvents simultaneously, or 2 separate LC systems. Fortunately, for

those without these capabilities, a semi-orthogonal alternative is to use two columns, one immediately preceding the other, which will resolve compounds of varying types (Chalcraft and McCarry, 2013; Davis et al., 2001).

4.1.2 Sample preparation

In the previous section, I described how efficient chromatography could reduce the amount of ion-suppression during analysis, however there are several endogenous substances that can be removed prior to separation to also reduce ion suppression. Metabolite extractions have different amounts of ion suppressing compounds depending on the solvent conditions and can also vary between extractions (Annesley, 2003). In general, these substances are poorly retained on columns, or the manner in which they interact with the column generates long, asymmetrical, elution profiles (Müller et al., 2002). Untargeted approaches such as ours aim to analyze the widest set of metabolites possible and in effort to avoid losing metabolites through various sample clean-up procedures, minimal sample preparation is performed. This limited-processing approach leaves a maximum of possible metabolites in the homogenate, but the simple protein precipitation procedure also leaves other substances such as salts and phospholipids in the homogenate, which may contribute to ion suppression (Annesley, 2003). It is possible that in our effort to avoid the loss of metabolites, ion suppression effects may have muted the signals of some metabolites, counteracting our goal of comprehensive metabolite analysis.

There are several commercially available sample preparation options that may be explored in the future. These options generally include a solid phase extraction (SPE) mechanism. SPE is essentially a preparative chromatography step that combines size exclusion and chromatographic principles to remove protein and debris and also various types of other compounds. Commercial SPE cartridges have been available since the late 1970's with a wide variety of sorbent materials (Hennion, 1999). SPE can be automized and even be included "on-line" (Negreira et al., 2013), meaning cleaning of the sample can be performed within a chromatographic run. Specialized equipment is required for automation and on-line capabilities, but a moderately high-throughput option is to use a 96-well plate format. The 96-well plate format options also require lower volumes of solvents, an important consideration when working with the small sample masses characteristic of *Drosophila melanogaster*, although the required volumes are larger than the

ones used in this thesis. A hindrance encountered with initial sample preparation protocols was the inability to evaporate/concentrate our samples, which made SPE impractical. A newly acquired vacuum concentrator in the Merritt lab has now removed this hindrance and work is currently underway to use higher extraction volumes and SPE, which can then be concentrated for LC-MS analysis.

Amongst the wide variety of SPE sorbent types, ion exchange SPE and phospholipid specific SPE are the most probable candidates for future use in the Merritt lab. Ion exchange based SPE has been successfully applied to remove protein and phospholipids from samples (Negreira et al., 2013). Ion exchange could also be used to remove the early eluting compounds from our ion-pairing protocol, which would leave the negatively charged polar compounds in the analysis. The positively charged compounds isolated from ion exchange could also be fractioned for analysis using a complementary method to the method developed in this thesis. This type of SPE would remove one type of charged species while allowing for the analysis of another and could be useful in the ion-pairing protocol. Removal of compounds would, however, conflict with our final goal of comprehensive metabolomics, particularly if a chromatography protocol is developed which separates compounds of acidic, basic, and neutral properties.

Alternatives to a classical mode of SPE include any of the several phospholipid specific removal SPE techniques. Three examples of formats specifically designed for the removal of phospholipids are Waters Ostro™ (Waters Corporation), HybridSPE™ (Supelco Analytical, Sigma Aldrich), Phree™ (Phenomenex). Each manufacturer claims these formats remove virtually all phospholipids while yielding high recovery of metabolites. A metabolite recovery, matrix effect, and cost analysis would need to be performed on these technologies if utilized. These types of SPE are designed to be specific to phospholipids, but it is likely that some other compounds may have an affinity to the sorbent, and be lost for analysis.

Sample clean-up techniques such as SPE remove large macromolecules, which can shorten column lifetimes. An alternative method to remove large macromolecules from biological samples is the use of centrifugal filters (Wang et al., 2003), which work on a simple size exclusion principle. This technique would remove large particulate matter that can lead to column blockage, however endogenous substances such as salts and phospholipids would

remain. Centrifugal filters are meant as a size exclusive mechanism, however any surface would have some affinity to some compounds and it has been demonstrated that centrifugal filters do lead to poor recovery of certain types of compounds (Elhamili et al., 2011).

In conclusion, sample preparation is a critical step in LC-MS analysis that is sometimes overlooked and can have large impacts on an analytical run. Our sample analyses would benefit from lower levels of ion suppression and our UHPLC columns would have longer lifetimes. Implementing one of the potential cleaning methods would require each one to be assessed, which would have a time and financial commitment, but may provide long-term benefits.

4.1.3 Broadening the scope of mass analyzer

We have developed a simple protocol for the metabolic profiling of *D. melanogaster* and have successfully applied it to three biological systems. In these three systems, the ion guides are optimized for compounds between 100-850 Da. This mass range could potentially cover thousands of metabolites, however there are several metabolites that are of particular interest in the Merritt lab, for example pyruvate and glycine, which are below this mass range. Previous work in the Merritt lab has focused on NADP reducing enzymes including Malic enzyme, which catalyzes the conversion of malate to pyruvate (Lum and Merritt, 2011; Rzezniczak and Merritt, 2012; Rzezniczak et al., 2012). Pyruvate is an important metabolite to analyze, particularly in a Malic enzyme knock-out, but we have not yet been able to quantify it. Current work is under way to expand the mass range to approximately 50-1000 Da, which will generally cover the metabolites we are interested in quantifying. The mass range used in this thesis was selected in an effort to achieve the highest sensitivity and broadening the range of masses we can analyze may also results in a decrease in sensitivity. Initial screening does suggest, however, that the proposed expansion of mass range will have limited effects on sensitivity. Analyzing a broader mass range will give us more complete picture of metabolism and aid in further understanding the processes affected by our systems.

4.2 Expanding biological significance

4.2.1 Genetic background and oxidative stress

The work described in this thesis provides a more complete understanding of the pleiotropic effects of a *Sod-null* allele generated decades ago. Metabolic rearrangements could have different phenotypic manifestations depending on the genetic background, therefore the general applicability of this study to oxidative stress, SOD deficient animals, or even *D. melanogaster*, is currently unknown. It has been demonstrated that *Sod-null* flies are subject to oxidative DNA damage (Woodruff et al., 2004), which may alter the overall genotype of the flies. Coupled with years of rearing in laboratory conditions and a hypothetical acclimatization to oxidative stress, the flies we studied are most likely a unique genetic system with a unique metabolic profile. We see striking differences between the altered metabolomes of the homologous *Sod-null* condition and those resulting from paraquat exposure in T5 control flies. These differences may reveal underlying cellular responses to the type and amount of oxidative stress these sources cause, and highlight the importance of investigating multiple sources of oxidative stress. A more complete picture of the general effects of loss of SOD activity will require varying levels and sources of oxidative stress, along with screening of multiple genetic backgrounds.

Drosophila melanogaster is a metropolitan species of fruit fly with a wide range of habitat, from tropical African rainforests to the boreal forest of Northern Ontario. Previous studies that have isolated *D. melanogaster* lines from different geographic locations documented large amounts of genetic variation between populations (Lachance and True, 2010; Oakeshott et al., 1984). Individual chromosomes that have originated from a certain location and that have a unique genomic structure are considered a genetic background. Wild type individuals have a range of genetic differences that confer a genetic potential that may only manifest when subject to a genetic lesion or stressor, potentially affecting the phenotypic response of the lesion or stress (Gibson and Reed, 2008). It is thus important to consider genetic background in any study involving a stress or genetic perturbation that results in a specific phenotype.

The concept of genetic background is an often overlooked aspect in various studies, however it can have large implications on the validity of a biological observation. For example, it has been demonstrated that the *scalloped*^{E3} wing mutant phenotype results in a variety of changes to wing

shape depending on the genetic background it is in (Dworkin et al., 2009). In this wing system, without prior knowledge of the genetic lesion, one could come to the conclusion that the different visible wing mutations are different genetic mutations, instead of the same mutations in different backgrounds. Genetic background effects also contribute to changes in functional genomic studies. Levels of transcripts and proteins can vary between the same species depending on genetic background (Sarup et al., 2011; Zhong et al., 2012). In most cases, there will be a lower number of significantly different features that are shared across all genetic backgrounds compared to the number of changes that appear to be background specific (Sarup et al., 2011).

Broad metabolic differences driven by different genetic backgrounds and external factors have hindered the widespread usage of LC-MS based screening for biomedical purposes (Johnson and Gonzalez, 2012). Human studies account for some variation in genetic background and environment depending on the level of random sampling, however this is often not enough to make broad based conclusions about the species as a whole. To give an example, a thorough investigation of 262 clinical samples was performed to discover biomarkers for the progression of benign, localized, and metastatic cancer progression (Sreekumar et al., 2009). Over 1000 common features were detected in this analysis, but even through the quite different pathophysiological conditions, only six metabolites were detected at significantly different levels between each stage of disease. In this investigation, the metabolite sarcosine was the most promising candidate for biomarker diagnosis and further genetic and cell invasion implications were investigated (Sreekumar et al., 2009). Two independent follow-up studies from Germany and The People's Republic of China attempted to replicate the results from Sreekumar *et al*. (2009). Using complimentary MS based techniques, the follow-up studies did not find a significant role for sarcosine as a biomarker for prostate cancer progression (Jentzmik et al., 2010; Wu et al., 2011). Whether the differences in metabolome between each study were driven by genetic background, environment, or a combination of both, is unknown, however these types of differences in the results of functional genomic studies highlight the need to look across different genetic backgrounds.

In model species such as *D. melanogaster* where there is the possibility of making lines virtually isogenic, it is especially important to consider the effects of genetic variation when studying key

metabolic processes. One of the major advantages of working with *Drosophila* is the ease of rearing and acquiring sample numbers, which makes accounting for genetic variation relatively simple. Genetic background effects often present themselves when an organism is subject to a stress or test condition, and these types of effects are referred to as cryptic genetic variation (reviewed in: Gibson and Reed, 2008). Cryptic genetic variation has been observed to affect the metabolic profiles of long lived *D. melanogaster* (Sarup et al., 2012), which has implications in the metabolic studies in the Merritt lab.

The metabolic response to oxidative stress in *D. melanogaster* may also be affected by genetic background variation. The Merritt lab is currently exploring possibilities to assess the variation in metabolomic signals in *D. melanogaster* as a result of oxidative stress. The *Sod-null* and the T5 transgenic control model are proving a difficult model to test for background effects. The native wild type copy of *cytosolic Superoxide dismutase* is located on the third chromosome, while the transgene inserted into the T5 line is located on the second chromosome (Parkes et al., 1993). Generally background, or chromosome, replacements, whereby entire chromosomes can be replaced with another, can be performed to add genetic variation to a model (Lum and Merritt, 2011; Rzezniczak and Merritt, 2012). However, since the *Sod* null allele and the *Sod* rescue transgene are on different chromosomes, changing any chromosome will make the models different and the transgene could no longer serve as a control. For this type of added variation to function double chromosomal replacements must be performed, or a method for transferring the transgene to the third chromosome may be performed.

A simpler way to add genetic variation to our study is by generating, via an alternative mutagenesis, a different SOD deficient fly and subsequent chromosomal replacement. Work is currently underway to generate knock-out alleles through *P*-element mutagenesis. *P*-element mutagenesis uses excision of mobile genetic elements inserted near a gene of interest to create local chromosomal lesions (Hummel and Klämbt, 2008). Fly lines with a *P*-element inserted near a gene of interest, but missing the transposase gene, the gene product that is required for *P*-element mobilization, are obtained from stock centers. *P*-element lines can be crossed with a line that contains a transposase source, which will mobilize the *P*-element. *P*-elements excise from the genome and at a low, but appreciable frequency, and take with them random segments of DNA flanking the element. Most alleles are repaired using the sister chromosome as a

template, generating 100%, "normal" or wild-type, activity alleles. When repair is not perfect the gene products can have altered activities, including reduced, increased or knocked-out activity alleles. Once created, *P*-element excision derived alleles can be established as individual lines. A suite of different alleles, differing in the genomic lesion, and in gene activity, can be collected and established as independent lines. This set would consist of control alleles ("normal" activity) and knock-down alleles, all of which are isogenic except for the small mutation at the excision site. These isogenic sets are then good models for experimental comparisons with virtually no genetic variation. To introduce controlled genetic variation, a homozygous *P*-element mutated fly can be mated with a fly of a different genetic background to create heterozygous flies that can be experimentally tested (Rzezniczak and Merritt, 2012). Unfortunately, not all *P*-element insertions are in a region of a gene whose deletion will generate alleles of interest and some complete knock-outs are non-viable, *i.e.* not all *P*-element excisions result in change of activity mutations (Hummel and Klämbt, 2008). Currently, the Merritt lab is attempting to generate such a matched set for *Sod*, but only one *P*-element is line is publicly available and, so far, this line has failed to produce knock-out excisions.

Finally, RNA interference (RNAi) may be a viable option for generating activity variant flies. RNAi induced suppression can be used to create, a suite of activity variant flies and has successfully been applied to generate SOD2 (the mitochondrial *Sod* locus) silenced flies (Kirby et al., 2002). A possible downside to this particular technique is that almost all genes have internal sequences with sequence similarity to other genes, meaning that RNAi may down-regulate many off-target sites (Seinen et al., 2010). Despite the possibility of off-target deregulation RNAi is a commonly used technique for altering gene activity and *Sod1* RNAi lines are available at the Vienna Drosophila RNAi Center (Transformant IDs: 31551 and 108307).

4.2.2 Paraquat induced stress and genetic background

In my thesis research, transgenic rescue control lines (T5) were treated with paraquat and then subject to LC-MS analysis. This is the first study that takes a broad based metabolomics approach to observe changes in metabolite levels after paraquat administration. Our results indicate that paraquat has a broad biological and metabolomic effect. We observed many changes to the metabolic profile of paraquat-induced stress. These observations bring us closer to

understanding the metabolic impact of oxidative stress. In this investigation, as in the *Sod-null* comparison, the importance of genetic background was not thoroughly assessed. Two separate fly lines, VT83 and 6326, were used to allow us to draw some general (*i.e.* not simply line-specific) conclusions about the metabolic impact of paraquat induced stress. T5 flies were included in this screen because they act as the wild-type controls for *Sod-null* flies. Because paraquat concentration had to be kept low to allow inclusion of the T5 control (which only has 60% SOD activity), neither wild-type line showed strong paraquat responses. This study did add another level of understanding past the use of a *Sod-null* allele alone, however more can be done in the future.

Testing genetic background effects on the metabolomic response to paraquat treatment is simpler than testing those effects in the *Sod-null* system. 6326 and VT83 lines were viable in concentrations of at least 5 mM paraquat, while T5 lines were only viable in a maximum of 0.5 mM paraquat. The low level of paraquat used was not sufficient to observe substantial changes to the metabolic profiles of the wild type lines. A first step in future studies with paraquat would simply be an assessment of the maximum paraquat concentration in which 6326, VT83, and a sample of isofemale lines from the wild, survive. Based on the response of the T5 lines to paraquat at their maximum tolerance level, this assessment at near-lethal concentrations of paraquat should elicit broad physiological and metabolomic changes in wild-type flies. Using multiple lines would also provide us a better understanding of what metabolic differences are altered in a genetic background specific manner, and which metabolite responses are shared across the backgrounds. Considering the genetic variation across multiple lines, there would most likely be a wide range of maximum concentrations in which the lines are viable. A concentration of paraquat in which a 50% decrease in viable adults is observed can be used to maintain a similar impact to all fly lines.

4.2.3 Species-specific metabolic profiles

As part of this thesis, I performed an exploratory investigation of species-specific metabolic profiles (Knee et al., 2013). There were substantial differences in the levels of metabolites in each species allowing the metabolic profiles to be resolved using PCA or heat maps. There is also evidence that within species metabolic profiles differ enough to resolve different isofemale

lines (Fig. 7). This experiment was designed as a proof-of-principle pilot study and though it did indicate a number of interesting features, future work is required for a better understanding of species-specific metabolomics.

The largest limitation to this study was the small sample sizes used in the analysis: four samples of each isofemale line. I included three wild-caught isofemale lines for each species sampled, with the exception of *D. hydei* for which only one line was available. This investigation served as a good exploratory study, however sample replication and types must be much larger to draw conclusions about species-specific metabolite profiles. Despite the remarkable similarities in the global metabolic profiles of *D. hydei* and *D. immigrans* they were distinguishable by PCA (Appendix B), but because there were only four biological replicates from one isofemale line, broad based conclusions about the metabolic profile of *D. hydei* cannot be made. We cannot conclude whether all *D. hydei* have similar metabolic profiles to *D. immigrans*, or whether the *D. hydei* line we isolated was uniquely similar in metabolic profile to *D. immigrans* in which case if we sample more lines we may observe wider separation. In Appendix B there is evidence that the metabolic profiles of *D. melanogaster* can be resolved using PCA. In contrast, Appendix C illustrates an example where T5 control lines cannot be metabolically distinguished from 6326 lines. In collaboration with a group from the University of Guelph a metabolomic comparison was made between *D. suzkii* originating from British Columbia and Ontario, and the metabolite profiles between the fly lines could not be resolved using PCA (Data not shown). These examples highlight the need for larger numbers of lines to assay using LC-MS analysis, before making broad based conclusions about species-specific or line-specific metabolomes.

All four species in the LC-MS comparison are cosmopolitan species of *Drosophila*, however they were all reared on a medium optimized for *D. melanogaster* and had been reared in laboratory for several generations at the time of assay. The type and content of the food type *Drosophila* are reared under affects metabolism and related processes (Matzkin et al., 2011, 2013; Reed et al., 2010). Work is currently under way in the Merritt lab to assess the metabolic effects of rearing *Drosophila* under different food media using LC-MS analysis. Observing changes to the metabolic profiles from rearing flies under different conditions will provide better understanding of the processes involved in laboratory rearing of *Drosophila* and give us a better picture of the metabolic signature of different species under lab conditions. *Drosophila* under

lab conditions are remarkably different from *Drosophila* found in the wild, and it is has been shown that in very few generations, genomic sequences will already be altered in response to selection for laboratory conditions (Orozco-terWengel et al., 2012). The number of generations in which the flies used in this study were kept in the lab was minimized, however the extent to which lab adaptation had taken place is unknown. This unknown limits our ability to generalize our conclusions about the species-specific metabolome in the wild. Future studies involving *Drosophila* isolated from the wild will benefit from both assaying flies reared under different media and minimizing laboratory rearing times, with the possibility of assaying at various generations once established in the lab.

4.3 LC-MS technology beyond oxidative stress and *Drosophila*

The *Sod-null* induced stress and the paraquat induced stress models investigated in this thesis were chosen, in part, because of the large physiological changes that oxidative stress confer which we expected would result in changes to the metabolome. Being the first metabolomic investigation in the Merritt lab, method development consumed a substantial amount of time and effort, and conditions that were most likely to affect the metabolome were most appealing avenues for investigation. This approach was rewarded when almost one third of the detected metabolome of *Sod-nulls* were altered compared to controls; being able to detect these large-scale differences in a biological system validated our method. By analyzing three different systems, a *Sod-null* allele, paraquat induced stress, and the metabolome of different species, we demonstrated that the method we designed was versatile and robust. With alterations to sample preparation, the protocol used in this thesis can be employed on any model organism or for food and drug investigations, an advantage it shares with other LC-MS designs (Cubbon et al., 2010; Lee et al., 2010; Sreekumar et al., 2009).

Previous work in the Merritt lab has involved describing changes in the relatively small metabolic network of NADP reducing enzymes, particularly under different genetic backgrounds and stresses (Lum and Merritt, 2011; Rzezniczak and Merritt, 2012). Different excision alleles have been assessed for soluble triglyceride levels, total carbohydrate content, and soluble protein content (Rzezniczak and Merritt, 2012). These final phenotypes are useful yet non-specific, considering there are more than one type of each of these particular biological compounds. Soluble proteins for example, consist of a large suite of proteins with broad biochemical

functions, and the unique concentration of each protein has many biological implications that cannot be elucidated by quantifying the concentration of all proteins of this type. Broad based LC-MS metabolomics is expected to shed light on many processes currently not assessed in these previous investigations. Not only could this approach quantify the relative steady state concentrations of the substrates, products, and cofactors involved in the enzyme networks under investigation, it could identify changes to networks and processes that would otherwise be missed, or justify speculations made in these studies.

The Merritt lab is also interested in microbial communities of acid mine drainage (AMD) ponds (Auld et al., 2013). There are projects currently underway aimed at culturing a suite of microbes that live in AMD with the intention of using them for LC-MS metabolomics. Little is known about the unique microbial community found in the Sudbury AMD site other than what microbes are present (Auld et al., 2013). The protocol presented in this thesis can be used to elucidate unique metabolic profiles of different microbes in AMD to gain a better understanding of what metabolic requirements are needed to survive in AMD and what certain microbes are contributing to the community.

4.4 Conclusion

The results from my research describe the metabolic profiles of *D. melanogaster* under chronic oxidative stress and the metabolic profiles of four *Drosophila* species. The metabolic profiles of the *Drosophila* were elucidated by a newly developed, and herein validated, LC-MS protocol for the quantification of polar metabolites. The *Sod-null* allele and paraquat administration are both sources of oxidative stress, which result in substantial, but unique changes to the metabolic profile of *D. melanogaster*. Developing new sample preparation and chromatographic protocols will allow for quantification of a broader suite of metabolites, which will increase our understanding of the metabolic processes affected by genetic lesion or stress. To obtain general conclusions about oxidative stress in *Drosophila melanogaster* LC-MS analysis of oxidative stress in different genetic backgrounds need to be performed.

References

Adams, M.D., Celniker, S.E., Holt, R.A., Evans, C.A., Gocayne, J.D., Amanatides, P.G., Scherer, S.E., Li, P.W., Hoskins, R.A., Galle, R.F., et al. (2000). The genome sequence of Drosophila melanogaster. Science *287*, 2185–2195.

Alpert, A.J. (1990). Hydrophilic-interaction chromatography for the separation of peptides, nucleic acids and other polar compounds. J. Chromatogr. A *499*, 177–196.

Alvarez-Peral, F.J., Zaragoza, O., Pedreno, Y., and Argüelles, J.-C. (2002). Protective role of trehalose during severe oxidative stress caused by hydrogen peroxide and the adaptive oxidative stress response in Candida albicans. Microbiol. Read. Engl. *148*, 2599–2606.

Annesley, T.M. (2003). Ion suppression in mass spectrometry. Clin. Chem. *49*, 1041–1044.

Auld, R.R., Myre, M., Mykytczuk, N.C.S., Leduc, L.G., and Merritt, T.J.S. (2013). Characterization of the microbial acid mine drainage microbial community using culturing and direct sequencing techniques. J. Microbiol. Methods *93*, 108–115.

Bais, P., Moon, S.M., He, K., Leitao, R., Dreher, K., Walk, T., Sucaet, Y., Barkan, L., Wohlgemuth, G., Roth, M.R., et al. (2010). PlantMetabolomics.org: a web portal for plant metabolomics experiments. Plant Physiol. *152*, 1807–1816.

Bajad, S.U., Lu, W., Kimball, E.H., Yuan, J., Peterson, C., and Rabinowitz, J.D. (2006). Separation and quantitation of water soluble cellular metabolites by hydrophilic interaction chromatography-tandem mass spectrometry. J. Chromatogr. A *1125*, 76–88.

Barabási, A.-L., and Oltvai, Z.N. (2004). Network biology: understanding the cell's functional organization. Nat. Rev. Genet. *5*, 101–113.

Barber, S.C., and Shaw, P.J. (2010). Oxidative stress in ALS: key role in motor neuron injury and therapeutic target. Free Radic. Biol. Med. *48*, 629–641.

Bernard, K.E., Parkes, T.L., and Merritt, T.J.S. (2011). A Model of Oxidative Stress Management: Moderation of Carbohydrate Metabolizing Enzymes in SOD1-Null Drosophila melanogaster. PLoS ONE *6*, e24518.

Bogdanov, M., Matson, W.R., Wang, L., Matson, T., Saunders-Pullman, R., Bressman, S.S., and Beal, M.F. (2008). Metabolomic profiling to develop blood biomarkers for Parkinson's disease. Brain *131*, 389–396.

Botella, J.A., Bayersdorfer, F., and Schneuwly, S. (2008). Superoxide dismutase overexpression protects dopaminergic neurons in a Drosophila model of Parkinson's disease. Neurobiol. Dis. *30*, 65–73.

Böttcher, C., Roepenack-Lahaye, E. v., Willscher, E., Scheel, D., and Clemens, S. (2007). Evaluation of Matrix Effects in Metabolite Profiling Based on Capillary Liquid Chromatography

Electrospray Ionization Quadrupole Time-of-Flight Mass Spectrometry. Anal. Chem. *79*, 1507–1513.

Bratty, M.A., Hobani, Y., Dow, J.A.T., and Watson, D.G. (2011). Metabolomic profiling of the effects of allopurinol on Drosophila melanogaster. Metabolomics *7*, 542–548.

Brunetti, D., Dusi, S., Morbin, M., Uggetti, A., Moda, F., D'Amato, I., Giordano, C., d' Amati, G., Cozzi, A., Levi, S., et al. (2012). Pantothenate kinase-associated neurodegeneration: altered mitochondria membrane potential and defective respiration in Pank2 knock-out mouse model. Hum. Mol. Genet. *21*, 5294–5305.

Brunner, E., Ahrens, C.H., Mohanty, S., Baetschmann, H., Loevenich, S., Potthast, F., Deutsch, E.W., Panse, C., de Lichtenberg, U., Rinner, O., et al. (2007). A high-quality catalog of the Drosophila melanogaster proteome. Nat. Biotechnol. *25*, 576–583.

Buonocore, G., Perrone, S., and Tataranno, M.L. (2010). Oxygen toxicity: chemistry and biology of reactive oxygen species. Semin. Fetal. Neonatal Med. *15*, 186–190.

Buszewski, B., and Noga, S. (2012). Hydrophilic interaction liquid chromatography (HILIC)--a powerful separation technique. Anal. Bioanal. Chem. *402*, 231–247.

Campbell, S.D., Hilliker, A.J., and Phillips, J.P. (1986). Cytogenetic analysis of the cSOD microregion in Drosophila melanogaster. Genetics *112*, 205–215.

Center for Drug Evaluation and Research (CDER), and Food and Drug Adminstration (FDA) (2001). Guidance for Industry: Bioanalytical Method Validation. Retrieved from: http://www.fda.gov/downloads/Drugs/Guidances/ucm070107.pdf

Chalcraft, K.R., and McCarry, B.E. (2013). Tandem LC columns for the simultaneous retention of polar and nonpolar molecules in comprehensive metabolomics analysis†. J. Sep. Sci. 1–8.

Chambers, M.C., Song, K.H., and Schneider, D.S. (2012). Listeria monocytogenes Infection Causes Metabolic Shifts in Drosophila melanogaster. PLoS ONE *7*, e50679.

Chandler, C.H., Chari, S., and Dworkin, I. (2012). Does your gene need a background check? How genetic background impacts the analysis of mutations, genes, and evolution. Trends Genet.

Chang, Y.-C., Tang, H.-W., Liang, S.-Y., Pu, T.-H., Meng, T.-C., Khoo, K.-H., and Chen, G.-C. (2013). Evaluation of Drosophila metabolic labeling strategies for in vivo quantitative proteomic analyses with applications to early pupa formation and amino acid starvation. J. Proteome Res. *12*, 2138–2150.

Cheng, Z., Tsuda, M., Kishita, Y., Sato, Y., and Aigaki, T. (2013). Impaired energy metabolism in a Drosophila model of mitochondrial aconitase deficiency. Biochem. Biophys. Res. Commun. *433*, 145–150.

Clark, J.B. (1998). N-Acetyl Aspartate: A Marker for Neuronal Loss or Mitochondrial Dysfunction. Dev. Neurosci. *20*, 271–276.

Clark, A.G., and Wang, L. (1994). Comparative Evolutionary Analysis of Metabolism in Nine Drosophila Species. Evolution *48*, 1230–1243.

Coulier, L., Bas, R., Jespersen, S., Verheij, E., van der Werf, M.J., and Hankemeier, T. (2006). Simultaneous quantitative analysis of metabolites using ion-pair liquid chromatography-electrospray ionization mass spectrometry. Anal. Chem. *78*, 6573–6582.

Cubbon, S., Antonio, C., Wilson, J., and Thomas-Oates, J. (2010). Metabolomic applications of HILIC-LC-MS. Mass Spectrom. Rev. *29*, 671–684.

Cui, Q., Lewis, I.A., Hegeman, A.D., Anderson, M.E., Li, J., Schulte, C.F., Westler, W.M., Eghbalnia, H.R., Sussman, M.R., and Markley, J.L. (2008). Metabolite identification via the Madison Metabolomics Consortium Database. Nat. Biotechnol. *26*, 162–164.

Czech, B., Preall, J.B., McGinn, J., and Hannon, G.J. (2013). A Transcriptome-wide RNAi Screen in the Drosophila Ovary Reveals Factors of the Germline piRNA Pathway. Mol. Cell *50*, 749–761.

Davis, M.T., Beierle, J., Bures, E.T., McGinley, M.D., Mort, J., Robinson, J.H., Spahr, C.S., Yu, W., Luethy, R., and Patterson, S.D. (2001). Automated LC-LC-MS-MS platform using binary ion-exchange and gradient reversed-phase chromatography for improved proteomic analyses. J. Chromatogr. B. Biomed. Sci. App. *752*, 281–291.

De Hoffmann, E. (2005). Mass Spectrometry. In Kirk-Othmer Encyclopedia of Chemical Technology, (5^{th} Ed., Vol. 15, pp. 1–20). John Wiley & Sons, Inc.

Dettmer, K., Aronov, P.A., and Hammock, B.D. (2007). Mass spectrometry-based metabolomics. Mass Spectrom. Rev. *26*, 51–78.

Dhalla, N.S., Temsah, R.M., and Netticadan, T. (2000). Role of oxidative stress in cardiovascular diseases. J. Hypertens. *18*, 655–673.

Dixon, S.P., Pitfield, I.D., and Perrett, D. (2006). Comprehensive multi-dimensional liquid chromatographic separation in biomedical and pharmaceutical analysis: a review. Biomed. Chromatogr. *20*, 508–529.

Dole, M., Mack, L.L., Hines, R.L., Mobley, R.C., Ferguson, L.D., and Alice, M.B. (1968). Molecular Beams of Macroions. J. Chem. Phys. *49*, 2240–2249.

Dunn, W.B., Broadhurst, D., Brown, M., Baker, P.N., Redman, C.W.G., Kenny, L.C., and Kell, D.B. (2008). Metabolic profiling of serum using Ultra Performance Liquid Chromatography and the LTQ-Orbitrap mass spectrometry system. J. Chromatogr. B Analyt. Technol. Biomed. Life. Sci. *871*, 288–298.

Dworkin, I., Kennerly, E., Tack, D., Hutchinson, J., Brown, J., Mahaffey, J., and Gibson, G. (2009). Genomic consequences of background effects on scalloped mutant expressivity in the wing of Drosophila melanogaster. Genetics *181*, 1065–1076.

Elhamili, A., Samuelsson, J., Bergquist, J., and Wetterhall, M. (2011). Optimizing the extraction, separation and quantification of tricyclic antidepressant drugs in human plasma with CE-ESI-TOF-MS using cationic-coated capillaries. Electrophoresis *32*, 647–658.

Elia, A.J., Parkes, T.L., Kirby, K., St George-Hyslop, P., Boulianne, G.L., Phillips, J.P., and Hilliker, A.J. (1999). Expression of human FALS SOD in motorneurons of Drosophila. Free Radic. Biol. Med. *26*, 1332–1338.

Eyres, G.T., Urban, S., Morrison, P.D., Dufour, J.-P., and Marriott, P.J. (2008). Method for Small-Molecule Discovery Based on Microscale-Preparative Multidimensional Gas Chromatography Isolation with Nuclear Magnetic Resonance Spectroscopy. Anal. Chem. *80*, 6293–6299.

Fiehn, O. (2002). Metabolomics – the link between genotypes and phenotypes. Plant Mol. Biol. *48*, 155–171.

Fox, R.E., Hopkins, I.B., Cabacungan, E.T., and Tildon, J.T. (1996). The Role of Glutamine and Other Alternate Substrates as Energy Sources in the Fetal Rat Lung Type II Cell1. Pediatr. Res. *40*, 135–141.

Francis, J.S., Strande, L., Markov, V., and Leone, P. (2012). Aspartoacylase supports oxidative energy metabolism during myelination. J. Cereb. Blood Flow Metab. *32*, 1725–1736.

Gamache, P.H., Meyer, D.F., Granger, M.C., and Acworth, I.N. (2004). Metabolomic applications of electrochemistry/Mass spectrometry. J. Am. Soc. Mass Spectrom. *15*, 1717–1726.

Gibson, G., and Reed, L.K. (2008). Cryptic genetic variation. Curr. Biol. CB *18*, R989–R990.

Gika, H.G., Theodoridis, G.A., Wingate, J.E., and Wilson, I.D. (2007). Within-Day Reproducibility of an HPLC−MS-Based Method for Metabonomic Analysis: Application to Human Urine. J. Proteome Res. *6*, 3291–3303.

Girardot, F., Monnier, V., and Tricoire, H. (2004). Genome wide analysis of common and specific stress responses in adult drosophila melanogaster. BMC Genomics *5*, 74.

Giri, S., Idle, J.R., Chen, C., Zabriskie, T.M., Krausz, K.W., and Gonzalez, F.J. (2006). A metabolomic approach to the metabolism of the areca nut alkaloids arecoline and arecaidine in the mouse. Chem. Res. Toxicol. *19*, 818–827.

Goeman, J.J., and Bühlmann, P. (2007). Analyzing gene expression data in terms of gene sets: methodological issues. Bioinformatics *23*, 980–987.

Goto, S.G., and Kimura, M.T. (2001). Phylogenetic Utility of Mitochondrial COI and Nuclear Gpdh Genes in Drosophila. Mol. Phylogenet. Evol. *18*, 404–422.

Graveley, B.R., Brooks, A.N., Carlson, J.W., Duff, M.O., Landolin, J.M., Yang, L., Artieri, C.G., van Baren, M.J., Boley, N., Booth, B.W., et al. (2011). The developmental transcriptome of Drosophila melanogaster. Nature *471*, 473–479.

Hellstrand, K., Brune, M., Dahlgren, C., Hansson, M., Hermodsson, S., Lindnér, P., Mellqvist, U.H., and Naredi, P. (2000). Alleviating oxidative stress in cancer immunotherapy: a role for histamine? Med. Oncol. Northwood Lond. Engl. *17*, 258–269.

Hennion, M.-C. (1999). Solid-phase extraction: method development, sorbents, and coupling with liquid chromatography. J. Chromatogr. A *856*, 3–54.

Ho, H.-Y., Cheng, M.-L., Shiao, M.-S., and Chiu, D.T.-Y. (2013). Characterization of global metabolic responses of glucose-6-phosphate dehydrogenase-deficient hepatoma cells to diamide-induced oxidative stress. Free Radic. Biol. Med. *54*, 71–84.

Holland, C., Lipsett, D.B., and Clark, D.V. (2011). A Link Between Impaired Purine Nucleotide Synthesis and Apoptosis in Drosophila melanogaster. Genetics *188*, 359–367.

Hosamani, R., and Muralidhara (2013). Acute exposure of Drosophila melanogaster to paraquat causes oxidative stress and mitochondrial dysfunction. Arch. Insect Biochem. Physiol. *83*, 25–40.

Hoskins, R.A., Phan, A.C., Naeemuddin, M., Mapa, F.A., Ruddy, D.A., Ryan, J.J., Young, L.M., Wells, T., Kopczynski, C., and Ellis, M.C. (2001). Single nucleotide polymorphism markers for genetic mapping in Drosophila melanogaster. Genome Res. *11*, 1100–1113.

Hsieh, Y., Chintala, M., Mei, H., Agans, J., Brisson, J.-M., Ng, K., and Korfmacher, W.A. (2001). Quantitative screening and matrix effect studies of drug discovery compounds in monkey plasma using fast-gradient liquid chromatography/tandem mass spectrometry. Rapid Commun. Mass Spectrom. *15*, 2481–2487.

Huck, J.H.J., Struys, E.A., Verhoeven, N.M., Jakobs, C., and van der Knaap, M.S. (2003). Profiling of pentose phosphate pathway intermediates in blood spots by tandem mass spectrometry: application to transaldolase deficiency. Clin. Chem. *49*, 1375–1380.

Hummel, T., and Klämbt, C. (2008). P-element mutagenesis. Methods Mol. Biol. Clifton NJ *420*, 97–117.

Iribarne, J.V., and Thomson, B.A. (1976). On the evaporation of small ions from charged droplets. J. Chem. Phys. *64*, 2287–2294.

James, S.J., Cutler, P., Melnyk, S., Jernigan, S., Janak, L., Gaylor, D.W., and Neubrander, J.A. (2004). Metabolic biomarkers of increased oxidative stress and impaired methylation capacity in children with autism. Am. J. Clin. Nutr. *80*, 1611–1617.

Jardon, M.A., Sattha, B., Braasch, K., Leung, A.O., Côté, H.C.F., Butler, M., Gorski, S.M., and Piret, J.M. (2012). Inhibition of glutamine-dependent autophagy increases t-PA production in CHO Cell fed-batch processes. Biotechnol. Bioeng. *109*, 1228–1238.

Jenner, P. (2003). Oxidative stress in Parkinson's disease. Ann. Neurol. *53 Suppl 3*, S26–36; discussion S36–38.

Jentzmik, F., Stephan, C., Miller, K., Schrader, M., Erbersdobler, A., Kristiansen, G., Lein, M., and Jung, K. (2010). Sarcosine in Urine after Digital Rectal Examination Fails as a Marker in Prostate Cancer Detection and Identification of Aggressive Tumours. Eur. Urol. *58*, 12–18.

Johnson, C.H., and Gonzalez, F.J. (2012). Challenges and opportunities of metabolomics. J. Cell. Physiol. *227*, 2975–2981.

Jozefczuk, S., Klie, S., Catchpole, G., Szymanski, J., Cuadros-Inostroza, A., Steinhauser, D., Selbig, J., and Willmitzer, L. (2010). Metabolomic and transcriptomic stress response of Escherichia coli. Mol. Syst. Biol. *6*, 1–15.

Kamleh, M.A., Hobani, Y., Dow, J.A.T., and Watson, D.G. (2008). Metabolomic profiling of Drosophila using liquid chromatography Fourier transform mass spectrometry. FEBS Lett. *582*, 2916–2922.

Kirby, K., Hu, J., Hilliker, A.J., and Phillips, J.P. (2002). RNA interference-mediated silencing of Sod2 in Drosophila leads to early adult-onset mortality and elevated endogenous oxidative stress. Proc. Natl. Acad. Sci. USA. *99*, 16162–16167.

Knee, J.M., Rzezniczak, T.Z., Guo, K.K., Barsch, A., and Merritt, T.J.S. (2013). A novel ion pairing LC-MS metabolomics protocol for study of a variety of biologically relevant metabolites. J. Chromatogr. B *936*, 63–73.

Kochar, N.I., and Umathe, S.N. (2009). Beneficial effects of L-arginine against diabetes-induced oxidative stress in gastrointestinal tissues in rats. Pharmacol. Reports PR *61*, 665–672.

Koek, M.M., Jellema, R.H., van der Greef, J., Tas, A.C., and Hankemeier, T. (2011). Quantitative metabolomics based on gas chromatography mass spectrometry: status and perspectives. Metabolomics Off. J. Metabolomic Soc. *7*, 307–328.

Krishnan, N., Dickman, M.B., and Becker, D.F. (2008). Proline modulates the intracellular redox environment and protects mammalian cells against oxidative stress. Free Radic. Biol. Med. *44*, 671–681.

Kristensen, M., Engelsen, S.B., and Dragsted, L.O. (2012). LC–MS metabolomics top-down approach reveals new exposure and effect biomarkers of apple and apple-pectin intake. Metabolomics *8*, 64–73.

Lachance, J., and True, J.R. (2010). X-autosome incompatibilities in Drosophila melanogaster: tests of Haldane's rule and geographic patterns within species. Evol. Int. J. Org. Evol. *64*, 3035–3046.

Layne, J., Farcas, T., Rustamov, I., and Ahmed, F. (2001). Volume-load capacity in fast-gradient liquid chromatography: Effect of sample solvent composition and injection volume on chromatographic performance. J. Chromatogr. A *913*, 233–242.

Lee, D.Y., Bowen, B.P., and Northen, T.R. (2010). Mass spectrometry-based metabolomics, analysis of metabolite-protein interactions, and imaging. BioTechniques *49*, 557–565.

Lemire, J., Milandu, Y., Auger, C., Bignucolo, A., Appanna, V.P., and Appanna, V.D. (2010). Histidine is a source of the antioxidant, alpha-ketoglutarate, in Pseudomonas fluorescens challenged by oxidative stress. FEMS Microbiol. Lett. *309*, 170–177.

Li, M., Feng, B., Liang, Y., Zhang, W., Bai, Y., Tang, W., Wang, T., and Liu, H. (2013). Lipid profiling of human plasma from peritoneal dialysis patients using an improved 2D (NP/RP) LC-QToF MS method. Anal. Bioanal. Chem. *405*, 6629–6638.

Liu, J., Litt, L., Segal, M.R., Kelly, M.J.S., Pelton, J.G., and Kim, M. (2011). Metabolomics of Oxidative Stress in Recent Studies of Endogenous and Exogenously Administered Intermediate Metabolites. Int. J. Mol. Sci. *12*, 6469–6501.

Liu, R., Li, Q., Ma, R., Lin, X., Xu, H., and Bi, K. (2013). Determination of polyamine metabolome in plasma and urine by ultrahigh performance liquid chromatography-tandem mass spectrometry method: Application to identify potential markers for human hepatic cancer. Anal. Chim. Acta *791*, 36–45.

Lu, W., Bennett, B.D., and Rabinowitz, J.D. (2008). Analytical strategies for LC–MS-based targeted metabolomics. J. Chromatogr. B *871*, 236–242.

Lum, T.E., and Merritt, T.J.S. (2011). Nonclassical regulation of transcription: interchromosomal interactions at the malic enzyme locus of Drosophila melanogaster. Genetics *189*, 837–849.

Luo, B., Groenke, K., Takors, R., Wandrey, C., and Oldiges, M. (2007). Simultaneous determination of multiple intracellular metabolites in glycolysis, pentose phosphate pathway and tricarboxylic acid cycle by liquid chromatography–mass spectrometry. J. Chromatogr. A *1147*, 153–164.

Mackay, T.F.C., Richards, S., Stone, E.A., Barbadilla, A., Ayroles, J.F., Zhu, D., Casillas, S., Han, Y., Magwire, M.M., Cridland, J.M., et al. (2012). The Drosophila melanogaster Genetic Reference Panel. Nature *482*, 173–178.

Mahmood, D., Khanam, R., Pillai, K.K., and Akhtar, M. (2012). Reversal of oxidative stress by histamine H_3 receptor-ligands in experimental models of schizophrenia. Arzneimittelforschung. *62*, 222–229.

Mallet, C.R., Lu, Z., and Mazzeo, J.R. (2004a). A study of ion suppression effects in electrospray ionization from mobile phase additives and solid-phase extracts. Rapid Commun. Mass Spectrom. *18*, 49–58.

Mallet, C.R., Lu, Z., and Mazzeo, J.R. (2004b). A study of ion suppression effects in electrospray ionization from mobile phase additives and solid-phase extracts. Rapid Commun. Mass Spectrom. *18*, 49–58.

Matés, J.M., Pérez-Gómez, C., de Castro, I.N., Asenjo, M., and Márquez, J. (2002). Glutamine and its relationship with intracellular redox status, oxidative stress and cell proliferation/death. Int. J. Biochem. Cell Biol. *34*, 439–458.

Matés, J.M., Segura, J.A., Alonso, F.J., and Márquez, J. (2006). Pathways from glutamine to apoptosis. Front. Biosci. J. Virtual Libr. *11*, 3164–3180.

Matuszewski, B.K., Constanzer, M.L., and Chavez-Eng, C.M. (1998). Matrix effect in quantitative LC/MS/MS analyses of biological fluids: a method for determination of finasteride in human plasma at pictogram per milliliter concentrations. Anal. Chem. *70*, 882-889.

Matzkin, L.M., Johnson, S., Paight, C., Bozinovic, G., and Markow, T.A. (2011). Dietary protein and sugar differentially affect development and metabolic pools in ecologically diverse Drosophila. J. Nutr. *141*, 1127–1133.

Matzkin, L.M., Johnson, S., Paight, C., and Markow, T.A. (2013). Preadult Parental Diet Affects Offspring Development and Metabolism in Drosophila melanogaster. PLoS ONE *8*, e59530.

Merritt, T.J.S., Duvernell, D., and Eanes, W.F. (2005). Natural and synthetic alleles provide complementary insights into the nature of selection acting on the Men polymorphism of Drosophila melanogaster. Genetics *171*, 1707–1718.

Mischak, H., Coon, J.J., Novak, J., Weissinger, E.M., Schanstra, J.P., and Dominiczak, A.F. (2009). Capillary electrophoresis-mass spectrometry as a powerful tool in biomarker discovery and clinical diagnosis: an update of recent developments. Mass Spectrom. Rev. *28*, 703–724.

Mockett, R.J., Radyuk, S.N., Benes, J.J., Orr, W.C., and Sohal, R.S. (2003). Phenotypic effects of familial amyotrophic lateral sclerosis mutant Sod alleles in transgenic Drosophila. Proc. Natl. Acad. Sci. USA. *100*, 301–306.

Montooth, K.L., Marden, J.H., and Clark, A.G. (2003). Mapping Determinants of Variation in Energy Metabolism, Respiration and Flight in Drosophila. Genetics *165*, 623–635.

Müller, C., Schäfer, P., Störtzel, M., Vogt, S., and Weinmann, W. (2002). Ion suppression effects in liquid chromatography-electrospray-ionisation transport-region collision induced dissociation mass spectrometry with different serum extraction methods for systematic toxicological analysis with mass spectra libraries. J. Chromatogr. B Analyt. Technol. Biomed. Life. Sci. *773*, 47–52.

Neckameyer, W.S., and Weinstein, J.S. (2005). Stress affects dopaminergic signaling pathways in Drosophila melanogaster. Stress Amst. Neth. *8*, 117–131.

Negreira, N., López de Alda, M., and Barceló, D. (2013). On-line solid phase extraction–liquid chromatography–tandem mass spectrometry for the determination of 17 cytostatics and metabolites in waste, surface and ground water samples. J. Chromatogr. A *1280*, 64–74.

Neu, J., Shenoy, V., and Chakrabarti, R. (1996). Glutamine nutrition and metabolism: where do we go from here ? FASEB J. *10*, 829–837.

Noor, R., Mittal, S., and Iqbal, J. (2002). Superoxide dismutase--applications and relevance to human diseases. Med. Sci. Monit. Int. Med. J. Exp. Clin. Res. *8*, RA210–215.

Oakeshott, J.G., McKechnie, S.W., and Chambers, G.K. (1984). Population genetics of the metabolically related Adh, Gpdh and Tpi polymorphisms in Drosophila melanogaster I. Geographic variation in Gpdh and Tpi allele frequencies in different continents. Genetica *63*, 21–29.

Hrydziuszko, O., and Viant, M.R. (2012). Missing values in mass spectrometery based metabolomics: an undervalued step in the dat processing pipeline. Metabolomics 8, 161-174.

Orozco-terWengel, P., Kapun, M., Nolte, V., Kofler, R., Flatt, T., and Schlötterer, C. (2012). Adaptation of Drosophila to a novel laboratory environment reveals temporally heterogeneous trajectories of selected alleles. Mol. Ecol. *21*, 4931–4941.

Owen, J.B., and Butterfield, D.A. (2010). Measurement of oxidized/reduced glutathione ratio. Methods Mol. Biol. Clifton NJ *648*, 269–277.

Parkes, T.L., Hilliker, A.J., and Phillips, J.P. (1993). Genetic and biochemical analysis of glutathione-S-transferase in the oxygen defense system of Drosophila melanogaster. Genome *36*, 1007–1014.

Parkes, T.L., Elia, A.J., Dickinson, D., Hilliker, A.J., Phillips, J.P., and Boulianne, G.L. (1998a). Extension of Drosophila lifespan by overexpression of human SOD1 in motorneurons. Nat. Genet. *19*, 171–174.

Parkes, T.L., Kirby, K., Phillips, J.P., and Hilliker, A.J. (1998b). Transgenic analysis of the cSOD-null phenotypic syndrome in *Drosophila*. Genome *41*, 642–651.

Passador-Gurgel, G., Hsieh, W.-P., Hunt, P., Deighton, N., and Gibson, G. (2007). Quantitative trait transcripts for nicotine resistance in Drosophila melanogaster. Nat. Genet. *39*, 264–268.

Pederzolli, C.D., Sgaravatti, Â.M., Braum, C.A., Prestes, C.C., Zorzi, G.K., Sgarbi, M.B., Wyse, A.T.S., Wannmacher, C.M.D., Wajner, M., and Dutra-Filho, C.S. (2007a). 5-Oxoproline Reduces Non-Enzymatic Antioxidant Defenses in vitro in Rat Brain. Metab. Brain Dis. *22*, 51–65.

Pederzolli, C.D., Mescka, C.P., Scapin, F., Rockenbach, F.J., Sgaravatti, Â.M., Sgarbi, M.B., Wyse, A.T.S., Wannmacher, C.M.D., Wajner, M., and Dutra-Filho, C.S. (2007b). N-Acetylaspartic acid promotes oxidative stress in cerebral cortex of rats. Int. J. Dev. Neurosci. *25*, 317–324.

Phillips, J.P., Campbell, S.D., Michaud, D., Charbonneau, M., and Hilliker, A.J. (1989). Null mutation of copper/zinc superoxide dismutase in Drosophila confers hypersensitivity to paraquat and reduced longevity. Proc. Natl. Acad. Sci. USA. *86*, 2761–2765.

Piva, T.J., and Mcevoy-Bowe, E. (1998). Oxidation of glutamine in HeLa cells: Role and control of truncated TCA cycles in tumour mitochondria. J. Cell. Biochem. *68*, 213–225.

Reed, L.K., Williams, S., Springston, M., Brown, J., Freeman, K., DesRoches, C.E., Sokolowski, M.B., and Gibson, G. (2010). Genotype-by-Diet Interactions Drive Metabolic Phenotype Variation in Drosophila melanogaster. Genetics *185*, 1009–1019.

Reitman, Z.J., Jin, G., Karoly, E.D., Spasojevic, I., Yang, J., Kinzler, K.W., He, Y., Bigner, D.D., Vogelstein, B., and Yan, H. (2011). Profiling the effects of isocitrate dehydrogenase 1 and 2 mutations on the cellular metabolome. Proc. Natl. Acad. Sci. USA. *108*.

Riley, P.A. (1994). Free radicals in biology: oxidative stress and the effects of ionizing radiation. Int. J. Radiat. Biol. *65*, 27–33.

Rodrigues Pereira, N., Bandeira Moss, M., Assumpção, C.R., Cardoso, C.B., Mann, G.E., Brunini, T.M.C., and Mendes-Ribeiro, A.C. (2010). Oxidative stress, l-arginine-nitric oxide and arginase pathways in platelets from adolescents with anorexia nervosa. Blood Cells. Mol. Dis. *44*, 164–168.

Rubin, G.M., and Lewis, E.B. (2000). A Brief History of Drosophila's Contributions to Genome Research. Science *287*, 2216–2218.

Rzezniczak, T.Z., and Merritt, T.J.S. (2012). Interactions of NADP-reducing enzymes across varying environmental conditions: a model of biological complexity. G3 Bethesda Md *2*, 1613–1623.

Rzezniczak, T.Z., Douglas, L.A., Watterson, J.H., and Merritt, T.J.S. (2011). Paraquat administration in Drosophila for use in metabolic studies of oxidative stress. Anal. Biochem. *419*, 345–347.

Rzezniczak, T.Z., Lum, T.E., Harniman, R., and Merritt, T.J.S. (2012). A combination of structural and cis-regulatory factors drives biochemical differences in Drosophila melanogaster malic enzyme. Biochem. Genet. *50*, 823–837.

Sarup, P., Sørensen, J.G., Kristensen, T.N., Hoffmann, A.A., Loeschcke, V., Paige, K.N., and Sørensen, P. (2011). Candidate genes detected in transcriptome studies are strongly dependent on genetic background. PloS One *6*, e15644.

Sarup, P., Pedersen, S.M.M., Nielsen, N.C., Malmendal, A., and Loeschcke, V. (2012). The Metabolic Profile of Long-Lived Drosophila melanogaster. PLoS ONE *7*, e47461.

Schauer, N., Steinhauser, D., Strelkov, S., Schomburg, D., Allison, G., Moritz, T., Lundgren, K., Roessner-Tunali, U., Forbes, M.G., Willmitzer, L., et al. (2005). GC-MS libraries for the rapid identification of metabolites in complex biological samples. FEBS Lett. *579*, 1332–1337.

Seinen, E., Burgerhof, J.G.M., Jansen, R.C., and Sibon, O.C.M. (2010). RNAI Experiments in D. melanogaster: Solutions to the Overlooked Problem of Off-Targets Shared by Independent dsRNAs. PLoS ONE *5*.

Sentman, M.-L., Granstrom, M., Jakobson, H., Reaume, A., Basu, S., and Marklund, S. (2006). Phenotypes of Mice Lacking Extracellular Superoxide Dismutase and Copper- and Zinc-containing Superoxide Dismutase. J. Biol. Chem. *281*, 6904–6909.

Serkova, N.J., Jackman, M., Brown, J.L., Liu, T., Hirose, R., Roberts, J.P., Maher, J.J., and Niemann, C.U. (2006). Metabolic profiling of livers and blood from obese Zucker rats. J. Hepatol. *44*, 956–962.

Singh, R., Lemire, J., Mailloux, R.J., and Appanna, V.D. (2008). A Novel Strategy Involved Anti-Oxidative Defense: The Conversion of NADH into NADPH by a Metabolic Network. PLoS ONE *3*.

Smith, C.A., Want, J.E., O'Maille, G., Abagyan, R., and Siuzdak, G. (2006). XCMS: Processing mass spectrometry data for metabolite profiling using nonlinear peak alignment, matching, and identification. Anal. Chem. *78*, 779-787.

Smith, J.E., Lay, J.O., and Bluhm, B.H. (2012). Metabolic fingerprinting reveals a new genetic linkage between ambient pH and metabolites associated with desiccation tolerance in Fusarium verticillioides. Metabolomics *8*, 376–385.

Soga, T., Igarashi, K., Ito, C., Mizobuchi, K., Zimmermann, H.-P., and Tomita, M. (2009). Metabolomic profiling of anionic metabolites by capillary electrophoresis mass spectrometry. Anal. Chem. *81*, 6165–6174.

Son, D.O., Satsu, H., and Shimizu, M. (2005). Histidine inhibits oxidative stress- and TNF-α-induced interleukin-8 secretion in intestinal epithelial cells. FEBS Lett. *579*, 4671–4677.

Sreekumar, A., Poisson, L.M., Rajendiran, T.M., Khan, A.P., Cao, Q., Yu, J., Laxman, B., Mehra, R., Lonigro, R.J., Li, Y., et al. (2009). Metabolomic profiles delineate potential role for sarcosine in prostate cancer progression. Nature *457*, 910–914.

Ståhlberg, J. (1999). Retention models for ions in chromatography. J. Chromatogr. A *855*, 3–55.

Thomson, B.A., and Iribarne, J.V. (1979). Field induced ion evaporation from liquid surfaces at atmospheric pressure. J. Chem. Phys. *71*, 4451–4463.

Tissot van Patot, M.C., Serkova, N.J., Haschke, M., Kominsky, D.J., Roach, R.C., Christians, U., Henthorn, T.K., and Honigman, B. (2009). Enhanced leukocyte HIF-1alpha and HIF-1 DNA binding in humans after rapid ascent to 4300 m. Free Radic. Biol. Med. *46*, 1551–1557.

T' Kindt, R., Scheltema, R.A., Jankevics, A., Brunker, K., Rijal, S., Dujardin, J.-C., Breitling, R., Watson, D.G., Coombs, G.H., and Decuypere, S. (2010). Metabolomics to Unveil and Understand Phenotypic Diversity between Pathogen Populations. PLoS Negl Trop Dis *4*, e904.

Tolstikov, V.V., and Fiehn, O. (2002). Analysis of highly polar compounds of plant origin: combination of hydrophilic interaction chromatography and electrospray ion trap mass spectrometry. Anal. Biochem. *301*, 298–307.

Trethewey, R.N., Krotzky, A.J., and Willmitzer, L. (1999). Metabolic profiling: a Rosetta Stone for genomics? Curr. Opin. Plant Biol. *2*, 83–85.

Van Dam, J.C., Eman, M.R., Frank, J., Lange, H.C., van Dedem, G.W.., and Heijnen, S.J. (2002). Analysis of glycolytic intermediates in Saccharomyces cerevisiae using anion exchange chromatography and electrospray ionization with tandem mass spectrometric detection. Anal. Chim. Acta *460*, 209–218.

Van Raamsdonk, J.M., and Hekimi, S. (2009). Deletion of the Mitochondrial Superoxide Dismutase sod-2 Extends Lifespan in Caenorhabditis elegans. PLoS Genet. *5*, e1000361.

Verhoeven, H.A., Vos, C.H.R. de, Bino, R.J., and Hall, R.D. (2006). Plant Metabolomics Strategies Based upon Quadrupole Time of Flight Mass Spectrometry (QTOF-MS). In Plant Metabolomics, P.D.K. Saito, P.D.R.A. Dixon, and P.D.L. Willmitzer, eds. (Springer Berlin Heidelberg), pp. 33–48.

Vo Duy, S., Besteiro, S., Berry, L., Perigaud, C., Bressolle, F., Vial, H.J., and Lefebvre-Tournier, I. (2012). A quantitative liquid chromatography tandem mass spectrometry method for metabolomic analysis of Plasmodium falciparum lipid related metabolites. Anal. Chim. Acta *739*, 47–55.

Wang, W., Zhou, H., Lin, H., Roy, S., Shaler, T.A., Hill, L.R., Norton, S., Kumar, P., Anderle, M., and Becker, C.H. (2003). Quantification of Proteins and Metabolites by Mass Spectrometry without Isotopic Labeling or Spiked Standards. Anal. Chem. *75*, 4818–4826.

Want, E.J., Masson, P., Michopoulos, F., Wilson, I.D., Theodoridis, G., Plumb, R.S., Shockcor, J., Loftus, N., Holmes, E., and Nicholson, J.K. (2013). Global metabolic profiling of animal and human tissues via UPLC-MS. Nat. Protoc. *8*, 17–32.

Watson, M.R., Lagow, R.D., Xu, K., Zhang, B., and Bonini, N.M. (2008). A Drosophila Model for Amyotrophic Lateral Sclerosis Reveals Motor Neuron Damage by Human SOD1. J. Biol. Chem. *283*, 24972–24981.

Weckwerth, W., Loureiro, M.E., Wenzel, K., and Fiehn, O. (2004). Differential metabolic networks unravel the effects of silent plant phenotypes. Proc. Natl. Acad. Sci. USA. *101*, 7809–7814.

Weeks, M.E., Sinclair, J., Butt, A., Chung, Y.-L., Worthington, J.L., Wilkinson, C.R.M., Griffiths, J., Jones, N., Waterfield, M.D., and Timms, J.F. (2006). A parallel proteomic and metabolomic analysis of the hydrogen peroxide- and Sty1p-dependent stress response in Schizosaccharomyces pombe. Proteomics *6*, 2772–2796.

Wei, J.-P.J., Srinivasan, C., Han, H., Valentine, J.S., and Gralla, E.B. (2001). Evidence for a Novel Role of Copper-Zinc Superoxide Dismutase in Zinc Metabolism. J. Biol. Chem. *276*, 44798–44803.

Wilm, M. (2011). Principles of Electrospray Ionization. Mol. Cell. Proteomics *10*, 1–8.

Wilm, M.S., and Mann, M. (1994). Electrospray and Taylor-Cone theory, Dole's beam of macromolecules at last? Int. J. Mass Spectrom. Ion Process. *136*, 167–180.

Wishart, D.S. (2008). Quantitative metabolomics using NMR. TrAC Trends Anal. Chem. *27*, 228–237.

Wishart, D.S., Jewison, T., Guo, A.C., Wilson, M., Knox, C., Liu, Y., Djoumbou, Y., Mandal, R., Aziat, F., Dong, E., et al. (2013). HMDB 3.0--The Human Metabolome Database in 2013. Nucleic Acids Res. *41*, D801–807.

Woodruff, R.C., Phillips, J.P., and Hilliker, A.J. (2004). Increased spontaneous DNA damage in Cu/Zn superoxide dismutase (SOD1) deficient Drosophila. Genome Natl. Res. Counc. Can. Génome Cons. Natl. Rech. Can. *47*, 1029–1035.

Wu, H., Liu, T., Ma, C., Xue, R., Deng, C., Zeng, H., and Shen, X. (2011). GC/MS-based metabolomic approach to validate the role of urinary sarcosine and target biomarkers for human prostate cancer by microwave-assisted derivatization. Anal. Bioanal. Chem. *401*, 635–646.

Wu, H., Liu, X., You, L., Zhang, L., Yu, J., Zhou, D., Zhao, J., and Feng, J. (2012). Salinity-Induced Effects in the Halophyte Suaeda salsa Using NMR-based Metabolomics. Plant Mol. Biol. Report. *30*, 590–598.

Xia, J., Psychogios, N., Young, N., and Wishart, D.S. (2009). MetaboAnalyst: a web server for metabolomic data analysis and interpretation. Nucleic Acids Res. *37*, W652–W660.

Xia, J., Mandal, R., Sinelnikov, I.V., Broadhurst, D., and Wishart, D.S. (2012). MetaboAnalyst 2.0—a comprehensive server for metabolomic data analysis. Nucleic Acids Res.

Ying, W. (2008). NAD+/NADH and NADP+/NADPH in cellular functions and cell death: regulation and biological consequences. Antioxidants Redox Signal. *10*, 179–206.

Zelko, I.N., Mariani, T.J., and Folz, R.J. (2002). Superoxide dismutase multigene family: a comparison of the CuZn-SOD (SOD1), Mn-SOD (SOD2), and EC-SOD (SOD3) gene structures, evolution, and expression. Free Radic. Biol. Med. *33*, 337–349.

Zhong, D.-N., Ning, Q.-Y., Wu, J.-Z., Zang, N., Wu, J.-L., Hu, D.-F., Luo, S.-Y., Huang, A.-C., Li, L.-L., and Li, G.-J. (2012). Comparative proteomic profiles indicating genetic factors may involve in hepatocellular carcinoma familial aggregation. Cancer Sci. *103*, 1833–1838.

Zou, S., Meadows, S., Sharp, L., Jan, L.Y., and Jan, Y.N. (2000). Genome-wide study of aging and oxidative stress response in Drosophila melanogaster. Proc. Natl. Acad. Sci. USA. *97*, 13726–13731.

Appendices

Appendix A: PCA loadings and score plots representing the metabolic profiles of A) paraquat treated T5 lines vs. T5 control lines, and B) four *Drosophila* species.

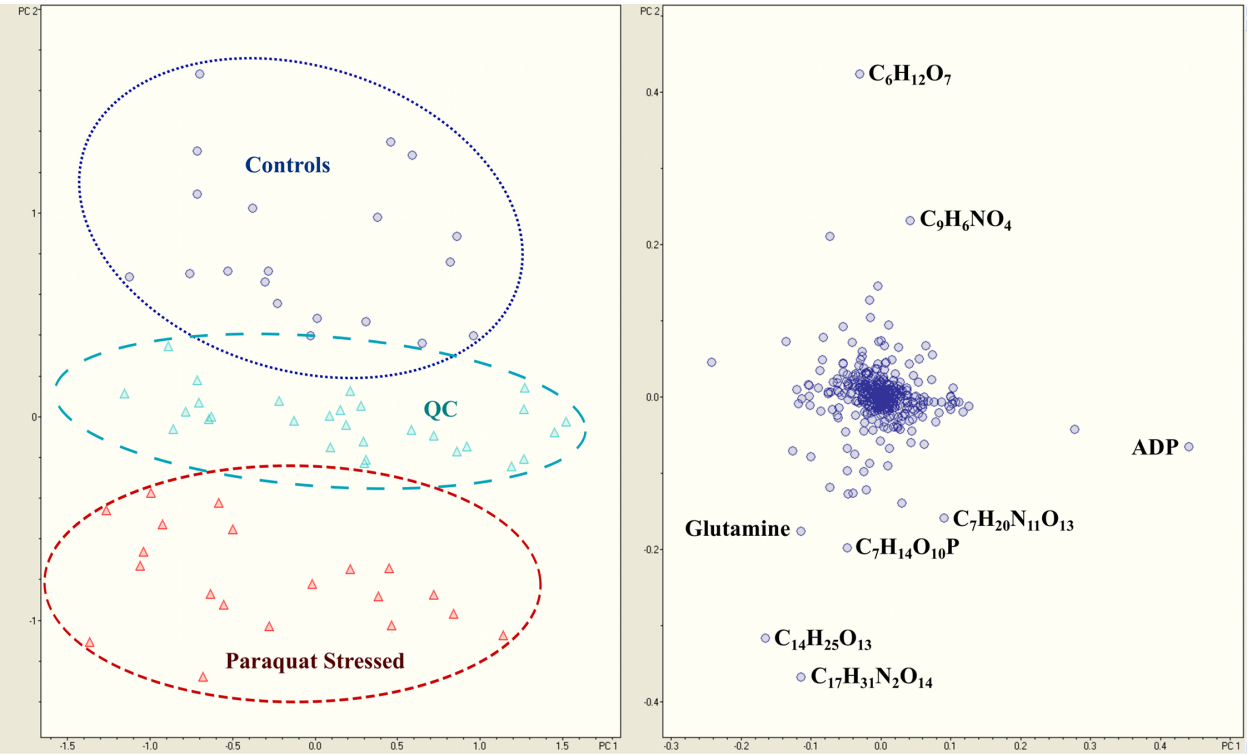

Appendix B: PCA loadings and score plots representing the metabolic profiles of four *Drosophila* species.

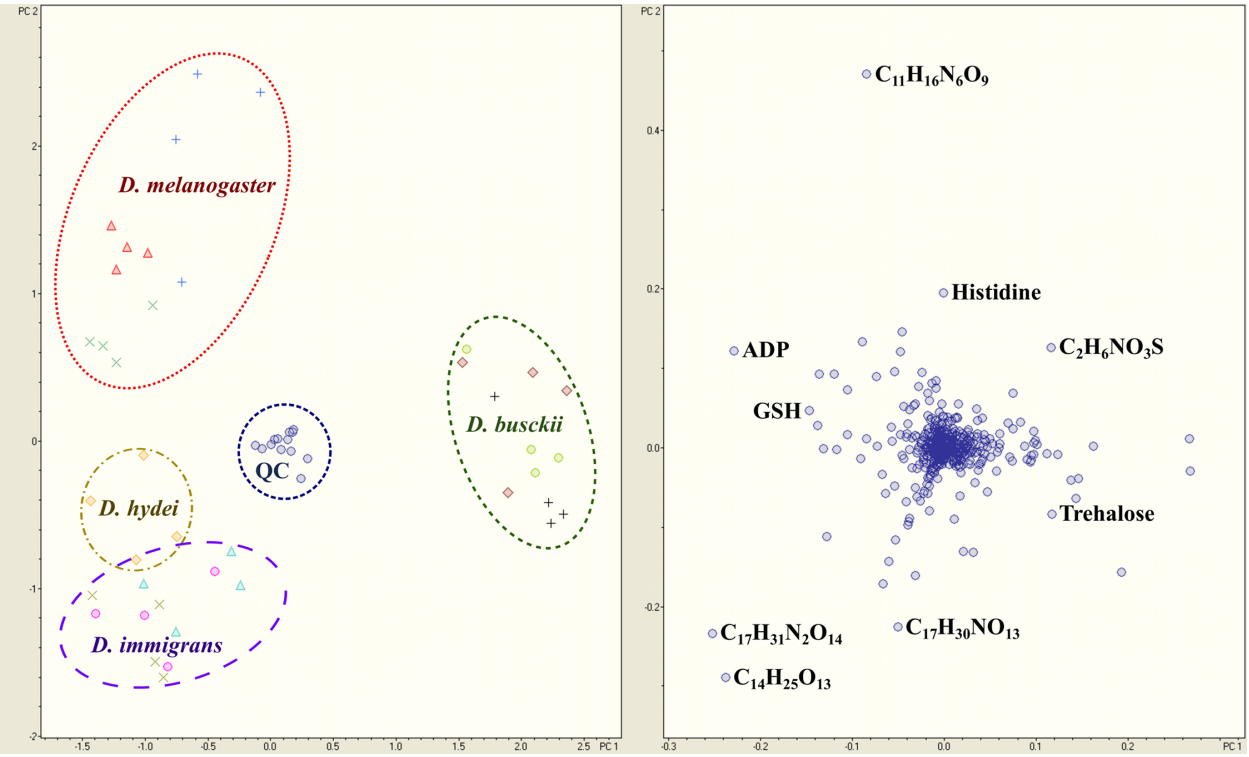

Appendix C: Comparison of transgenic rescue lines with wild-type lines

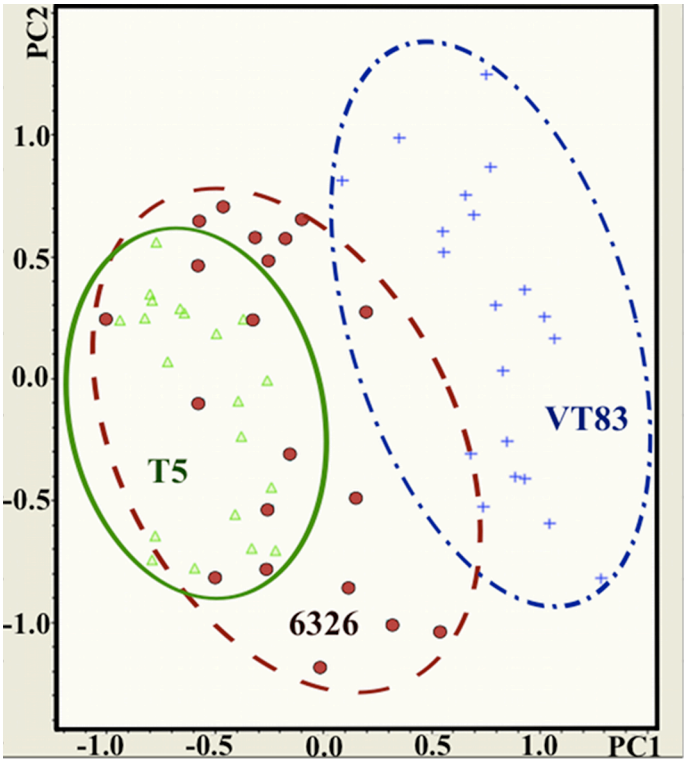

Appendix D: Relative standard deviations (RSD) of the area under the curve, for five replicates, of injections containing 16 compounds that elute near the void volume.

Metabolite	RSD (%)		
	0.8 ppm	**5 ppm**	**50 ppm**
Arginine	3.58	6.38	2.02
Asparagine	10.68	11.52	2.56
Cysteine	36.54	2.14	2.50
Dopamine		125.92	2.49
Glutamine	3.47	5.02	2.04
Histidine	4.77	3.98	1.70
Leucine	14.67	4.03	2.80
Lysine	12.86	5.45	2.07
Methionine	45.24	4.03	4.24
Ornithine	4.86	2.78	3.51
Proline	5.22	4.33	2.26
Serine	10.42	9.24	6.11
Threonine	14.14	4.15	2.78
Trehalose	3.58	3.67	3.65
Tryosine	5.51	5.75	1.02
Valine	19.44	9.97	3.34

Appendix E: Significantly altered metabolites in the *Sod-null* genotype (post-tandem MS)

Metabolite	*P*-value	Ratio (*Sod-nulls*/controls)	Fold (*Sod-nulls*/controls)	Pathway placement (From: Table 5)
Pantothenate	0	0.47	-2.11	1
Dopamine	0	0.7	-1.43	15
Histamine	0	0.73	-1.37	17
Glutamine	0	1.42	1.42	2,3,4,5,6,7,18,39
Threonine	0	1.49	1.49	7,10,11,44
UDP-n-acetyl glucosamine	0	0.78	-1.29	9
Trehalose	0	0.77	-1.29	13
Gluconate	0	2.01	2.01	8
Methionine	0	1.77	1.77	7,12
Sedoheptulose 7-phosphate	0	1.79	1.79	8
Cytidine	0	0.68	-1.48	4
N-acetlyaspartate	0	0.76	-1.31	6
Phosphotyrosine	0	1.59	1.59	-
glucose/fructose/etc	0	0.82	-1.22	-
AMP	0	0.93	-1.08	18
Glycerophosphates	0	0.84	-1.2	-
GSSG	0	1.48	1.48	26
Histidine	0.00001	0.88	-1.13	7,17
Arginine	0.00001	1.11	1.11	2,7
UMP	0.00007	0.76	-1.32	4
Asparagine	0.00026	1.44	1.44	6,7,43
Pyroglutamate	0.00047	1.2	1.2	19
Valine	0.00074	1.37	1.37	1,7,10,30,41,43
Trehalose 6-phosphate	0.00119	0.72	-1.38	13
NAD	0.00168	0.84	-1.19	24
FAD	0.00176	0.86	-1.16	33
(Iso)leucine	0.0028	1.13	1.13	-
Ornithine	0.00289	1.11	1.11	2,19
n-acetyl-glutamate	0.0029	1.4	1.4	2
Hexose-phosphates	0.00436	1.19	1.19	-
Biopterin	0.00443	1.54	1.54	-
Urate	0.00724	0.59	-1.7	18

Metabolite	*P*-value	Ratio (*Sod-nulls*/controls)	Fold (*Sod-nulls*/controls)	Pathway placement (From: Table 5)
CoA	0.00855	0.84	-1.2	1,25
ATP	0.01047	0.74	-1.35	18
Acetyl-CoA	0.0136	0.73	-1.37	10,21,23,25,26,27, 28,29,30,31,32,34, 38,39,41,42,
Proline	0.01899	0.9	-1.11	2,7
ADP	0.06343	0.89	-1.12	18
Cysteine	0.12442	0.87	-1.15	1,7,11,12,19
Tyrosine	0.14594	1.07	1.07	7,15,20,21,45
Phospho ethanolamine	0.15359	0.96	-1.04	14,37
Phenylalanine	0.17352	0.94	-1.07	7,20,21,43
Malate	0.23028	1.09	1.09	23,38,39,42
Serine	0.23335	0.87	-1.15	7,11,12,38,39,42,4 3
Oxoglutarate	0.24111	1.15	1.15	5,6,17,23,26,39
Lysine	0.33527	1.1	1.1	7,27,40
Inosine	0.61143	1.08	1.08	18
Mannose 6-Phosphate	0.63373	1.12	1.12	9,36
NADH	0.67924	0.93	-1.07	-
Aspartate	0.78293	0.96	-1.04	1,2,6,7,11,12,17,24 ,41,43
Succinate	0.82429	1	1	6,15,21,23,26
Glutamate	0.87853	1	1	2,3,5,6,7,17,19,26, 39,44
Fumarate	0.89018	1.02	1.02	23,6,2,15,21,26,24
GSH	0.95284	1	-1	19
(Iso)citrate	0.99008	1	-1	-
NADP		Absent in *Sod-nulls*		19

Appendix F: Significantly altered metabolites in paraquat treated flies (post-tandem MS)

Metabolite	*P*-value	Ratio (PQ/controls)	Fold (PQ/controls)	Pathway placement (From: Table 5)
Sedoheptulose 7-phosphate	0	4.64	4.64	8
Panothenate	0	0.55	-1.83	1
Gluconate	0	0.12	-8.37	8
Glutamine	0	1.9	1.9	2,3,4,5,6,7,18,39
GSH	0	1.31	1.31	19
Trehalose	0	1.2	1.2	13
(Iso)leucine	0.00048	0.79	-1.27	-
Lysine	0.00063	1.51	1.51	7,27,40
Tyrosine	0.00074	1.27	1.27	7,15,20,21,45
Histidine	0.00179	0.87	-1.15	7,17
Hexose-phosphates	0.0022	1.33	1.33	-
Trehalose 6-phosphate	0.00284	1.38	1.38	13
Proline	0.00318	0.78	-1.28	2,7
Asparagine	0.00483	1.54	1.54	6,7,43
Phenylalanine	0.01427	0.8	-1.25	7,20,21,43
UMP	0.01984	1.17	1.17	4
GSSG	0.02696	1.24	1.24	26
Arginine	0.06045	0.85	-1.17	2,7
Phospho ethanolamine	0.06951	0.85	-1.17	14,37
Threonine	0.09878	0.81	-1.24	7,10,11,44
Phosphotyrosine	0.10366	0.84	-1.18	-
(Iso)citrate	0.10632	1.2	1.2	-
Aspartate	0.14159	1.1	1.1	1,2,6,7,11,12,17,24,41,43
Biopterin	0.18875	1.19	1.19	-
CoA	0.25249	0.81	-1.23	1,25
Mannose 6-phosphate	0.27072	1.37	1.37	9,36
Malate	0.33153	0.74	-1.36	23,38,39,42
Dopamine	0.37476	1.06	1.06	15
Succinate	0.39438	1.05	1.05	6,15,21,23,26
N-acetylaspartate	0.40839	0.91	-1.09	6
Inosine	0.43673	0.87	-1.15	18
ATP	0.44062	0.84	-1.19	18
Glutamate	0.56141	1.04	1.04	2,3,5,6,7,17,19,26,39,44
Glyceraldehyde 3-phosphate	0.5772	1.1	1.1	8,29,34,36,42
AMP	0.66482	1.02	1.02	18
Glycerophosphates	0.71192	0.96	-1.04	-
UDP-n-acetyl glucosamine	0.74556	1.05	1.05	9
Ornithine	0.77702	0.97	-1.03	2,19

Metabolite	*P*-value	Ratio (PQ/controls)	Fold (PQ/controls)	Pathway placement (From: Table 5)
NADH	0.78073	1.06	1.06	-
(Iso)citrate	0.82373	0.95	-1.06	-
NAD	0.82795	0.98	-1.02	24
ADP	0.88741	0.98	-1.02	18
Histamine	0.8878	1.01	1.01	17
Pyroglutamate	0.89187	0.99	-1.01	19
FAD	0.96348	1.01	1.01	33